Monitoring Survey at the Isles of Shoals North Disposal Site, October 2021

Disposal Area Monitoring System - DAMOS

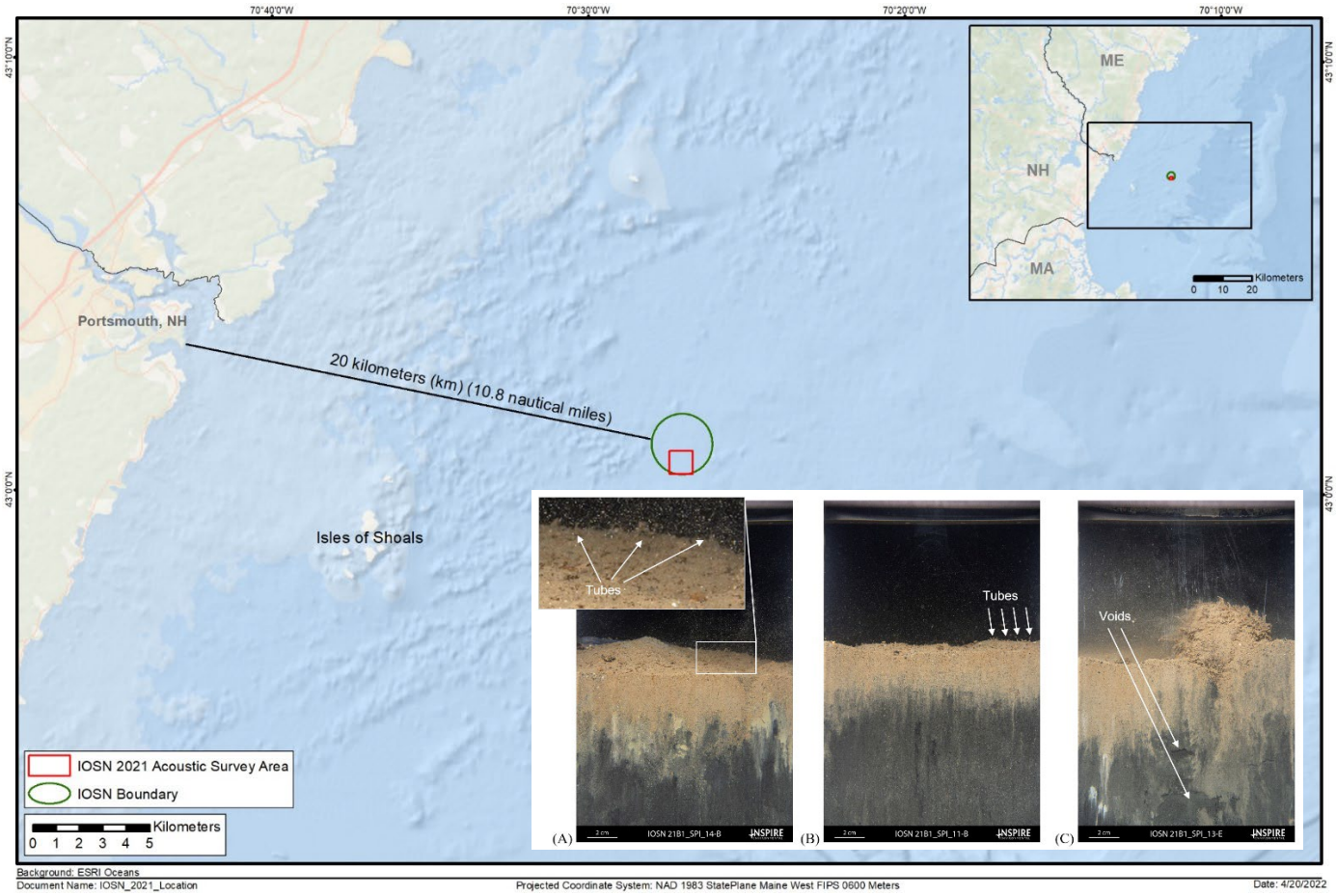

US Army Corps of Engineers
New England District

D A M O S
DISPOSAL AREA MONITORING SYSTEM

Contribution 214
September 2022

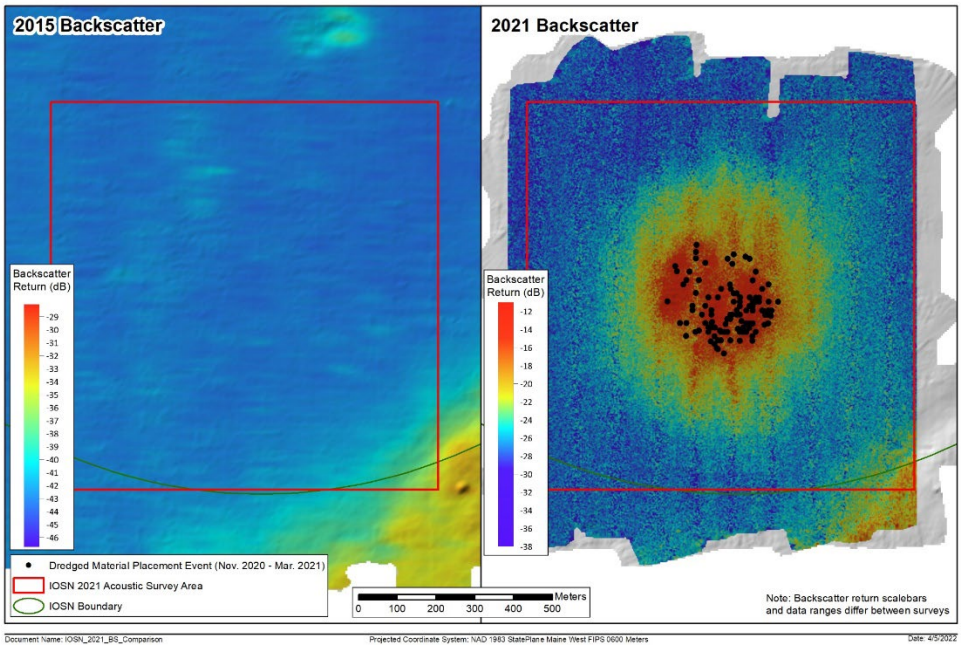

REPORT DOCUMENTATION PAGE

form approved OMB No. 0704-0188

1. AGENCY USE ONLY (LEAVE BLANK)	2. REPORT DATE	3. REPORT TYPE AND DATES COVERED
	September 2022	FINAL Contribution, October 2021 Survey

4. TITLE AND SUBTITLE
Monitoring Survey at the Isles of Shoals North Disposal Site, October 2021

5. FUNDING NUMBERS
Contract No. W912WJ-19-D-0010

6. AUTHOR(S)
Kaitlin Sylvester, INSPIRE Environmental

7. PERFORMING ORGANIZATION NAME(S) AND ADDRESS(ES)
INSPIRE Environmental
513 Broadway
Newport, RI 02840

8. PERFORMING ORGANIZATION REPORT NUMBER

9. SPONSORING/MONITORING AGENCY NAME(S) AND ADDRESS(ES)
US Army Corps of Engineers-New England District
696 Virginia Rd
Concord, MA 01742-2751

10. SPONSORING/MONITORING AGENCY REPORT NUMBER
Contribution No. 214

11. SUPPLEMENTARY NOTES
Available from DAMOS Program Manager, Environmental Branch
USACE-NAE, 696 Virginia Rd, Concord, MA 01742-2751

12a. DISTRIBUTION/AVAILABILITY STATEMENT
Approved for public release; distribution unlimited

12b. DISTRIBUTION CODE

13. ABSTRACT

The Isles of Shoals North Disposal Site (IOSN) was designated as a new Ocean Dredged Material Disposal Site (ODMDS) in September 2020; since the official designation, and at the time of the 2021 survey, it had received approximately 46,000 m^3 (60,000 yd^3) of dredged material. The overall objective of the 2021 IOSN survey was to conduct an initial confirmatory survey for the newly designated site after the initial placement of dredged material. The acoustic survey was designed to characterize the seafloor topography over the active portion of the site (southern central area) and confirm the location of recent dredged material disposals. The sediment profile and plan view imaging (SPI/PV) survey was designed to assess surficial sediments and benthic habitat status of the new dredged material mound, baseline areas within IOSN, and reference areas.

The 2021 IOSN survey included the collection of high-resolution acoustic data and the collection of SPI/PV imagery. The acoustic survey covered a 1,000 x 1,000 m area located in the southern central portion of the site. SPI/PV imagery was collected at 15 stations within IOSN and at three stations within each of the three reference areas. Nine stations were placed over the active portion of IOSN, in an area where dredged material placement occurred, and an additional six stations were placed in baseline areas of the site where dredged material has not yet been placed.

The bathymetric data revealed a relatively flat surface that gradually sloped from 93 m (305 ft) deep along the western boundary of the survey area to approximately 95 m (312 ft) deep along the eastern boundary, with a slight elevation increase visible within the central portion of the survey area where dredged material had accumulated. The bathymetric depth differencing model revealed an elevated area within the central portion of the survey grid rising approximately 0.7 m (2 ft) above the ambient seafloor. The acoustic backscatter data displayed a footprint of coarser material that spread approximately 600 m (1,968 ft) in diameter around the disposal target.

Benthic recolonization status was assessed using SPI/PV imagery and was observed to be progressing along the successional stage model as expected. The mean apparent redox potential discontinuity (aRPD) depth within the active area of IOSN was statistically shallower than the reference areas, however, the infaunal successional stage within the active portion of IOSN was statistically equivalent to the reference areas. This difference in statistical results indicates that deep burrows are present but have yet to establish an aRPD depth equivalent to the reference areas due to the recent disposal activity.

The results of the 2021 survey led to the following recommendations:

R1: Targeted placement of dredged material disposal successfully limited temporary benthic community impacts to a small area within IOSN. Future dredged material placement can occur throughout the disposal site utilizing the targeted placement approach.

R2: A confirmatory acoustic and SPI/PV survey should be conducted at IOSN after it receives additional dredged material. The survey should occur over the area of newly placed dredged material and over the active area surveyed in 2021 to evaluate benthic habitat conditions.

R3: The reference areas are comparable to the site and can continue to be used for future surveys.

14. SUBJECT TERMS	15. NUMBER OF TEXT PAGES:
DAMOS, dredged material, IOSN, Isles of Shoals, acoustic, multibeam, backscatter, side-scan sonar, SPI, PV, sediment profile imaging	46 pp plus Figures and Appendices
	16. PRICE CODE

17. SECURITY CLASSIFICATION OF REPORT	18. SECURITY CLASSIFICATION OF THIS PAGE	19. SECURITY CLASSIFICATION OF ABSTRACT	20. LIMITATION OF ABSTRACT
Unclassified			

MONITORING SURVEY AT THE ISLES OF SHOALS NORTH DISPOSAL SITE OCTOBER 2021

CONTRIBUTION #214

September 2022

Contract No. W912WJ-19-D-0010
Delivery Order W912WJ21F0113

Funded and Managed by:
New England District
U.S. Army Corps of Engineers
696 Virginia Road
Concord, MA 01742-2751

Prepared by:
INSPIRE ENVIRONMENTAL
INSPIRE Environmental
513 Broadway
Newport, RI 02840

This report should be cited as:

USACE. 2022. Monitoring Survey at the Isles of Shoals North Disposal Site, October 2021. DAMOS Contribution No. 214. Prepared by INSPIRE Environmental, Newport, RI for the U.S. Army Corps of Engineers, New England District, Concord, MA. 46 pp plus Figures and Appendices.

Note on units of this report: As a scientific data summary, information and data are presented in the metric system. However, given the prevalence of English units in the dredging industry of the United States, conversions to English units are provided for general information in Section 1.0. A table of common conversions can be found in Appendix A.

TABLE OF CONTENTS

Page

TABLE OF CONTENTS (CONTINUED)

Page

LIST OF TABLES

Page

LIST OF FIGURES

LIST OF FIGURES (CONTINUED)

Figure Page

LIST OF FIGURES (CONTINUED)

Figure Page

LIST OF FIGURES (CONTINUED)

Figure Page

LIST OF ACRONYMS

aRPD	apparent redox potential discontinuity
ASCII	American Standard Code for Information Interchange
CI	confidence interval
CLT	Central Limit Theorem
DAMOS	Disposal Area Monitoring System
DGPS	Digital Global Positioning System
EGN	Empirical Gain Normalization
EPA	U.S. Environmental Protection Agency
ER-L	effects range low
ER-M	effects range median
ft	feet
GIS	Geographic information system
GPS	Global Positioning System
GRD	gridded data
INSPIRE	INSPIRE Environmental
IOSN	Isles of Shoals North Disposal Site
m	meter
MBES	multibeam echosounder
MLLW	Mean Lower Low Water
MPRSA	Marine Protection, Research, and Sanctuaries Act
MRU	motion reference unit
NAD83	North American Datum of 1983
NAE	USACE, New England Division

LIST OF ACRONYMS (CONTINUED)

NEF	Nikon Electronic Format
NMFS	National Marine Fisheries Service
NOAA	National Oceanic and Atmospheric Association
NOS	National Ocean Service
ODMDS	Ocean Dredged Material Disposal Site
PAHs	Polycyclic aromatic hydrocarbons
PCBs	polychlorinated biphenyls
PSD	Photoshop Document
PV	Plan View
QAPP	Quality Assurance Project Plan
RTK	Real Time Kinematic
R/V	research vessel
SMMP	Site Management and Monitoring Plan
SOP	Standard Operating Procedures
SPI	Sediment Profile Imaging
SVP	sound velocity profile
TIF	tagged image file
USACE	U.S. Army Corps of Engineers
VDATUM	Vertical Datum Transformation
yd	yard

EXECUTIVE SUMMARY

The Isles of Shoals North Disposal Site (IOSN) was designated as a new Ocean Dredged Material Disposal Site (ODMDS) in September 2020; since the official designation, and at the time of the 2021 survey, it had received approximately 46,000 m^3 (60,000 yd^3) of dredged material. The overall objective of the 2021 IOSN survey was to conduct an initial confirmatory survey for the newly designated site after the initial placement of dredged material. The acoustic survey was designed to characterize the seafloor topography over the active portion of the site (southern central area) and confirm the location of recent dredged material disposals. The sediment profile and plan view imaging (SPI/PV) survey was designed to assess surficial sediments and benthic habitat status of the new dredged material mound, baseline areas within IOSN, and reference areas.

The 2021 IOSN survey included the collection of high-resolution acoustic data and the collection of SPI/PV imagery. The acoustic survey covered a 1,000 x 1,000 m area located in the southern central portion of the site. SPI/PV imagery was collected at 15 stations within IOSN and at three stations within each of the three reference areas. Nine stations were placed over the active portion of IOSN, in an area where dredged material placement occurred, and an additional six stations were placed in baseline areas of the site where dredged material has not yet been placed.

The bathymetric data revealed a relatively flat surface that gradually sloped from 93 m (305 ft) deep along the western boundary of the survey area to approximately 95 m (312 ft) deep along the eastern boundary, with a slight elevation increase visible within the central portion of the survey area where dredged material had accumulated. The bathymetric depth differencing model revealed an elevated area within the central portion of the survey grid rising approximately 0.7 m (2 ft) above the ambient seafloor. The acoustic backscatter data displayed a footprint of coarser material that spread approximately 600 m (1,968 ft) in diameter around the disposal target.

Benthic recolonization status was assessed using SPI/PV imagery and was observed to be progressing along the successional stage model as expected. The mean apparent redox potential discontinuity (aRPD) depth within the active area of IOSN was statistically shallower than the reference areas, however, the infaunal successional stage within the active portion of IOSN was statistically equivalent to the reference areas. This difference in statistical results indicates that deep burrows are present but have yet to establish an aRPD depth equivalent to the reference areas due to the recent disposal activity.

The results of the 2021 survey led to the following recommendations:

R1: Targeted placement of dredged material disposal successfully limited temporary benthic community impacts to a small area within IOSN. Future dredged material placement can occur throughout the disposal site utilizing the targeted placement approach.

R2: A confirmatory acoustic and SPI/PV survey should be conducted at IOSN after it receives additional dredged material. The survey should occur over the area of newly placed dredged material and over the active area surveyed in 2021 to evaluate benthic habitat conditions.

R3: The reference areas are comparable to the site and can continue to be used for future surveys.

1.0 INTRODUCTION

INSPIRE Environmental (INSPIRE) conducted an acoustic and Sediment Profile and Plan View Imaging (SPI/PV) monitoring survey at the Isles of Shoals North Disposal Site (IOSN) in October 2021 as part of the U.S. Army Corps of Engineers (USACE) New England District (NAE) Disposal Area Monitoring System (DAMOS) Program. DAMOS is a comprehensive monitoring and management program designed and conducted to address environmental concerns surrounding the placement of dredged material at aquatic disposal sites throughout the New England region. An introduction to the DAMOS Program and IOSN, including brief descriptions of previous dredged material disposal and site monitoring activities, is provided below.

1.1 Overview of the DAMOS Program

The DAMOS Program features a tiered management protocol designed to ensure that any potential adverse environmental impacts associated with dredged material disposal are promptly identified and addressed (Germano et al. 1994). For over 40 years, the DAMOS Program has collected and evaluated dredged material disposal site data throughout New England. Based on these data, patterns of physical, chemical, and biological responses of seafloor environments to dredged material disposal activity have been documented (Fredette and French 2004).

DAMOS monitoring surveys fall into two general categories: confirmatory studies and focused studies. The data collected and evaluated during these studies provide answers to strategic questions in determining next steps in the disposal site management process. DAMOS monitoring results guide the management of disposal activities at existing sites, support planning for use of future sites, and evaluate the long-term status of historical sites (Wolf et al. 2012).

Confirmatory studies are designed to test hypotheses related to expected physical and ecological response patterns following placement of dredged material on the seafloor at established, active disposal sites. Two primary goals of DAMOS confirmatory monitoring surveys are to document the physical location and stability of dredged material placed into the aquatic environment and to evaluate the biological recovery of the benthic community following placement of dredged material. Several survey techniques are employed in order to characterize these responses to dredged material placement. Sequential acoustic

monitoring surveys (including bathymetric, acoustic backscatter, and side-scan sonar data collection) are performed to characterize the height and spread of discrete dredged material deposits or mounds created at open-water sites as well as the accumulation/consolidation of dredged material into confined aquatic disposal cells.

SPI and PV imaging surveys are performed in confirmatory studies to provide further physical characterization of the material and to support evaluation of seafloor (benthic) habitat conditions and recovery over time. Each type of data collection activity is conducted periodically at disposal sites, and the conditions found after a defined period of disposal activity are compared with the long-term data set at specific sites to determine the next step in the disposal site management process (Germano et al. 1994).

Focused studies are periodically undertaken within the DAMOS Program to evaluate candidate sites, as baseline surveys at new sites, to evaluate inactive or historical disposal sites, and to contribute to the development of dredged material management and monitoring techniques. Focused DAMOS monitoring surveys may also feature additional types of data collection activities as deemed appropriate to achieve specific survey objectives, such as grab or core sampling of sediment for physical/chemical/biological analyses, sub-bottom profiling, or video image files.

The 2021 IOSN survey was a confirmatory monitoring survey conducted over the southern central portion of the newly designated site and associated reference areas. Acoustic imagery paired with SPI/PV data were used to support assessment of physical modifications and initial benthic community response to dredged material placement. SPI/PV imagery was collected within the three reference areas for comparative purposes. An additional set of SPI/PV stations were captured over the northern portion of the site to further investigate the baseline benthic habitat conditions within the site.

1.2 Introduction to the Isles of Shoals North Disposal Site

IOSN is located approximately 20 kilometers (km) (10.8 nautical miles) east of Portsmouth, New Hampshire, in the Gulf of Maine (Figure 1-1). IOSN is circular in shape and approximately 2.5 km (1.3 nmi) in diameter. Based on a 2015 acoustic survey conducted under the DAMOS Program, water depths at the site range from approximately 77 to 104 meters (m) (252 to 341 feet [ft]) Mean Lower Low Water (MLLW) (Figure 1-2) (Guarinello et al. 2016). The seafloor at IOSN slopes gradually and increases in depth from the western boundary to the eastern boundary of the site. Outside of IOSN boundaries to the northwest

and southeast, hard bottom features rise approximately 10 to 20 m (33 to 66 ft) above the surrounding seafloor (Guarinello et al. 2016). Three reference areas (REF-A, REF-B, and REF-C) are defined as 250-m (~820-ft) radius circles and are located to the southwest and northeast of the site (Figure 1-2). Water depths at the reference areas range from 93 to 95 m (305 to 312 ft).

In September 2020, the U.S. Environmental Protection Agency Region 1 (EPA Region 1) designated IOSN as an Ocean Dredged Material Disposal Site (ODMDS) under Section 102(c) of the Marine Protection, Research, and Sanctuaries Act (MPRSA). The site is managed by EPA Region 1 and USACE NAE following the Site Management and Monitoring Plan (SMMP) (USACE/EPA 2020).

1.3 Previous IOSN Monitoring Events

In 2015, a baseline acoustic and SPI/PV survey was conducted at IOSN and at the three potential reference areas to characterize the seafloor topography, surficial features, and assess the benthic status of the proposed site and reference areas (Table 1-1; Guarinello et al. 2016). Acoustic results from the 2015 survey documented baseline topographic conditions (Figure 1-2), which are briefly described above. SPI/PV results indicated that the site and reference areas were composed of fine-grained sediment, with one location within REF-C observed to consist of anomalous material, potentially indicative of historical dredged material placement. Mature stage III infauna were observed throughout IOSN and the reference areas (Guarinello et al. 2016).

Additional baseline sediment, water, and benthic characterization surveys were conducted in 2019 and 2020 within IOSN and the reference areas prior to site designation and dredged material placement within the site. The 2019 and 2020 baseline efforts included the collection of sediment grab samples to assess sediment chemistry and benthic community structure, and the collection of water column profiles and water quality samples (for analysis of chemical and nutrient concentrations) at the proposed site and potential reference areas (Table 1-1; USACE 2021). Sediment chemistry results inclusive of metals, polycyclic aromatic hydrocarbons (PAHs), polychlorinated biphenyls (PCBs), and pesticides from the 2019 and 2020 surveys were below respective effects range low (ER-L) values for all locations at IOSN and reference areas with the exception of arsenic and nickel at both IOSN and reference areas. However, measured concentrations of arsenic and nickel were considered to be representative of native sediment within the region because levels of each metal were similar between the site and reference areas (USACE 2021). The benthic

community analysis revealed healthy benthic communities with similar trophic guilds within the site and reference areas. Water chemistry results for PCBs and pesticides were observed to be below the method detection limit, and metals concentrations were detected at concentrations below conservative values presented within the National Oceanic and Atmospheric Association's (NOAA) screening tables. PAHs were detected infrequently and only at low levels. Water column nutrient concentrations measured at both IOSN and the reference areas were found to be within expected ranges for the region (USACE 2021).

1.4 Recent Dredged Material Disposal Activity

Since the official designation of IOSN in September 2020, approximately 46,000 cubic meters (m^3) (60,000 cubic yards [yd^3]) of dredged material were placed at a target area in the southern central portion of IOSN (Table 1-2; Figure 1-3). This material originated from both federal and permitted (non-federal) dredging projects in Rye, New Hampshire.

A detailed record of dredged material disposal activity at IOSN for the period November 2020 to March 2021, including the origin, volume, and disposal location, is provided in Appendix B. The October 2021 monitoring survey was the first to assess dredged material placed at IOSN since official site designation.

1.5 2021 Survey Objectives

The overall objective of the 2021 IOSN survey was to conduct a confirmatory survey for the newly designated site after the initial placement of dredged material. The specific survey objectives were to:

- Characterize the seafloor topography and surficial features of IOSN, including the active disposal area by conducting a multibeam bathymetric survey.
- Use SPI/PV imaging to assess the recolonization status of benthic organisms and surficial sediment characteristics at the active area of IOSN and three references areas.
- Compare physical and benthic community conditions of the baseline area of the site to the reference areas.

Table 1-1.

Overview of Survey Activities at IOSN

Date	Purpose of Survey	Bathymetry Area	SPI Stations (location - #)	Additional Studies	DAMOS Report/ Contribution No.	Reference
Sept 2015	Baseline Acoustic and SPI/PV	3500 x 3500 m	45	-	2015-D-01	Guarinello et al. 2016
Sept/Oct 2019 and Sept 2020	Baseline Sediment Characterization, Benthic Community Structure, and Water Quality	-	-	17 Sediment Grab Samples 4 Water Quality Profiles/Samples	DR-2020-1	USACE 2021

Table 1-2.

Disposal Activity at IOSN since Site Designation in September 2020
(per dredged material disposal logs provided by USACE, February 2022)

Permit number	Project Name	Disposal Dates	Load volume (m^3)	Load volume (yd^3)
NAE-2016-2159	Tom Bluoin Property, Rye, NH	2/2021 – 3/2021	2,133	2,790
W912WJ-20-C-0016*	Rye Harbor Federal Navigation Project	11/2020 – 2/2021	44,065	57,635
Total			**46,198**	**60,425**

* The FNP contract included dredging approximately 8,150 cubic yards from the Rye Harbor State Anchorage (permit number NAE-2019-02222) at 100% non-Federal cost through a Memorandum of Understating with the State of New Hampshire.

2.0 METHODS

The SPI/PV survey was conducted by INSPIRE Environmental onboard the 55-foot R/V *Jamie Hanna* on 6 October 2021. The acoustic data collection survey was conducted by CR Environmental onboard the 42-foot M/V *Gunsmoke* on 7 October 2021. A fishing gear observation was conducted during the acoustic survey to inventory active fishing gear in and around the site.

2.1 Navigation and Onboard Data Acquisition

Navigation for the acoustic survey was accomplished using a Hemisphere VS-330 Real Time Kinematic (RTK) Global Positioning System (GPS) which received base station corrections through the SmartNet NTRIP broadcast. Horizontal position accuracy in fixed RTK mode was approximately 1 cm, vertical (tidal) accuracy was approximately 2 cm. The digital GPS (DGPS) system was serially interfaced to a laptop computer running HYPACK hydrographic survey software. HYPACK continually recorded vessel position and GPS satellite quality and provided a steering display for the captain allowing him to accurately maintain the position of the vessel along pre-established acoustic survey transects. Vessel heading measurements were provided by an IxBlue Octans III fiber optic gyrocompass. The Hemisphere VS-330 served as a backup source for heading corrections.

Navigation for the SPI/PV survey was accomplished using a Hemisphere VS330 Global Navigation Satellite System (GNSS) compass with dual antennas using Wide Area Augmentation System (WAAS) differential correctors to accurately record vessel heading and position accuracy within 1 m. At each station, the vessel was positioned at the target coordinates and the camera was deployed within a defined station tolerance of 7.5 m. At least four replicate SPI and PV images were collected at each station. The navigation system was interfaced to HYPACK® software via laptop serial ports to provide a method to locate target coordinates and record actual sampling locations. Throughout the survey, the HYPACK® data acquisition system received DGPS data. The incoming data stream was digitally integrated and stored on the PC's hard drive. After all stations were sampled, the navigator exported all recorded positional data into a Microsoft Excel© spreadsheet. The spreadsheet includes the station name, replicate number, date, time, depth, and coordinate positions for every SPI/PV replicate.

2.2 Acoustic Survey

The acoustic survey included bathymetric, backscatter, and side-scan sonar data collection and processing. The bathymetric data provided measurements of water depth that, when processed, were used to map the seafloor topography. The processed data were also compared with previous surveys to track changes in the size and location of seafloor features. This technique is the primary tool of the DAMOS Program for mapping the distribution of dredged material at disposal sites. The methodology for acoustic data acquisition is described in detail in the Project Quality Assurance Project Plan (QAPP; INSPIRE 2020a) and INSPIRE acoustic standard operating procedures (SOP; INSPIRE 2020b).

Multibeam backscatter and side-scan sonar data provided images that supported the characterization of surface sediment texture and roughness. Backscatter data are processed into a seamless image with corrections for topography (depth-normalized) while side-scan sonar data retains a higher resolution image without correction for topography. Comparison of synoptic acoustic data types is very useful for assessing dredged material placed on the seafloor.

2.2.1 Acoustic Survey Planning

A certified hydrographer obtained site coordinates from USACE NAE, imported them to HYPACK and ArcView geographic information system (GIS) software, and created maps to guide survey activities. The proposed IOSN acoustic survey design was then reviewed and approved by the NAE DAMOS Program Manager.

The acoustic survey covered the active, southern central portion of IOSN (Figure 2-1). A 1000 × 1000-m acoustic survey was selected and tracklines were generated to provide greater than 100-percent coverage of the IOSN seafloor surveyed. Survey tracklines were collected in a north-south orientation and spaced 100 m apart and cross lines were collected in an east-west orientation and spaced 200 m apart (Figure 2-1). The acoustic survey did not include coverage of the entire IOSN or the three reference areas, these areas were surveyed during the baseline monitoring effort in 2015 (Guarinello et al. 2016).

2.2.2 Acoustic Data Collection

The 2021 multibeam bathymetric survey of IOSN was conducted on 7 October 2021. Bathymetric, acoustic backscatter, and side-scan sonar data were collected using a Teledyne Reson T-20R multibeam echosounder (MBES). This 200-400 kHz system forms 256 1–2-

degree beams (frequency dependent) distributed equiangularly or equidistantly across a 160-degree swath. The system was operated using a frequency of 250 kHz and a 0.08-millisecond pulse to optimize bathymetric and backscatter data quality. The MBES transducer was mounted amidships to the port rail of the survey vessel using a high strength adjustable boom. Offsets between the primary GPS antenna and the sonar were precisely measured and entered into HYPACK. The transducer depth below the water surface (draft) was checked and recorded at the beginning and end of data acquisition and confirmed using the "bar check" method. Tide corrections were applied using RTK GPS data.

An IxBlue Octans V motion reference unit (MRU) was interfaced to the MBES topside processor and to the acquisition computer. Precise linear offsets between the MRU and MBES were recorded and applied during acquisition. Depth and backscatter data were synchronized using pulse per second timing and transmitted to the HYPACK MAX® acquisition computer via Ethernet communications. Patch tests were conducted before and after the survey to allow computation of angular offsets between the MBES system components.

An AML Minos-X sound velocity profiler system was used to collect sound velocity profile (SVP) casts at frequent intervals throughout each survey day to determine the speed of sound in the local water mass for use in calibrating the MBES system. Three SVP casts were acquired during the survey. Additional confirmations of proper calibration, including static draft, were obtained using the "bar check" method, in which a metal plate was lowered beneath the MBES transducer to a known depth (e.g., 5.0 m) below the water surface. Bar-check calibrations conducted offshore were accurate to within 0.01 m in tests conducted at the beginning and end of the survey.

2.2.3 Bathymetric Data Processing

Bathymetric data were processed using HYPACK HYSWEEP® software. Processing components are described below and included:

- Conversion of RTK GPS tide data from NAVD88 elevations to MLLW elevations using NOAA's VDatum model
- Adjustment of data for tide fluctuations
- Correction of ray bending (refraction) due to density variation in the water column
- Removal of spurious points associated with water column interference or system errors

- Development of a grid surface representing depth solutions
- Statistical estimation of sounding solution uncertainty
- Generation of data visualization products

Correction of sounding depth and position (range and azimuth) for refraction due to water column stratification was conducted using a series of three SVPs acquired by the survey team. The water column was stratified during the survey, with an approximately 25-meters per second gradient between the surface and bottom. Stratification resulted in data artifacts associated with refraction that remained in the bathymetric surface model at a relatively fine scale (approximately 5 to 10 cm) relative to the surveyed water depth.

Bathymetric data were filtered to accept only beams falling within an angular limit of 52 degrees to minimize refraction artifacts. Spurious sounding solutions were flagged or rejected based on the careful examination of data in sweep and profile views.

The Reson MBES system was operated at 250 kHz. At this frequency, the system has a published beam width of 1.75 degrees. Assuming an average depth of 94 m and a maximum beam angle of 52 degrees, the beam footprint ranged from approximately 2.9 × 2.9 m (8.4 m^2) at nadir to 7.6 x 4.7 m 52 degrees from nadir. Data were reduced to a cell (grid) size of 5.0 × 5.0 m, acknowledging the system's fine range resolution while accommodating beam position uncertainty. This data reduction was accomplished by calculating and exporting the average elevation for each cell in accordance with USACE recommendations (USACE 2013).

The combined uncertainties associated with all system elements, including calibrations, tide corrections and refraction caused by water column stratification were quantified by comparing primary survey transects with perpendicular "cross-line" transects. Data for primary transects were exported at a cell resolution of 25 m^2 using the average elevation within each cell. Data for cross-line transects were compared to the pseudo "reference surface" created using the primary transects.

Comparisons were made between cross-line and mainstay swaths to +/- 55 degrees from nadir using 5.0 × 5.0-m cell average elevations and 5-degree beam-angle increments. The mean difference between the mainstay reference surface and cross-line data was -0.03 m. The average standard deviation between cross-lines and primary lines was 0.11 m, with a mean 95% Root Mean Square confidence limit uncertainty of 0.22 m. Mean elevation differences across the swaths ranged from 0.0 to 0.10 m with the greatest difference at 62

degrees from nadir. This comparison documents negligible tide bias and quantifies uncertainty associated with refraction. This analysis shows compliance with USACE accuracy recommendations and National Ocean Service (NOS) standards. Note that the NOS standard for this project depth (Special Order) would call for a 95th percentile confidence interval (95% CI) of 0.76 m at the maximum site depth (96.1 m) and 0.75 m at the mean site depth (94.4 m).

Reduced data were exported in ASCII text format with fields for Easting, Northing, and MLLW elevation (meters). All data were projected to the Maine West State Plane grid, NAD83 (metric). A variety of data visualizations were generated using a combination of ESRI ArcMap (V.10.8), and Golden Software Surfer (V. 17). Visualizations and data products included:

- ASCII data files of all processed soundings including MLLW depths and elevations,
- Contours of seabed elevation (20-cm, 50-cm, and 1.0-m intervals) in SHP format suitable for plotting using GIS and CAD software,
- 3-dimensional surface maps of the seabed created using 5× vertical exaggeration and artificial illumination to highlight fine-scale features not visible on contour layers (delivered in grid and TIF formats), and,
- An acoustic relief map of the survey area created using 5× vertical exaggeration, delivered in georeferenced TIF format.

2.2.4 Backscatter Data Processing

MBES backscatter data were processed using HYPACK®'s implementation of GeoCoder software developed by NOAA's Center for Coastal and Ocean Mapping Joint Hydrographic Center (CCOM/JHC). GeoCoder was used to create a mosaic best suited for substratum characterization using innovative beam-angle correction algorithms. Data acquired were processed using Reson Snippets beam time series data. A trend-adaptive angle-varying gain function in Geocoder was applied to minimize artifacts associated with substrate variation within survey transects.

Backscatter data for IOSN were next exported in ASCII format with fields for Easting, Northing, and backscatter (in dB units) using a 3.0 × 3.0-m resolution. Data were converted to grid format using Golden Software Surfer software. This grid was used to generate a seamless mosaic of backscatter in GeoTIF format. A Gaussian filter was next applied to backscatter data to minimize nadir artifacts and the filtered data were used to

develop a backscatter model using a 3.0 × 3.0-m grid. The grid was exported to an ESRI binary GRD format to facilitate comparison with other data layers.

2.2.5 Side-Scan Sonar Data Processing

Multibeam side-scan sonar data were processed using Chesapeake Technology, Inc. SonarWiz software. Time-varied gain adjustments were applied to data and a mosaic was constructed using the root-mean squared intensity value to represent overlapping pixels. Empirical Gain Normalization (EGN) was found to best detect features associated with disposals. This mosaic was exported in GeoTIF format using a resolution of 0.2 m per pixel. Because fine details are partially obscured in side-scan mosaics, individual GeoTIF images of each sonar file with resolutions of 0.2 m per pixel were also produced and delivered.

2.2.6 Acoustic Data Analysis

The processed bathymetric grids were converted to rasters, and bathymetric contour lines and acoustic relief models were generated and displayed using GIS. The backscatter mosaics and filtered backscatter grid were combined with acoustic relief models in GIS to facilitate visualization of relationships between acoustic datasets. This was done by rendering images and color-coded grids with sufficient transparency to allow the three-dimensional acoustic relief model to be visible underneath.

Surfer software was used to calculate elevation difference grids between the 2021 bathymetric dataset and the DAMOS survey conducted in 2015. Elevation difference grids were calculated by subtracting the earlier survey elevation estimates from the 2021 survey depth estimates at each point throughout the grid. The resulting elevation differences were contoured and displayed using GIS.

2.3 Sediment Profile and Plan View Imaging Survey

Sediment profile imaging and plan view imaging (SPI/PV) are monitoring techniques used to provide data on the physical characteristics of the seafloor and the status of the benthic biological community.

2.3.1 SPI and PV Survey Planning

The IOSN SPI/PV survey featured image collection at 24 stations. Fifteen stations were distributed within IOSN; nine stations were positioned over the active disposal area that recently received dredged material (within the acoustic survey footprint), and six stations

were positioned within the baseline portion of the site. Three stations were randomly located within each of the three reference areas (REF A, REF B, and REF C; Figure 2-2). SPI/PV target station locations are provided in Table 2-1, and actual SPI/PV station replicate locations are provided in Appendix C. The methodology for data acquisition and analysis for these images was consistent with the sampling methods described in detail in the Project QAPP (INSPIRE 2020a) and INSPIRE SPI/PV standard operating procedures (INSPIRE 2019).

2.3.2 Sediment Profile Imaging

Sediment profile imaging (SPI) is a monitoring technique used to provide data on the physical characteristics of the seafloor and the status of the benthic biological community. The technique involves deploying an underwater camera system to photograph a cross section of the sediment–water interface. In the 2021 survey at IOSN, high-resolution SPI images were acquired using a Nikon® D7100 digital single-lens reflex camera mounted inside an Ocean Imaging® Model 3731 pressure housing system. The pressure housing sat atop a wedge-shaped steel prism with a plexiglass front faceplate and a back mirror. The mirror was mounted at a 45-degree angle to reflect the profile of the sediment–water interface. The camera lens looked down at the mirror, which reflected the image from the faceplate. The prism had an internal strobe mounted inside at the back of the wedge to provide illumination for the image; this chamber was filled with distilled water, so the camera always had an optically clear path. The descent of the prism into the sediment was controlled by a hydraulic piston. As the prism penetrated the seafloor, a trigger activated a time-delay circuit that fired an internal strobe to obtain a cross-sectional image of the upper 15–20 cm of the sediment column (Figure 2-3). The camera remained on the seafloor for approximately 20 seconds to ensure that a successful image had been obtained.

Test exposures of a Color Calibration Target were made on deck at the beginning and end of the 2021 survey to verify that all internal electronic systems consistently met design specifications and to provide a color standard against which final images could be checked to ensure proper color balance. Details of the camera settings for each digital image are available in the associated parameters file embedded in each electronic image file. For this survey, the ISO-equivalent was set at 640, shutter speed was 1/250, f-stop was f11, and storage was in compressed raw Nikon Electronic Format (NEF) files (approximately 30 MB each). All camera settings and any setting changes were recorded in the field log (INSPIRE 2020c).

Each time the camera system was brought onboard, the frame counter was checked to ensure that the requisite number of replicates had been obtained. In addition, a prism penetration depth indicator on the camera frame was checked to verify that the optical prism had penetrated the bottom to a sufficient depth. If images were missed or the penetration depth was insufficient, the camera frame stop collars were adjusted and/or weights were added or removed, and additional replicate images were taken. Frame counts, time of image acquisition, and the number of weights used were recorded in the field log for each replicate image.

Each image was assigned a unique time stamp in the digital file attributes by the camera's data logger and cross-checked with the time stamp in the navigational system's computer data file. In addition, the field crew kept redundant written sample logs. Images were downloaded periodically to verify successful sample acquisition and/or to assess what type of sediment/depositional layer was present at a particular station. Digital image files were renamed with the appropriate station names after downloading as a further quality assurance step.

2.3.3 Plan View Imaging

An Ocean Imaging® Model DSC24000 plan view underwater camera (PV) system with two Ocean Imaging® Model 400-37 Deep Sea Scaling lasers was attached to the sediment profile camera frame and used to collect plan view images of the seafloor surface. Both SPI and PV images were collected during each "drop" of the system. The PV system consisted of a Nikon D-7100 encased in an aluminum housing, a 24 VDC autonomous power pack, a 500 W strobe, and a bounce trigger. A weight was attached to the bounce trigger with a stainless-steel cable so that the weight hung below the camera frame; the scaling lasers projected two red dots that are separated by a constant distance (26 cm) regardless of the field-of-view of the PV system. The field-of-view can be varied by increasing or decreasing the length of the trigger wire and, thereby, the camera height above the bottom when the picture is taken. As the SPI/PV camera system was lowered to the seafloor, the weight attached to the bounce trigger contacted the seafloor prior to the camera frame reaching the seafloor and triggered the PV camera (Figure 2-3).

During set-up and testing of the PV camera, the positions of lasers on the PV camera were checked and calibrated to ensure separation of 26 cm. Test images were also captured to confirm proper camera settings for site conditions. Details of the camera settings for each digital image are available in the associated parameters file embedded in each electronic

image file; for this survey, the ISO-equivalent was set at 640. The additional camera settings used were as follows: shutter speed 1/30, f18, white balance set to flash, color mode set to Adobe RGB, sharpening set to none, noise reduction off, and storage in compressed raw NEF files (approximately 30 MB each). Images were checked periodically throughout the survey to confirm that the initial camera settings were still resulting in the highest quality images possible. All camera settings and any setting changes were recorded in the field log.

Prior to field operations, the internal clock in the digital PV system was synchronized with the GPS navigation system and the SPI camera. For each PV image, a time stamp was recorded in the digital file and redundant time notes were made in the field and navigation logs. Throughout the survey, PV images were downloaded at the same time as the SPI images and evaluated to confirm image acquisition and image clarity.

The ability of the PV system to collect usable images was dependent on the clarity of the water column. Water conditions at IOSN allowed use of a 0.8-m trigger wire, resulting in a mean image width of 0.7 m and a mean field-of-view of 0.3 m^2.

2.3.4 SPI and PV Data Collection

The SPI/PV survey was conducted at IOSN and reference areas on 6 October 2021 onboard the *Jamie Hanna.* At each station, the vessel was positioned at the target coordinates and the camera was deployed within a defined station tolerance of 7.5 m. At least four replicate SPI and PV images were collected at each station. The three replicate images with the best quality (adequate prism penetration, no or minimal sampling artifacts) at each station were selected for analysis (Appendices D and E).

The DGPS described above was interfaced to HYPACK® software via laptop serial ports to provide a method to locate target coordinates and record actual sampling locations. Throughout the survey, the HYPACK® data acquisition system received DGPS data. The incoming data stream was digitally integrated and stored on the PC's hard drive. Actual SPI/PV sampling locations were recorded using this system.

2.3.5 Image Conversion and Calibration

Following completion of field operations, quality control checks were conducted on the field log, image date/time stamps were verified, and project-specific filenames were generated. After these procedures, the NEF raw image files were color calibrated in Adobe Camera Raw® by synchronizing the raw color profiles to the Color Calibration Target that

was photographed prior to field operations with the SPI camera. The raw SPI and PV images were then converted to high-resolution Photoshop Document (PSD) format files, using a lossless conversion file process and maintaining an Adobe RGB (1998) color profile. The PSD images were then calibrated and analyzed in Adobe Photoshop®. Length and area measurements were recorded as number of pixels and converted to scientific units using the calibration information. Detailed results of all SPI and PV image analyses are presented in Appendices D and E.

2.3.6 SPI and PV Data Analysis

Computer-aided analysis of the resulting images provided a set of standard measurements to allow comparisons between different locations and different surveys. The DAMOS Program has successfully used this technique for over 30 years to map the distribution of disposed dredged material and to monitor benthic recolonization at disposal sites (Germano et al. 2011).

Measured parameters for SPI and PV images were recorded in Microsoft Excel© spreadsheets. These data were subsequently checked by one of INSPIRE's senior scientists as an independent quality assurance/quality control review before final interpretation was performed. Spatial distributions of SPI and PV parameters were mapped using ESRI ArcGIS 10.5. Map backgrounds, unless otherwise indicated in the figure footnote, use ESRI Oceans regional hillshaded model accessed through the ArcGIS Online platform.

2.3.6.1 Sediment Profile Image Analysis Parameters

The parameters discussed below were assessed and/or measured and recorded for each replicate SPI image selected for analysis (Appendix D). Descriptive comments were also recorded for each. Many variables can be seen and annotated in context in SPI images from soft bottom coastal and estuarine environments (Figure 2-4).

Sediment Type–The sediment grain size major mode and range were estimated visually from the images using a grain size comparator at a similar scale. Results were reported using the phi scale. Conversion to other grain size scales is provided in Appendix F. The presence and thickness of disposed dredged material were also assessed as described below.

Penetration Depth–The depth to which the camera penetrated into the seafloor was measured to provide an indication of the sediment density and bearing capacity. The

penetration depth can range from a minimum of 0 cm (i.e., no penetration on hard substrata) to a maximum of 20 cm (full penetration on very soft substrata).

Surface Boundary Roughness–Surface boundary roughness is a measure of the vertical relief of features at the sediment–water interface in the sediment profile image. Surface boundary roughness was determined by measuring the vertical distance between the highest and lowest points of the sediment–water interface. The surface boundary roughness (sediment surface relief) measured over the width of sediment profile images typically ranges from 0 to 4 cm, and may be related to physical structures (e.g., ripples, rip-up structures, mud clasts) or biogenic features (e.g., burrow openings, fecal mounds, foraging depressions). Biogenic roughness typically changes seasonally and is related to the interaction of bottom turbulence and bioturbation activities.

Apparent Redox Potential Discontinuity (aRPD) Depth–The aRPD depth provides a measure of the integrated time history of the balance between near-surface oxygen conditions and biological reworking of sediments. Sediment particles exposed to oxygenated waters oxidize and lighten in color to brown or light gray. As the particles are buried or moved down by biological activity, they are exposed to reduced oxygen concentrations in subsurface pore waters and their oxic coating slowly reduces, changing color to dark gray or black. When biological activity is high, the aRPD depth increases; when it is low or absent, the aRPD depth decreases. The aRPD depth was measured by assessing color and reflectance boundaries within the images.

Mud Clasts – When fine-grained, cohesive sediments are disturbed, either by physical bottom scour or faunal activity (e.g., decapod foraging) intact clumps of sediment are often scattered across the seafloor. The number of clasts observed at the sediment–water interface was counted and their oxidation state assessed. The detection of reduced mud clasts in an obviously aerobic setting suggests a recent origin (Germano 1983). Mud clasts that are artifacts of SPI sampling (mud clots can fall off the back of the prism or wiper blade) are not recorded in the analysis sheet but may be noted in the "Comments" field.

Dredge Material Layer Depth and Thickness – The depth below the sediment–water interface that the top of dredge material layer occurred was measured. Additionally, the thickness of the dredged material layer, from 1 mm to 20 cm (the height of the SPI optical window) was measured. If the layer extended below the depth of prism penetration this was noted.

Biological Mixing – The depth to which sediments are bioturbated, or the biological mixing depth, can be an important parameter for studying nutrient or contaminant flux, as well as organic enrichment, in sediments. In this study, the minimum and maximum linear distances from the sediment surface to subsurface voids were measured. The latter parameter represents the maximum observed particle mixing depth of head-down feeders, mainly polychaetes. The number of subsurface voids were counted for each SPI replicate.

Infaunal Successional Stage – Infaunal successional stage is a measure of the biological community inhabiting the seafloor. Current theory holds that organism–sediment interactions in fine-grained sediments follow a predictable sequence of development after a major disturbance (e.g., dredged material disposal) (Pearson and Rosenberg 1978; Rhoads and Germano 1982; Rhoads and Boyer 1982). This continuum has been divided subjectively into four stages: Stage 0, indicative of a sediment column that is largely devoid of macrofauna, occurs immediately following a physical disturbance or in close proximity to an organic enrichment source; Stage 1 is the initial recolonizing tiny, densely populated polychaete assemblages; Stage 2 is the start of the transition to head-down deposit feeders; and Stage 3 is the mature, equilibrium community of deep-dwelling, head-down deposit feeders (Figure 2-5). Successional stage was assigned by assessing the types of species and related activities (e.g., feeding voids) apparent in the images. Biogenic particle mixing depths can be estimated by measuring the maximum and minimum depths of imaged fauna, burrows, or feeding voids in the sediment column.

Additional components of the SPI analysis included calculating the means and ranges for the quantitative parameters listed above and mapping of means of replicate values from each station. Station means were calculated from three replicates from each station and used in statistical analysis.

2.3.6.2 Plan View Image Analysis Parameters

The PV images provided a much larger field-of-view than the SPI images and provided valuable information about the landscape ecology and sediment topography in the area where the pinpoint “optical core” of the sediment profile was taken (Figure 2-6). Unusual surface sediment layers, textures, or structures detected in any of the sediment profile images can be interpreted within the larger context of surface sediment features, i.e., is a surface layer or topographic feature a regularly occurring feature and typical of the bottom in this general vicinity or just an isolated anomaly. The scale information provided by the underwater lasers allows for accurate density counts of attached epifaunal colonies,

sediment burrow openings, or larger macrofauna or fish which may have been missed in the sediment profile cross section. Information on sediment transport dynamics and bedform wavelength were also available from PV image analysis.

For each replicate PV image selected for analysis, analysts calculated the image size and field-of-view, and the following were recorded: sediment type; oxidation state of the surface sediment; presence and type of bedforms; presence of *Beggiatoa* and estimates of cover extent; dredged material presence; presence of burrows, tubes, tracks/trails, and debris; types of epifauna and flora; number of fish; and descriptive comments (Appendix E).

2.3.7 Data Quality Assurance and Quality Control

Measures were taken both during field data collection and during post-collection analysis for data quality assurance and control in alignment with the project QAPP (INSPIRE 2020a). These included but were not limited to:

- Systems were tested prior to and during survey activities to ensure calibration and operation,
- A full backup system (including tools, parts, and electronics) was carried in the field, and
- Image data collected was time stamped both digitally and in hand-written logs to ensure proper identification and synchronization with navigational data.

2.4 Statistical Analyses

One objective of the 2021 SPI/PV survey at IOSN was to assess the status of an active disposal area relative to reference area conditions. Statistical analyses were conducted to compare the following SPI variables: 1) aRPD depth and 2) successional stage. The aRPD depth and successional stage were compared because they are known to be key indicators of infaunal activity measured by SPI within soft sediment environments, such as those observed at IOSN. Standard boxplots were generated to provide a visual assessment of the central tendency and variability of these metrics within the sampled active disposal and reference areas. Tests evaluating the inequivalence, described in detail below, between the reference and active disposal area in 2021 were conducted.

Traditionally, the objective of this study would be addressed using point null hypotheses of the form “There is no difference in benthic conditions between the reference area and the disposal target areas.” However, in this instance, a bioequivalence or interval

testing approach was considered more informative than the point null hypothesis test of "no difference" (Germano 1999). One reason is that there is always some small difference between areas, and the statistical significance of this difference may or may not be ecologically meaningful. Without an associated power analysis, the results of traditional point null hypothesis testing often provide an inadequate ecological assessment.

In this application of bioequivalence (interval) testing the null hypothesis is chosen as one that presumes the difference is great, i.e., an inequivalence hypothesis (e.g., McBride 1999). This is recognized as a "proof of safety" approach because rejection of this inequivalence null hypothesis requires sufficient proof that the difference is actually small. The null and alternative hypotheses to be tested were:

$$H_0: \ d \leq -\delta \ \text{ or } \ d \geq \delta \text{ (presumes the difference is great)}$$

$$H_A: \ -\delta < d < \delta \text{ (requires proof that the difference is small)}$$

where d is the difference between a reference mean and a site mean. If the null hypothesis is rejected, then it can be concluded that the two means are equivalent to one another within $\pm\delta$ units. The size of δ should be determined from historical data and/or best professional judgment to identify a maximum difference that is within background variability/noise and is therefore not ecologically meaningful. Previously established δ values of 1 for aRPD, and 0.5 for successional stage rank on the 0–3 scale were used.

The test of this interval hypothesis can be broken down into two one-sided tests (TOST; McBride 1999 after Schuirmann 1987) which are based on the normal distribution, or on Student's *t*-distribution when sample sizes are small and variances must be estimated from the data (the typical case in the majority of environmental monitoring projects). The statistics used to test the interval hypotheses shown here are based on such statistical foundations as the Central Limit Theorem (CLT) and basic statistical properties of random variables. A simplification of the CLT states that the mean of any random variable is normally distributed. Linear combinations of normal random variables are also normal, so a linear function of means is also normally distributed. When a linear function of means is divided by its standard error the ratio follows a *t*-distribution with degrees of freedom associated with the variance estimate. Hence, the *t*-distribution can be used to construct a confidence interval around any linear function of means.

In the sampling design for the 2021 survey, four distinct areas were sampled: three of which were categorized as reference areas (REF-A, REF-B, REF-C) and one active disposal location within the disposal site. The difference equation of interest was the linear contrast of the average of the reference means minus the active disposal area mean, or

$$\hat{d} = [1/3 \text{ x } (\text{Mean}_{\text{REF-A}} + \text{Mean}_{\text{REF-B}} + \text{Mean}_{\text{REF-C}}) - (\text{Mean}_{\text{Active}})] \qquad \text{[Eq. 1]}$$

where $\text{Mean}_{\text{Active}}$ was the mean for the active disposal area.

The three reference areas collectively represented ambient conditions, but if the means were different among these three areas, then pooling them into a single reference group would inflate the variance estimate. Inflation would occur because it would include the variability between areas, rather than only the variability between stations within a single homogeneous area. The effect of keeping the three reference areas separate [Eq. 1] had no effect on the grand reference mean when sample size was equal among these areas, and it ensured that the variance was truly the residual variance within a single population, with a constant mean.

The standard error of each difference equation was calculated from the fact that the variance of a sum is the sum of the variances for independent variables, or

$$se(\hat{d}) = \sqrt{\sum_j \left(S_j^2 c_j^2 / n_j \right)} \qquad \text{[Eq. 2]}$$

Where:

$se(\hat{d})$ standard error of the difference equation

$\hat{d}$ observed difference in means between the reference areas and the disposal area

c_j coefficients for the j means in the difference equation, $\hat{d}$ (i.e., for [Eq. 1] shown above, the coefficients were 1/3 for each of the three reference locations, and -1 for the disposal area.

S_j^2 variance for the j^{th} area. If we can assume equal variances, a single pooled residual variance estimate can be substituted for each group, equal to the mean square error from an ANOVA.

n_j number of stations for the j^{th} area

The inequivalence null hypothesis was rejected (and equivalence was concluded) if the confidence interval on the difference of means, $\hat{d}$, was fully contained within the interval [–δ, +δ].

Thus, the decision rule was to reject H_0 if

$$D_L = \hat{d} - t_{\alpha,\upsilon} se(\hat{d}) > -\delta \qquad \text{and} \qquad D_U = \hat{d} + t_{\alpha,\upsilon} se(\hat{d}) < \delta \qquad \text{[Eq. 3]}$$

where:

$t_{\alpha,\upsilon}$ upper (1-α)*100$_{th}$ percentile of a Student's t-distribution with υ degrees of freedom (α = 0.05)

$se(\hat{d})$ standard error of the difference ([Eq. 2])

υ degrees of freedom for the standard error. If a pooled residual variance estimate was used, it was the residual degrees of freedom from an ANOVA on all groups (total number of samples minus the number of groups); if separate variance estimates were used, degrees of freedom were calculated based on the Welch-Satterthwaite estimation (Satterthwaite 1946).

Validity of the normality and equal variance assumptions was tested using Shapiro-Wilk's test for normality on the area residuals (α=0.05) and Levene's test for equality of variances among the four areas (α =0.05). If normality was not rejected but equality of variances was, then the variance for the difference equation was based on separate variances for each group. If systematic deviations from normality were identified, then a nonparametric bootstrapped interval was used. Bootstrapping methodology is outlined in Appendix G.

Table 2-1.

IOSN 2021 Survey Target SPI/PV Station Locations

Station ID	Latitude (NAD 1983)	Longitude (NAD 1983)	X (NAD 83 State Plane ME West meters)	Y (NAD 83 State Plane ME West meters)
REF-C-01	43.03889	-70.420752	879295.3995	22866.11601
REF-C-02	43.037207	-70.420745	879295.3995	22679.24101
REF-C-03	43.037663	-70.417613	879550.7952	22729.07441
REF-B-04	43.00547	-70.467067	875508.0668	19165.99171
REF-B-05	43.004913	-70.465689	875620.1918	19103.70011
REF-B-06	43.004285	-70.469659	875296.2752	19035.17921
REF-A-07	42.986861	-70.464303	875726.0876	17097.90881
REF-A-08	42.988258	-70.466066	875582.8168	17253.63791
REF-A-09	42.988319	-70.464234	875732.3168	17259.86711
IOSN-10	43.011933	-70.451333	876793.3237	19879.53951
IOSN-11	43.012766	-70.450214	876884.8164	19971.76151
IOSN-12	43.012652	-70.451621	876770.048	19959.42471
IOSN-13	43.010979	-70.450899	876828.283	19773.47671
IOSN-14	43.011441	-70.449281	876960.3564	19824.32791
IOSN-15	43.014361	-70.45496	876498.5041	20150.19991
IOSN-16	43.019261	-70.446119	877221.0873	20692.13731
IOSN-17	43.019224	-70.46268	875871.1458	20692.66171
IOSN-18	43.024116	-70.451439	876789.2681	21232.90801
IOSN-19	43.010046	-70.454158	876562.2621	19670.72551
IOSN-20	43.025559	-70.438504	877844.0039	21389.80381
IOSN-21	43.008383	-70.446715	877168.4873	19483.86661
IOSN-22	43.022581	-70.441319	877613.5248	21059.65801
IOSN-23	43.013124	-70.447978	877067.2367	20010.91071
IOSN-24	43.02697	-70.457618	876286.7125	21551.76211

3.0 RESULTS

In October 2021, an acoustic survey was conducted over the southern central portion of IOSN, and SPI/PV imagery was collected throughout IOSN and within the three reference areas. The survey objectives were to characterize the seafloor topography and surficial features of the active portion of the site and to assess the benthic recolonization status of the active portion of the site in comparison to the reference areas. The results from these surveys are presented below.

3.1 Acoustic Survey

3.1.1 Bathymetry

The 2021 multibeam bathymetric data were rendered as an acoustic relief model to provide a detailed representation of the survey area surface (Figure 3-1). The 2021 bathymetry of the southern central portion of IOSN revealed a relatively flat surface with a gentle slope from approximately 93 m deep along the western boundary to approximately 95 m deep along the eastern boundary. The mean depth across the survey area was 94.4 m. A slightly elevated area was visible in the central portion of the survey area. This central feature was approximately 94.0 m in depth and rose slightly above the ambient gentle seafloor slope.

3.1.2 Acoustic Backscatter and Side-Scan Sonar

Acoustic backscatter data provides a relative estimate of surface sediment texture (hard, soft, rough, and smooth). Stronger backscatter returns are indicative of coarser-grained, rougher, or harder sediment relative to surrounding sediments and weaker backscatter returns are indicative of finer-grained, smoother, or softer sediment relative to surrounding sediments.

The unfiltered backscatter data collected over the active portion of IOSN displayed a distinct area where a disposal footprint is evident as an area of stronger acoustic return in the central portion of the survey extent (Figure 3-2). Filtered backscatter highlighted an area of stronger backscatter returns (shown in red and yellow) within the central portion of the survey area, which varied from the ambient seafloor that was characterized by weaker backscatter returns (shown in blue; Figure 3-3). Apparent within the backscatter contours is the spread of material coarser than the ambient sediment (silt) at the dredged material

disposal location. It is apparent that dredged material (fine sand) spread approximately 600 m in diameter around the central disposal target area in a radial direction. The toe of the rock ledge in the southeast corner of the survey area also displays a stronger backscatter return than the ambient seafloor.

Side-scan sonar data are higher resolution and more responsive to minor surface textural features and slope than backscatter results and can reveal additional information about topographic and textural properties of the seafloor. Side-scan sonar imagery displayed the same distinct footprint within the central portion of the site (Figure 3-4). The toe of the rock ledge in the southeast corner of the site is also apparent within the side scan sonar imagery.

3.1.3 Comparison with Previous Bathymetry

The 2021 bathymetric data were quantitatively compared to 2015 bathymetric data to assess elevation change between the two surveys (Figure 3-5). Bottom depths measured during the 2015 survey were subtracted from those measured during the 2021 survey to obtain an elevation change map of each survey point throughout the combined study area. Positive values (represented as shades of yellow and green on the elevation change map) computed between surveys indicated an increase in elevation (i.e., sediment accumulation). Negative elevation change (represented in shades of blue and purple) computed between surveys indicated areas where elevation decreased (i.e., compaction, redistribution, smoothing).

Results of the depth differencing calculations displayed an area within the central portion of the survey extent where dredged material created a feature approximately 325 m in diameter rising to a maximum height of 0.7 m above the surrounding seafloor (Figure 3-5).

3.2 Fishing Gear Observations

The fishing gear observations resulted in identification of five fishing surface marker buoys (buoys). One buoy was located within the active survey area, three buoys were located within IOSN but outside of the active survey area, and one buoy was located just outside of the southern boundary of IOSN (Figure 3-6).

3.3 Sediment Profile and Plan View Imaging

The primary purpose of the SPI/PV survey at IOSN was to assess the status of benthic colonization in the active disposal area after initial dredged material placement. SPI/PV images collected within the active portion of the site were compared those of the three reference areas. SPI/PV images were also collected and analyzed from the baseline portion of IOSN and are described within this section to provide additional information on the baseline conditions within the site (Figure 3-7). Station summaries of selected physical and biological parameters from the SPI/PV images can be found in Tables 3-1 through 3-6; and a complete set of SPI/PV results are provided in Appendices D and E.

3.3.1 Reference Area Stations

A total of nine SPI/PV stations were sampled across the three references areas (REF-A, REF-B, and REF-C) during the October 2021 survey. Paired SPI and PV image collection occurred at all stations, and images were analyzed in triplicate. The data collected within the reference areas is intended to provide a representative comparison of baseline sediment conditions to the active disposal site.

3.3.1.1 Physical Sediment Characteristics

Measured water depths at the reference area stations ranged from a minimum of 84.4 m at REF-B-05 to 98.8 m at REF-A-08 and averaged 95.9 m for all reference stations (Table 3-1). Sediment grain size major mode at all reference area stations was consistently classified as silt/clay (Figure 3-8). Camera prism penetration depth ranged from 8.6 cm at REF-C-03 to 17.7 cm at REF-A-09 (Table 3-1; Figures 3-9 and 3-10). Intermediate penetration values were observed at REF-B. At REF-C, a clay deposit layer was observed at depth likely resulting in relatively shallow penetration camera depth at REF-C (Table 3-1; Figure 3-11). The clay-like material was observed at all stations within REF-C at depth and, in some instances, on the surface as clay clasts (Table 3-1; Figure 3-11).

Boundary roughness values across the reference areas ranged from a station average of 0.9 cm at REF-C-02 and REF-C-03 to 3.0 cm at REF-A-09, with an overall reference area mean of 1.6 cm (Table 3-1; Figure 3-12). The small-scale topographic variability can be attributed to biological processes and features such as small burrow openings, pits, mounds, etc., formed as a result of surface and subsurface benthic activity. Selected images from REF-B-05 and REF-C-09 display a large pit at the sediment–water interface and a mound formation at the surface, both from biological activity, respectively (Table 3-1; Figure 3-13).

3.3.1.2 Biological Conditions

The three reference areas displayed similar biological characteristics, consistent with the uniform physical characteristics that were observed. Surface sediment tracks were most abundant at REF-A, and burrows were observed most consistently at REF-B. Surface tubes were more abundant at Reference Areas A and B, however, were still present at REF-C. Shrimp were observed at all reference areas (Table 3-2; Figure 3-14).

The average aRPD depth at the reference areas was 3.2 cm, a maximum value of 4.0 cm was observed at REF-A-08, and a minimum value of 2.6 cm was observed at REF-C-03 (Table 3-2; Figures 3-15 and 3-16). No observation of low oxygen, methane, and/or *Beggiatoa* mats was recorded at any of the reference stations.

Evidence of mature, deposit-feeding (Stage 3) assemblages was observed at all reference stations, recorded as subsurface feeding voids, large burrows, and deep borrowing polychaetes (Figure 3-17). Stage 1 on 3 communities were most frequently observed at Reference Areas A and B, which displayed deep burrowing polychaetes and/or subsurface feeding voids paired with tubes at the sediment–water interface. Successional stage variation was noted at REF-C where all stations and replicates were characterized as Stage 2 on 3 (Table 3-2; Figure 3-17). The presence of Stage 3 fauna within the sediment profile images was also supported by the plan view images which displayed tubes, burrow openings, shrimp, and tracks (Figure 3-14).

3.3.2 IOSN Baseline Stations

SPI/PV images were collected at six stations located in the northern portion of IOSN where dredged material has not yet been placed and are considered representative of baseline conditions (Figure 3-7).

3.3.2.1 Physical Sediment Characteristics

Measured water depths at the IOSN baseline area SPI/PV stations ranged from 96.3 m at IOSN-17 to 99.4 m at IOSN-22, and average depth within the baseline area was 97.9 m. Sediment grain size at the baseline area was homogeneous and classified as silt/clay at all stations sampled (Figure 3-8). Camera penetration depths at the baseline area ranged from 13.8 cm at IOSN-20 to 16.9 cm at IOSN-17 and averaged 15.6 cm (Table 3-3; Figure 3-9).

Boundary roughness values within the baseline area of the site ranged from 0.7 cm at IOSN-16 to 1.7 cm at IOSN-20, with an average of 1.2 cm for the baseline area. Similar to

the reference area stations, boundary roughness within the baseline area of the site can be attributed to biological processes such as burrow openings, pits, mounds, etc. (Table 3-3; Figure 3-12).

3.3.2.2 Biological Conditions

Tubes, tracks, and burrows were observed at all locations within the baseline portion of the site. Shrimp were observed in images from all locations except for IOSN-16 and IOSN-24. No indication of low dissolved oxygen, methane, or *Beggiatoa* was observed during the survey.

The average aRPD depth at the baseline area was 3.5 cm, ranging from 2.3 cm at IOSN-22 to 4.7 cm at IOSN-16 (Table 3-4; Figure 3-15). Stage 1 on 3 was the most frequently observed classification among replicates at the baseline area (Figure 3-17). Sediment profile images from the baseline area of the site displayed benthic community characteristics that were similar to the reference areas, including the presence of deep feeding voids and surficial tubes at the sediment–water interface (Table 3-4; Figure 3-18).

3.3.3 IOSN Active Site Stations

A total of nine SPI/PV stations were sampled within the active disposal area. Five stations, IOSN-10 through IOSN-14, were sampled within the disposal target area; an area within the site that had directly received dredged material. Dredged material thickness over this area ranged from 11.0 to 8.7 cm. One location, IOSN-23, was sampled within the active disposal area where dredged material settled or had thinly spread after placement. Dredged material thickness at this location measured 10.1 cm. Three locations, IOSN-15, IOSN-19, and IOSN-21, were classified as being located within the active disposal area but were in limited contact with recently placed dredged material. These stations were classified as no dredged material present (Figure 3-19).

3.3.3.1 Physical Sediment Characteristics

Measured water depths at the SPI/PV stations at the IOSN active disposal area ranged from 96.9 m at IOSN-19 to 100 m at IOSN-23 (Table 3-5). Sediment grain size major mode over the area of the disposal site that recently received dredged material was classified as very fine sand, with one station (IOSN-12) characterized by very fine sand over fine sand (Figure 3-8). Grain size at IOSN-23, where dredged material was thinly spread, was classified as very fine sand over silt/clay. Grain size at IOSN-19 was similarly classified as

very fine sand over silt/clay; however, dredged material was not observed at this station (Figures 3-8 and 3-19). Stations IOSN-15 and IOSN-21 are located furthest from the active disposal area and were classified as silt/clay, displaying similar grain size characteristics to the baseline and reference areas; dredged material was not observed at these stations (Table 3-5; Figures 3-8 and 3-20).

Camera penetration depths within the active site ranged from 8.4 cm at IOSN-12, which is located in an area where measured dredged material thickness was greatest, to 15.9 cm at IOSN-15, which is in the area of limited dredged material contact (Figure 3-9). Dredged material was present at IOSN-10 numerically through IOSN-14 and at IOSN-23, which were all located within the dredged material disposal footprint. Dredged material measurement depths and penetration depths extended to the bottom of the SPI at stations IOSN-10 numerically through IOSN-14, indicating that dredged material thickness may not have been fully measured to depth due to penetration limitations (Table 3-5; Figure 3-19). IOSN-23 had the greatest penetration depth of all stations where dredged material was present and was the only station where penetration was greater than the dredged material measurement depth, displaying the native silt/clay below the dredged material. As previously mentioned, dredged material was not observed at IOSN-15, 19, and 21.

Boundary roughness ranged from 0.7 cm at IOSN-11 to 2.2 cm at IOSN-12, with both stations located in the area where measured dredged material thickness was greatest. Mean boundary roughness within the active disposal area was 1.4 cm (Table 3-5; Figure 3-12). Boundary roughness within the site was the result of biological processes such as burrows and foraging depressions.

3.3.3.2 Biological Conditions and Benthic Recolonization

Mean station aRPD depths within the active disposal area of IOSN ranged from a minimum of 1.5 cm at IOSN-23 to a maximum of 4.2 cm at IOSN-15. The mean aRPD for the survey area was 2.4 cm (Table 3-6; Figure 3-15). Overall aRPD depths within the active disposal area of IOSN were lower than those observed within the reference and baseline areas, which averaged 3.2 and 3.5 cm, respectively.

Tubes, tracks, and burrows were present at most stations within the active disposal area and epifauna such as shrimp and hermit crabs were observed at all stations within the active disposal area. Low dissolved oxygen, methane, and *Beggiatoa* were not observed.

Successional stage was variable within the active disposal area; IOSN-10 through IOSN-14 were in areas of thicker dredged material and were observed to have Stage 2 fauna within all station replicates. Feeding voids were not observed at IOSN-10 or IOSN-14. Stations IOSN-11 and IOSN-12 were classified as Stage 2 for two replicates and Stage 2 on 3 for one replicate each. Feeding voids were observed at IOSN-11; however, burrows were not present. Surface tubes were abundant for IOSN-12 and present at IOSN-11, and surface tracks were abundant at both stations (Figure 3-21). Stations that were located on the dredged material apron (i.e., area of thin dredged material spread) (IOSN-19 and IOSN-23) were classified predominately as Stage 2 on 3, with Stage 2 tubes at the surface and polychaetes and subsurface voids at depth. The two stations farthest from the active disposal area displayed similar characteristics to the baseline portion of the site, resulting in Stage 1 on 3 fauna at all stations, displaying deep burrowing polychaetes and/or subsurface voids paired with feeding tubes at the sediment–water interface (Table 3-6; Figures 3-17 and 3-21).

3.3.4 Statistical Comparisons

Statistical comparisons between IOSN and the reference areas were conducted on two variables; aRPD depth and successional stage ranking, which can provide a quantifiable metric for the health of a benthic community. Statistical analysis was conducted using the methods described in Section 2.4.

3.3.4.1 aRPD Depth Comparisons

Area mean aRPD depth at the active disposal area was 2.4 cm, lower than the grand mean of the reference areas (3.2 cm; Table 3-7; Figure 3-22). The active disposal area had more variability in aRPD depth compared to the reference areas (standard deviation of 0.8 and 0.5, respectively).

A statistical inequivalence test was performed to determine whether the differences observed in mean aRPD values between the grand mean of the three reference areas and the active disposal area were significantly similar. The station mean aRPD data from the two groups (reference areas and active disposal area) were combined to assess normality and estimate pooled variance. Results for the normality test indicated that each area's residuals, i.e., each observation minus the area mean, were not significantly different from a normal distribution (Shapiro-Wilk's test p-value = 0.16). Levene's test for equality of variances was not rejected ($p = 0.49$), so a single pooled variance estimate could be used for all groups. The confidence interval for the difference equations was constructed using parametric estimates.

The confidence region for the difference in means between reference areas (3.2 cm) and the active disposal area (2.4 cm) was not contained within the interval [-1 cm, +1 cm] (Table 3-7). The conclusion was that the aRPD depths at the active disposal area were not equivalent to the pooled reference area aRPD depths. The mean aRPD depth at the active disposal area was significantly shallower than the mean reference area aRPD depth.

3.3.4.2 Successional Stage Comparisons

To evaluate successional stages numerically, a successional stage rank variable was applied to each image. A value of 3 was assigned to Stages 3, 2 on 3, and 1 on 3 designations, a value of 2 was applied to Stage 2, and images from which the stage could not be determined were excluded from calculations. The maximum successional stage rank among replicates was used to represent the station value.

Results for the normality test indicated that mean successional stage ranks were significantly different from a normal distribution (Shapiro-Wilk's test p-value <0.001). Therefore, the confidence interval for the difference equations was constructed using non-parametric bootstrapped estimates between the mean successional stage at the active disposal area versus the pooled reference areas. The confidence interval for the difference between the mean maximum successional stage rank of the pooled reference areas (3.0) versus the disposal area (2.7) was contained within the interval [-0.5, +0.5] (Table 3-8). The conclusion was that the mean maximum successional stage rank at the active disposal area was statistically equivalent to that of the pooled reference areas.

Table 3-1.

Summary of IOSN Reference Area Sediment Profile and Plan View Imaging Physical Results, October 2021

Station ID	SPI Replicate (n)	Water Depth (m)	Mean Prism Penetration Depth (cm)	Mean Boundary Roughness (cm)	SPI Predominant Sediment Type	SPI Dredged Material Presence	Mean Dredged Material Thickness (cm)	Buried Dredged Material Presence	Mean Dredged Material Depth (cm)
REF-C-01	3	96.6	9.8	1.0	Silt/clay	No	N/A	N/A	N/A
REF-C-02	3	97.2	10.1	0.9	Silt/clay	No	N/A	N/A	N/A
REF-C-03	3	97.2	8.6	0.9	Silt/clay	No	N/A	N/A	N/A
REF-B-04	3	97.5	14.8	1.5	Silt/clay	No	N/A	N/A	N/A
REF-B-05	3	84.4	12.8	2.0	Silt/clay	No	N/A	N/A	N/A
REF-B-06	3	95.4	14.4	1.0	Silt/clay	No	N/A	N/A	N/A
REF-A-07	3	97.8	17.4	2.4	Silt/clay	No	N/A	N/A	N/A
REF-A-08	3	98.8	16.2	2.0	Silt/clay	No	N/A	N/A	N/A
REF-A-09	3	98.5	17.7	3.0	Silt/clay	No	N/A	N/A	N/A
	n = 9								
	Max	98.8	17.7	3.0					
	Min	84.4	8.6	0.9					
	Mean	95.9	13.5	1.6					
	Standard Deviation	4.4	3.4	0.8					

N/A=Not Applicable

Table 3-2.

Summary of IOSN Reference Area Sediment Profile and Plan View Imaging Biological Results, October 2021

Station ID	SPI Replicate (n)	Mean aRPD Depth (cm)	Mean Maximum Bioturbation Depth (cm)	Presence of Methane	Presence of Low Dissolved Oxygen	Void Presence	Successional Stage (by replicate)[1]			PV Replicate (n)	*Beggiatoa* Presence	Burrow Abundance	Track Abundance	Tube Abundance	Epifauna Present
REF-C-01	3	3.0	8.8	No	No	Yes	2 on 3	2 on 3	2 on 3	3	No	Sparse (<10%)	Present (10-25%)	Present (10-25%)	Shrimp
REF-C-02	3	2.8	9.5	No	No	Yes	2 on 3	2 on 3	2 on 3	3	No	Sparse (<10%)	Abundant (25-75%)	Present (10-25%)	Shrimp
REF-C-03	3	2.6	8.5	No	No	Yes	2 on 3	2 on 3	2 on 3	3	No	Sparse (<10%)	Present (10-25%)	Present (10-25%)	Crab, Hydroids, Shrimp
REF-B-04	3	3.0	13.1	No	No	Yes	1 on 3	1 on 3	1 on 3	3	No	Present (10-25%)	Abundant (25-75%)	Abundant (25-75%)	Shrimp
REF-B-05	3	3.1	12.0	No	No	Yes	1 on 3	1 on 3	1 on 3	3	No	Present (10-25%)	Abundant (25-75%)	Present (10-25%)	Shrimp
REF-B-06	3	3.3	13.6	No	No	Yes	1 on 3	1 on 3	1 on 3	3	No	Sparse (<10%)	Present (10-25%)	Present (10-25%)	Shrimp
REF-A-07	3	3.6	16.1	No	No	Yes	1 on 3	1 on 3	2 on 3	3	No	Present (10-25%)	Abundant (25-75%)	Present (10-25%)	Shrimp
REF-A-08	3	4.0	14.6	No	No	Yes	1 on 3	1 on 3	2 on 3	3	No	Sparse (<10%)	Abundant (25-75%)	Abundant (25-75%)	Shrimp
REF-A-09	3	3.9	17.0	No	No	Yes	1 on 3	1 on 3	1 on 3	3	No	Sparse (<10%)	Abundant (25-75%)	Present (10-25%)	Shrimp
	n = 9														
	Max	4.0	17.0												
	Min	2.6	8.5												
	Mean	3.2	12.6												
	Standard Deviation	0.5	3.1												

[1]Successional Stage: “on” indicates one Stage is found on top of another Stage (i.e., 1 on 3).

Table 3-3.

Summary of IOSN Baseline Site Sediment Profile and Plan View Imaging Physical Results, October 2021

Station ID	SPI Replicate (n)	Water Depth (m)	Mean Prism Penetration Depth (cm)	Mean Boundary Roughness (cm)	SPI Predominant Sediment Type	SPI Dredged Material Presence	Mean Dredged Material Thickness (cm)	Buried Dredged Material Presence	Mean Dredged Material Depth (cm)
IOSN-16	3	98.5	16.5	0.7	Silt/clay	No	N/A	N/A	N/A
IOSN-17	3	96.3	16.9	1.2	Silt/clay	No	N/A	N/A	N/A
IOSN-18	3	97.5	15.9	1.5	Silt/clay	No	N/A	N/A	N/A
IOSN-20	3	99.1	13.8	1.7	Silt/clay	No	N/A	N/A	N/A
IOSN-22	3	99.4	14.5	0.9	Silt/clay	No	N/A	N/A	N/A
IOSN-24	3	96.9	16.3	1.2	Silt/clay	No	N/A	N/A	N/A
	n = 6								
	Max	99.4	16.9	1.7					
	Min	96.3	13.8	0.7					
	Mean	97.9	15.6	1.2					
	Standard Deviation	1.2	1.3	0.4					

N/A=Not Applicable

Table 3-4.

Summary of IOSN Baseline Site Sediment Profile and Plan View Imaging Biological Results, October 2021

Station ID	SPI Replicate (n)	Mean aRPD Depth (cm)	Mean Maximum Bioturbation Depth (cm)	Presence of Methane	Presence of Low Dissolved Oxygen	Void Presence	Successional Stage (by replicate)[1]			PV Replicate (n)	*Beggiatoa* Presence	Burrow Abundance	Track Abundance	Tube Abundance	Epifauna Present
IOSN-16	3	4.7	15.8	No	No	Yes	1 on 3	1 on 3	1 on 3	3	No	Present (10-25%)	Abundant (25-75%)	Abundant (25-75%)	None
IOSN-17	3	4.4	16.4	No	No	Yes	1 on 3	1 on 3	1 on 3	3	No	Present (10-25%)	Present (10-25%)	Sparse (<10%)	Shrimp
IOSN-18	3	3.9	15.8	No	No	Yes	1 on 3	1 on 3	1 on 3	3	No	Sparse (<10%)	Present (10-25%)	Present (10-25%)	Shrimp
IOSN-20	3	3.4	13.1	No	No	Yes	1 on 3	1 on 3	2 on 3	3	No	Sparse (<10%)	Sparse (<10%)	Abundant (25-75%)	Shrimp
IOSN-22	3	2.3	12.3	No	No	Yes	1 on 3	1 on 3	1 on 3	3	No	Sparse (<10%)	Present (10-25%)	Present (10-25%)	Shrimp
IOSN-24	3	2.5	13.5	No	No	Yes	1 on 3	2 on 3	2 on 3	3	No	Present (10-25%)	Present (10-25%)	Present (10-25%)	None
n = 6															
Max		4.7	16.4												
Min		2.3	12.3												
Mean		3.5	14.5												
Standard Deviation		1.0	1.7												

[1]Successional Stage: "on" indicates one Stage is found on top of another Stage (i.e., 1 on 3).

Table 3-5.

Summary of IOSN Active Site Sediment Profile and Plan View Imaging Physical Results, October 2021

Station ID	SPI Replicate (n)	Water Depth (m)	Mean Prism Penetration Depth (cm)	Mean Boundary Roughness (cm)	SPI Predominant Sediment Type	SPI Dredged Material Presence	Mean Dredged Material Thickness (cm)	Dredged Material > Penetration	Buried Dredged Material Presence	Mean Dredged Material Depth (cm)
IOSN-10	3	99.4	8.8	1.2	Very fine sand	Yes	8.8	Yes	No	0.0
IOSN-11	3	99.4	11.1	0.7	Very fine sand	Yes	11.1	Yes	No	0.0
IOSN-12	3	99.4	8.4	2.2	Very fine sand over fine sand	Yes	8.4	Yes	No	0.0
IOSN-13	3	99.7	11.0	1.7	Very fine sand	Yes	11.0	Yes	No	0.0
IOSN-14	3	99.1	10.2	0.8	Very fine sand	Yes	10.2	Yes	No	0.0
IOSN-15	3	98.8	15.9	1.4	Silt/clay	No	N/A	No	N/A	N/A
IOSN-19	3	96.9	13.5	1.6	Very fine sand over silt/clay	No	N/A	No	N/A	N/A
IOSN-21	3	97.5	14.3	1.0	Silt/clay	No	N/A	No	N/A	N/A
IOSN-23	3	100.0	13.4	1.6	Very fine sand over silt/clay	Yes	10.1	No	No	0.0
n = 9										
Max		100.0	15.9	2.2			11.1			0.0
Min		96.9	8.4	0.7			8.4			0.0
Mean		98.9	11.8	1.4			9.9			0.0
Standard Deviation		1.0	2.6	0.5			1.1			0.0

N/A=Not Applicable

Table 3-6.

Summary of IOSN Active Site Sediment Profile and Plan View Imaging Biological Results, October 2021

Station ID	SPI Replicate (n)	Mean aRPD Depth (cm)	Mean Maximum Bioturbation Depth (cm)	Presence of Methane	Presence of Low Dissolved Oxygen	Void Presence	Successional Stage (by replicate)[1]			PV Replicate (n)	*Beggiatoa* Presence	Burrow Abundance	Track Abundance	Tube Abundance	Epifauna Present
IOSN-10	3	2.8	7.1	No	No	No	2	2	2	3	No	Present (10-25%)	Present (10-25%)	Present (10-25%)	Gastropod, Hermit Crab
IOSN-11	3	2.1	7.0	No	No	Yes	2	2	2 on 3	3	No	None	Abundant (25-75%)	Abundant (25-75%)	Hermit Crab, Shrimp
IOSN-12	3	1.8	6.8	No	No	No	2	2	2 on 3	3	No	Sparse (<10%)	Abundant (25-75%)	Present (10-25%)	Gastropod, Shrimp
IOSN-13	3	2.6	8.3	No	No	Yes	2	2 on 3	2 on 3	3	No	Sparse (<10%)	Present (10-25%)	Present (10-25%)	Shrimp
IOSN-14	3	2.0	8.1	No	No	No	2	2	2	3	No	Sparse (<10%)	Abundant (25-75%)	Present (10-25%)	Shrimp
IOSN-15	3	4.2	11.5	No	No	Yes	1 on 3	1 on 3	2 on 3	3	No	Sparse (<10%)	Present (10-25%)	Present (10-25%)	None
IOSN-19	3	2.4	13.1	No	No	Yes	2 on 3	2 on 3	2 on 3	3	No	Sparse (<10%)	Abundant (25-75%)	Abundant (25-75%)	Shrimp
IOSN-21	3	2.5	14.4	No	No	Yes	1 on 3	1 on 3	1 on 3	2	No	Sparse (<10%)	Present (10-25%)	Present (10-25%)	Shrimp
IOSN-23	3	1.5	12.0	No	No	Yes	2	2 on 3	2 on 3	3	No	Present (10-25%)	Abundant (25-75%)	Abundant (25-75%)	Shrimp
n = 9															
Max		4.2	14.4												
Min		1.5	6.8												
Mean		2.4	9.8												
Standard Deviation		0.8	2.9												

[1]Successional Stage: "on" indicates one Stage is found on top of another Stage (i.e., 1 on 3)

Table 3-7.

Summary Statistics and Results of Inequivalence Hypothesis Testing for aRPD Values

Difference Equation	Observed Difference ($\hat{d}$)	SE $\hat{d}$	*df* for SE	Confidence Bounds (D_L to D_U)[1]	Results[2]	n (REF)	n (Active)
$Mean_{REF} - Mean_{Active}$	0.82	0.30	16	0.29 to 1.35	d	9	9

1 DL and DU as defined in [Eq. 3]
2 s = Reject the null hypothesis of inequivalence: the two group means are significantly equivalent, within ± 1 cm.
d = Fail to reject the null hypothesis of inequivalence: the two group means are different.

Table 3-8.

Summary Statistics and Results of Inequivalence Hypothesis Testing for Successional Stage Values

Difference Equation	Observed Difference ($\hat{d}$)	SE $\hat{d}$	Number of Bootstrap Replicates	Confidence Bounds (D_L to D_U)[1]	Results[2]	n (REF)	n (Active)
$Mean_{REF} - Mean_{Active}$	0.22	0.14	1000	0.09 to 0.40	s	9	9

1 DL and DU as defined in [Eq. 3]

2 s = Reject the null hypothesis of inequivalence: the two group means are significantly equivalent, within ± 1 cm.
d = Fail to reject the null hypothesis of inequivalence: the two group means are different.

4.0 DISCUSSION

The objective of the 2021 monitoring effort was to conduct a confirmatory survey over the active area of IOSN, the baseline portion of the site, and reference areas. A multibeam acoustic survey was conducted over the area of IOSN that most recently received approximately 46,000 m³ of dredged material from two dredging projects in Rye, NH. SPI/PV images were collected at the active portion of the site, at the three reference areas, and at a baseline portion of the site that had never received dredged material at the time of the survey.

4.1 Dredged Material Distribution and Seafloor Topography

The acoustic survey displayed a relatively flat area within the site with a moderate elevation increase where dredged material had recently been placed. Placement of dredged material occurred within the planned target disposal area. A depth difference comparison using the 2015 acoustic survey data revealed a low-relief mound that displayed a maximum elevation change of 0.7 m over the area with the greatest sediment accumulation. This increase in elevation since 2015 spatially coincided with the area of higher acoustic returns in the backscatter and side-scan sonar data. Although, the acoustic data displayed areas where a thinner layer of recent dredged material was likely deposited that was outside the range of uncertainty (-0.4 to 0.1 m) of the depth difference model (Figures 3-3, 3-4, and 3-5).

The 2015 filtered backscatter dataset revealed a seafloor that was homogeneous in texture over the targeted disposal area, whereas the 2021 backscatter data displayed a distinct footprint of coarser material that covered a 600 m diameter footprint on the seafloor (Figure 4-1). This deposit was also visible within the side-scan sonar data. Also apparent within the side-scan sonar data is the toe of the rock ledge where a distinct texture that differs from the ambient seafloor and the recent disposal material is visible. The thin spread of material was anticipated and is consistent with the distribution of dredged material observed at other disposal sites (e.g., the Massachusetts Bay Disposal Site).

4.2 Benthic Recolonization and Community Composition

The objective of the IOSN SPI/PV survey was to determine the biological recovery timeline of the newly designated site by assessing the current status of benthic recolonization within the active disposal site compared to the three reference areas. Collection of these data provide a useful reference for future surveys by determining how quickly and effectively the

new site responds to material placement. The 2021 SPI survey was conducted less than one year from placement activity at the site. Despite this short timeframe from the physical disturbance, the biological community displayed signs of recovery.

The measured aRPD depths within the IOSN active disposal area were significantly lower than aRPD depths at the three reference areas. The shallower aRPD depths within the active disposal area may indicate that additional time is necessary for the biological community to fully rework surface sediments after dredged material placement has occurred. However, the maximum infaunal successional stage within the active disposal area was statistically similar to the reference areas. The reduced aRPD depth paired with the statistically equivalent successional stage may indicate that there is reduced activity among deep burrowing infauna working to deepen the aRPD depth. It is assumed that over time as deep burrowing organisms fully colonize the site the aRPD depths will become statistically equivalent to the reference area depths. The observed habitat conditions within the active portion of the site were consistent with the recovery expectations based on the successional stage model.

The baseline area of IOSN provides a useful measure of conditions prior to dredged material placement within the northern portion of the site. SPI/PV data displayed uniform characteristics between the baseline area stations and the reference area stations for sediment type, aRPD depth, and successional stage.

4.3 Reference Area C Applicability

IOSN is a newly designated disposal site and the survey conducted in 2021 was the first time that the REF-A, REF-B, and REF-C served as reference areas to assess benthic recovery at IOSN. The three reference areas, two located to the south of IOSN (REF-A and REF-B) and one located to the north (REF-C) were observed to have similar grain size characteristics to the baseline IOSN site (silt/clay). Reference area C was different from the other reference areas and IOSN because a clay layer was observed below the sediment surface in SPI at all REF-C stations. INSRIRE scientists consulted with Steve Dixon, a geologist at the State of Maine, and reached consensus that the clay material is likely due to a non-anthropogenic occurrence, such as Pleistocene mud deposit, iceberg scars, or potentially an anthropogenic anomaly (S. Dixon, personal communication, January 26, 2022). The presence of clay at REF-C was also observed during surveys conducted in 2015, 2019 and 2020 (Guarinello et al. 2016 and USACE 2021). REF-C remains a suitable reference area

for IOSN because the naturally occurring clay at REF-C may provide comparable habitat to the various sediment types that will likely be placed at IOSN in the future.

5.0 CONCLUSIONS AND RECOMMENDATIONS

The October 2021 acoustic and SPI/PV survey was conducted to provide information on the distribution of recently placed dredged material and to assess benthic habitat conditions at IOSN and reference areas. This survey provides useful information on how the newly designation IOSN received dredged material and how the benthic community recovery compared to the selected reference areas. The following conclusions and recommendations are provided based on the information collected during this survey:

- Dredged material was observed at the planned target area as confirmed by acoustic and SPI/PV sampling results.
- Dredged material placed within the active area of IOSN resulted in an elevation increase of 0.7 m above the seafloor at the highest point.
- Dredged material spread in a radial direction after impact and created a thin apron of sediment extending approximately 600 m in diameter.
- The benthic community within the active portion of IOSN is in a state of recovery. Measured aRPD depths within the active area were statistically less than those at the reference areas, however successional stage were statistically similar, indicating that the site is progressing towards full recovery.
- Baseline conditions within IOSN were observed to be similar to the IOSN reference areas and will provide a useful timestamp for the benthic community when the northern portion of the site receives dredged material.

R1: Future dredged material placements can occur throughout the disposal site but should be targeted to specific areas to limit temporary impacts to the benthic community.

R2: A confirmatory acoustic and SPI/PV survey should be conducted at IOSN after it receives additional dredged material. The survey should occur over the area of newly placed dredged material and over the active area surveyed in 2021 to evaluate benthic habitat conditions.

R3: The reference areas are comparable to the site and can continue to be used for future surveys.

6.0 REFERENCES

Battelle. 2008. Conceptual Plan for Nutrient Criteria Development in Maine Coastal Waters. Prepared for EPA Region 1, Boston, MA, Maine Department of Environmental Protection, Augusta, ME, and Oceans and Coastal Protection Division (USEPA), Washington, D.C. 34 pp.

Fredette, T. J.; French, G. T. 2004. Understanding the physical and environmental consequences of dredged material disposal: history in New England and current perspectives. Mar. Pollut. Bull. 49:93–102.

Germano, J. D. 1983. Infaunal succession in Long Island Sound: animal sediment interactions and the effects of predation [dissertation]. New Haven (CT): Yale University.

Germano, J. D. 1999. Ecology, statistics, and the art of misdiagnosis: The need for a paradigm shift. Environ. Rev. 7(4):167–190.

Germano, J. D.; Rhoads, D. C.; Lunz, J. D. 1994. An Integrated, Tiered Approach to Monitoring and Management of Dredged Material Disposal Sites in the New England Regions. DAMOS Contribution No. 87. U.S. Army Corps of Engineers, New England Division, Waltham, MA, 67 pp.

Germano, J. D.; Rhoads, D. C.; Valente, R. M.; Carey, D. A.; Solan, M. 2011. The use of sediment-profile imaging (SPI) for environmental impact assessments and monitoring studies: lessons learned from the past four decades. Oceanogr. Mar. Biol. Ann. Rev. 49:235–285.

Guarinello, M. L.; Carey, D. A.; Wright, C. 2016. Data Summary Report for the Monitoring Survey at the Isles of Shoals Disposal Site North, September 2015. U.S. Army Corps of Engineers, New England District, Concord, MA, 63 pp.

INSPIRE. 2019. Standard Operating Procedure (SOP) for Sediment Profile and Plan View Imaging Sample Collection and Image Analysis. Prepared by INSPIRE Environmental, Newport, RI. Revision 1 March 2019.

INSPIRE. 2020a. Quality Assurance Project Plan (QAPP) for the Disposal Area Monitoring System (DAMOS) Program. Prepared for the U.S. Army Corps of Engineers, New

England District under Contract No. W912WJ-19-D-0010. Submitted by INSPIRE Environmental, Newport, RI. September 2020.

INSPIRE. 2020b. Standard Operating Procedure (SOP) for Acoustic Surveys. Prepared by INSPIRE Environmental, Newport, RI. Revision 2 January 2020.

McBride, G. B. 1999. Equivalence tests can enhance environmental science and management. Aust. New Zeal. J. Stat. 41(1):19–29.

Pearson, T. H.; Rosenberg, R. 1978. Macrobenthic succession in relation to organic enrichment and pollution of the marine environment. Oceanogr. Mar. Biol. 16: 229-311.

Rhoads, D. C.; Boyer, L. F. 1982. The effects of marine benthos on physical properties of sediments. In: McCall, P.L. and M.J.S. Tevesz, editors. Animal-sediment relations. New York (NY): Plenum Press. p. 3-52.

Rhoads, D. C.; Germano, J. D. 1982. Characterization of organism-sediment relations using sediment profile imaging: an efficient method of remote ecological monitoring of the seafloor (REMOTS System). Mar. Ecol. Progr. 8: 115-128.

Satterthwaite, F. E. 1946. “An Approximate Distribution of Estimates of Variance Components”, Biometrics Bulletin, Vol. 2, No. 6, pp. 110-114.

Schuirmann, D. J. 1987. A comparison of the two one-sided tests procedure and the power approach for assessing the equivalence of average bioavailability. J. Pharmacokinet. Biopharm. 15:657–680.

USACE. 2013. Engineering and Design - Hydrographic Surveying. Manual No. EM 1110- 2-1003. November 2013.

USACE. 2021. Data Summary Report for the Baseline Surveys of the Isles of Shoals North Disposal Site, September/October 2019 and September 2020.

USACE/EPA Region 1. 2020. Isles of Shoals North Ocean Dredged Material Disposal Site - Site Management and Monitoring Plan. Prepared by the U.S. Army Corps of Engineers, New England District and the U.S. Environmental Protection Agency, Region 1. September 2020.

Wolf, S.; Fredette, T. J.; Loyd, R. B. 2012. Thirty-Five Years of Dredged Material Disposal Area Monitoring – Current Work and Perspectives of the DAMOS Program. WEDA Journal of Dredging Engineering, Vol. 12, No. 2, p. 24-41.

INDEX

MONITORING SURVEY AT THE ISLES OF SHOALS NORTH DISPOSAL SITE OCTOBER 2021

FIGURES

CONTRIBUTION #214

September 2022

Contract No. W912WJ-19-D-0010
DAMOS PWS #03 - Task 3c

Funded and Managed by:
New England District
U.S. Army Corps of Engineers
696 Virginia Road
Concord, MA 01742-2751

Prepared by:
INSPIRE ENVIRONMENTAL
INSPIRE Environmental
513 Broadway
Newport, RI 02840

LIST OF FIGURES

LIST OF FIGURES

Figure Page

LIST OF FIGURES

Figure Page

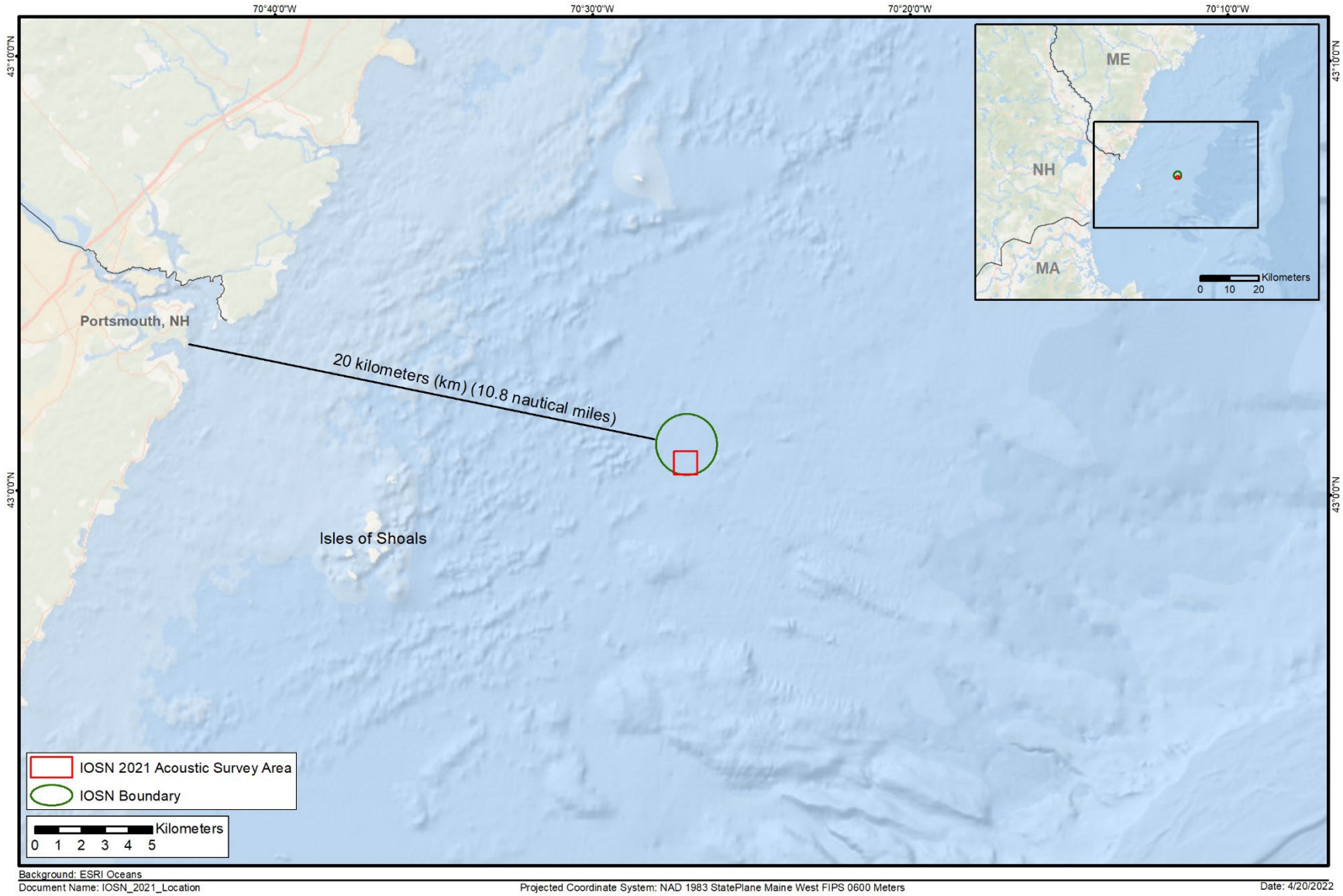

Figure 1-1. Location of the Isles of Shoals North Disposal Site (IOSN)

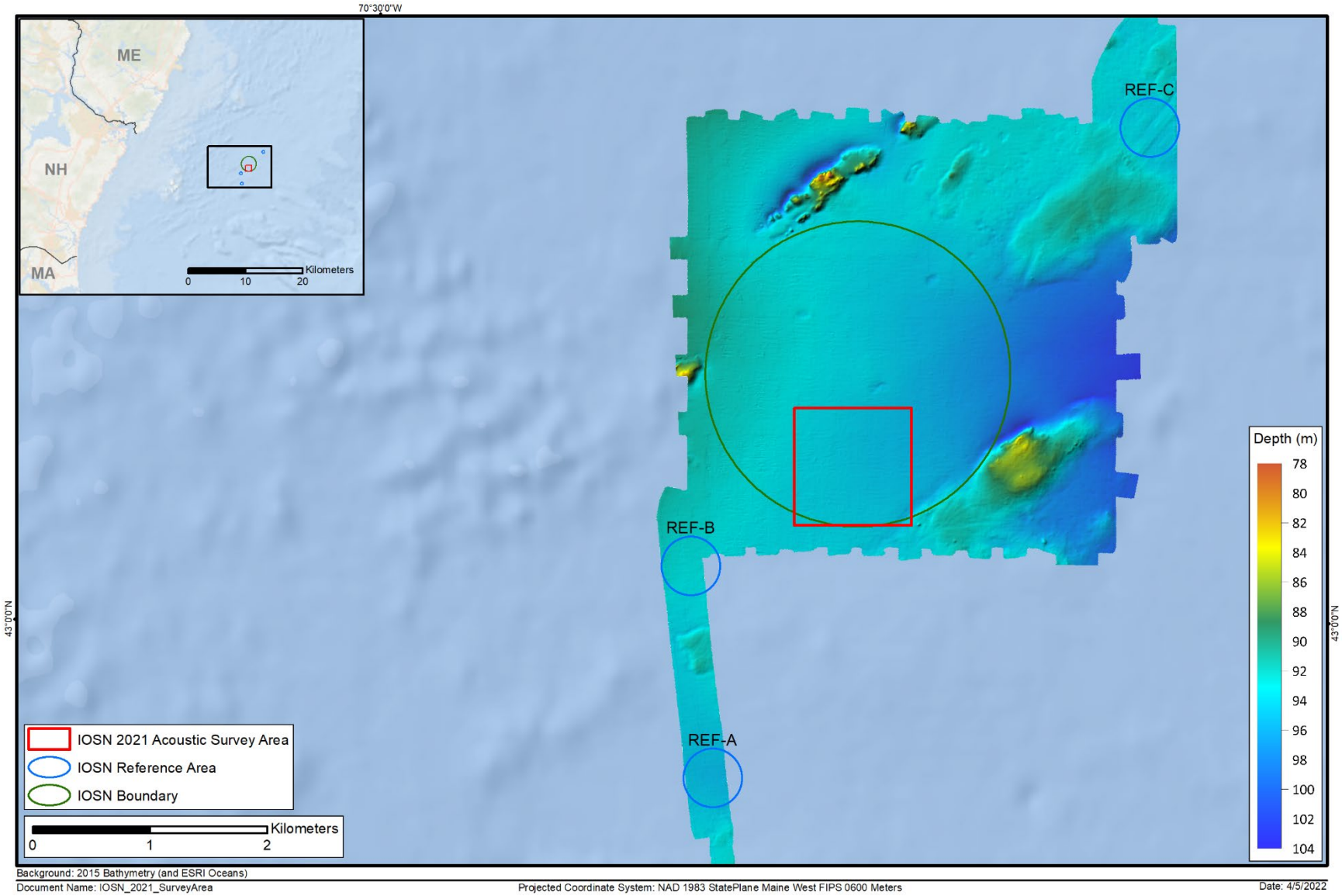

Figure 1-2. Overview of IOSN 2015 bathymetry and 2021 sampling areas

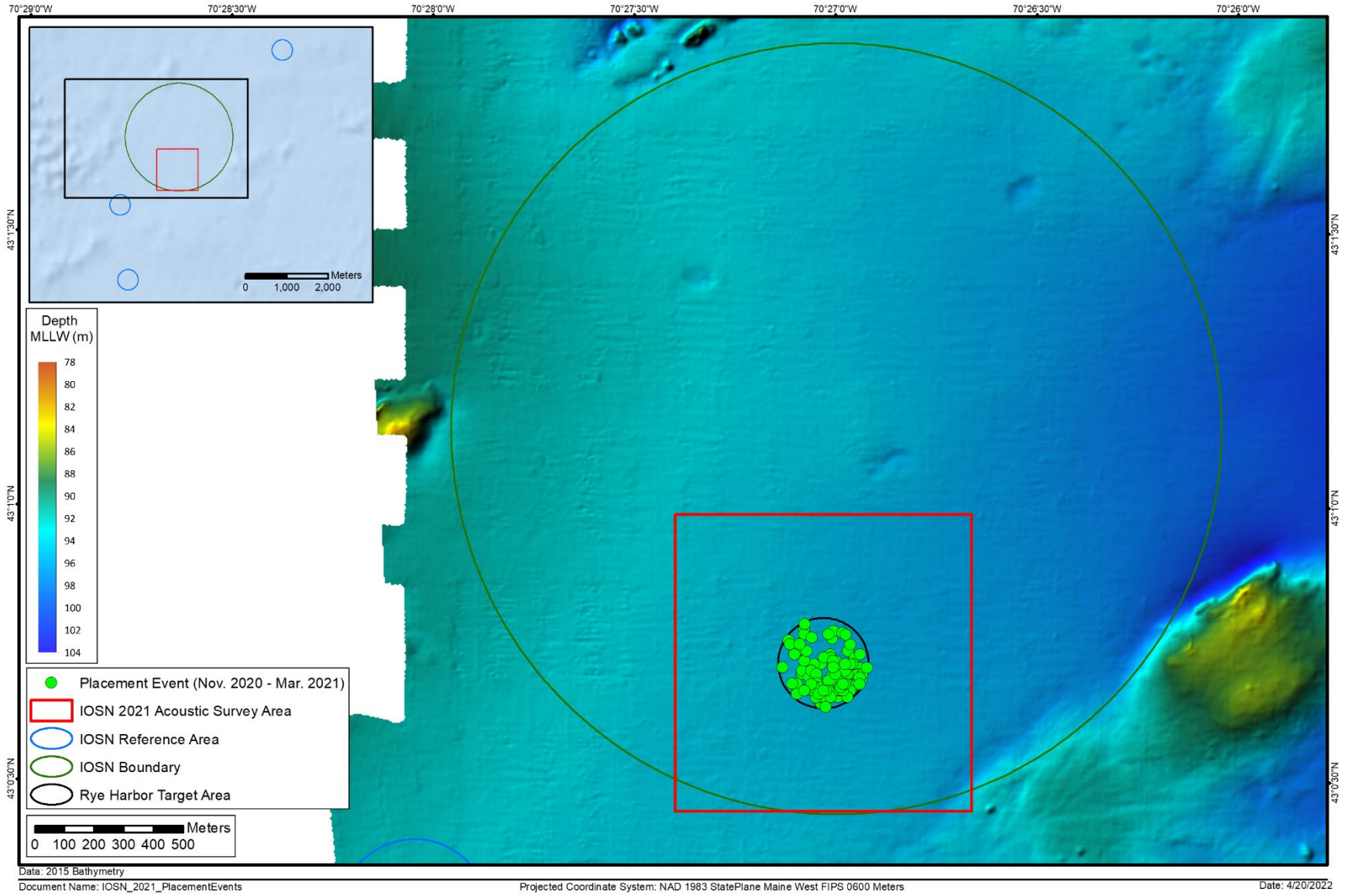

Figure 1-3. Recent dredged material disposal locations for the period November 2020 to March 2021

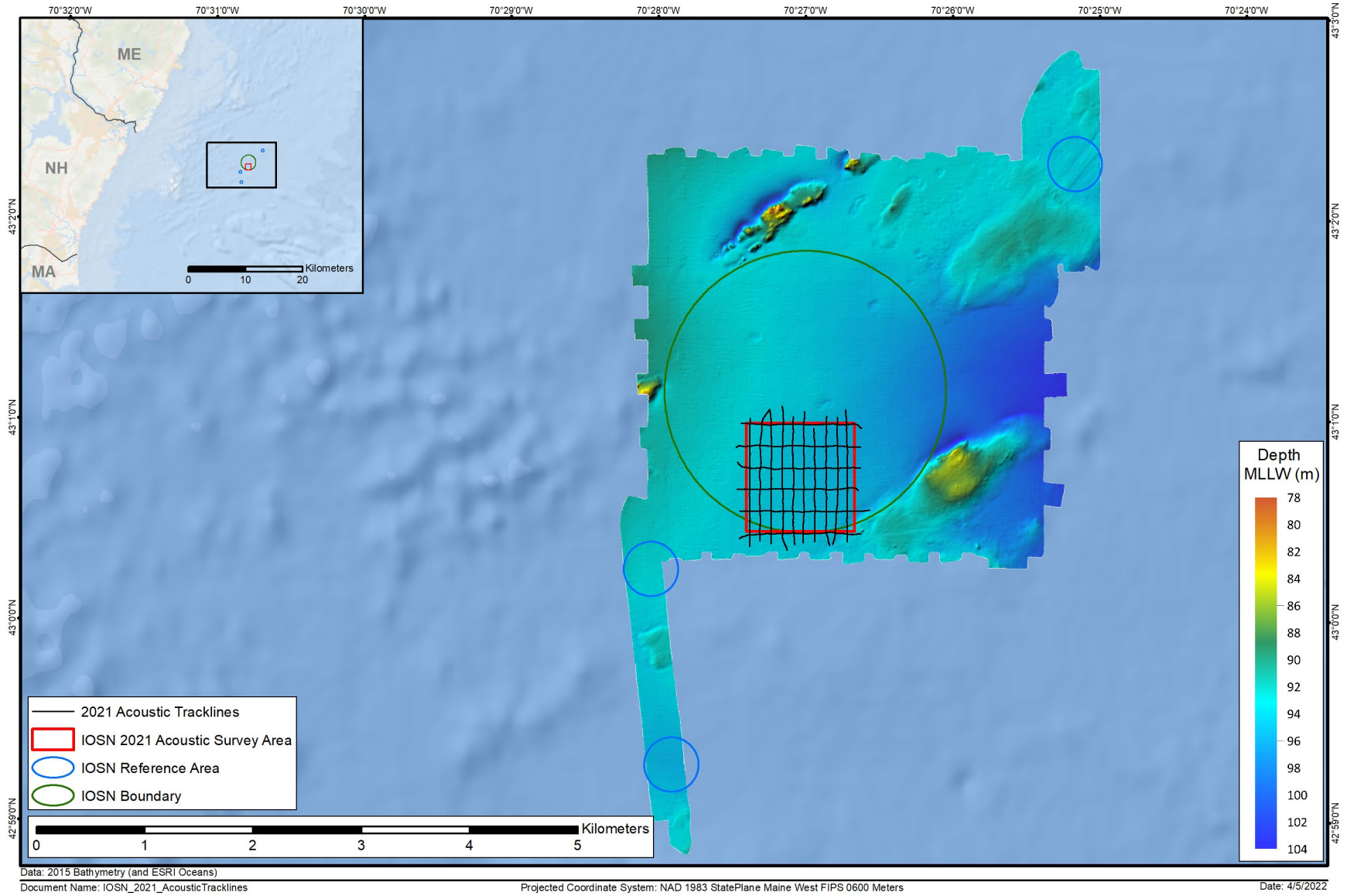

Figure 2-1. Actual acoustic survey tracklines at IOSN, October 2021

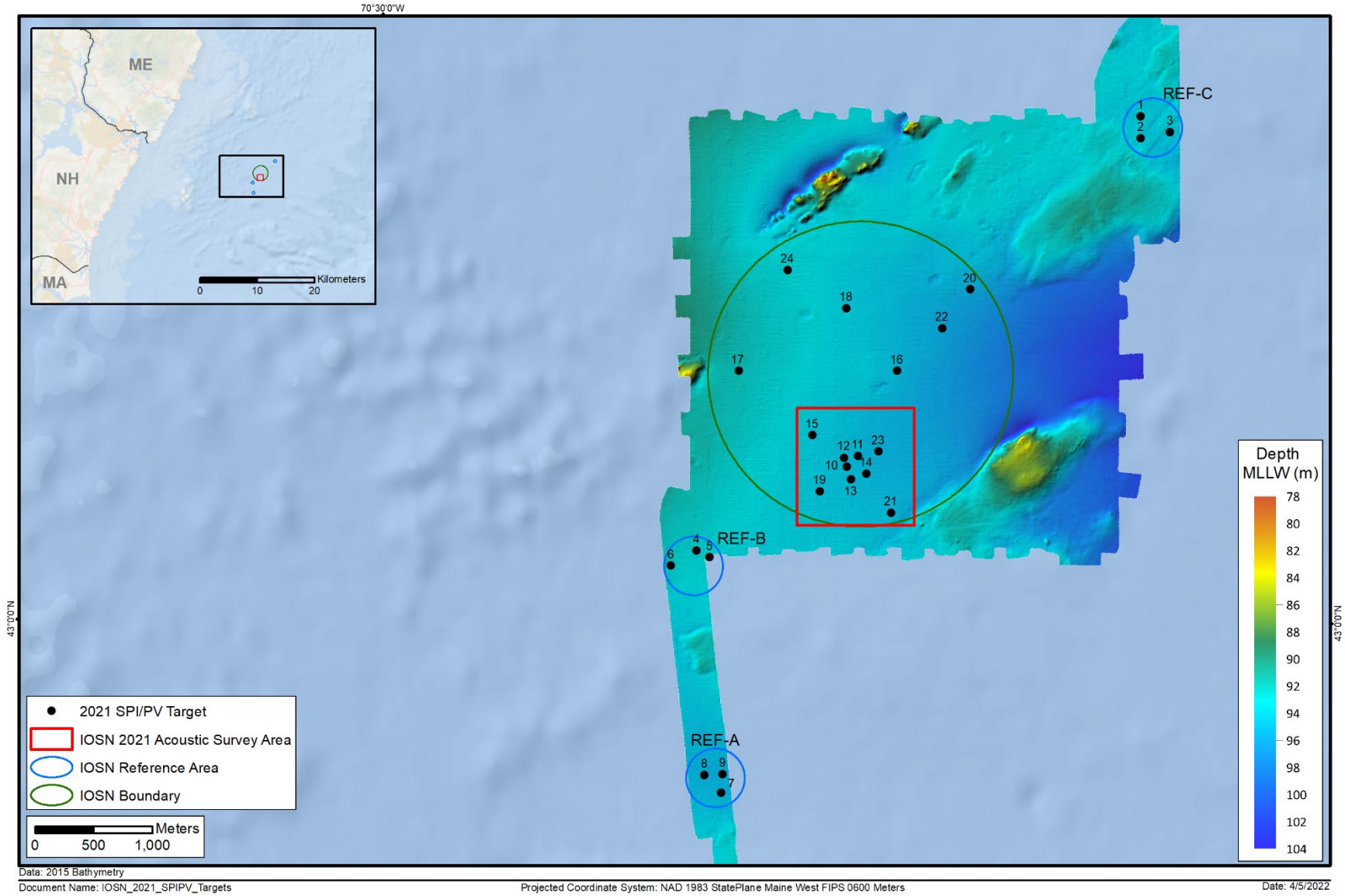

Figure 2-2. SPI/PV target station locations at IOSN and reference areas

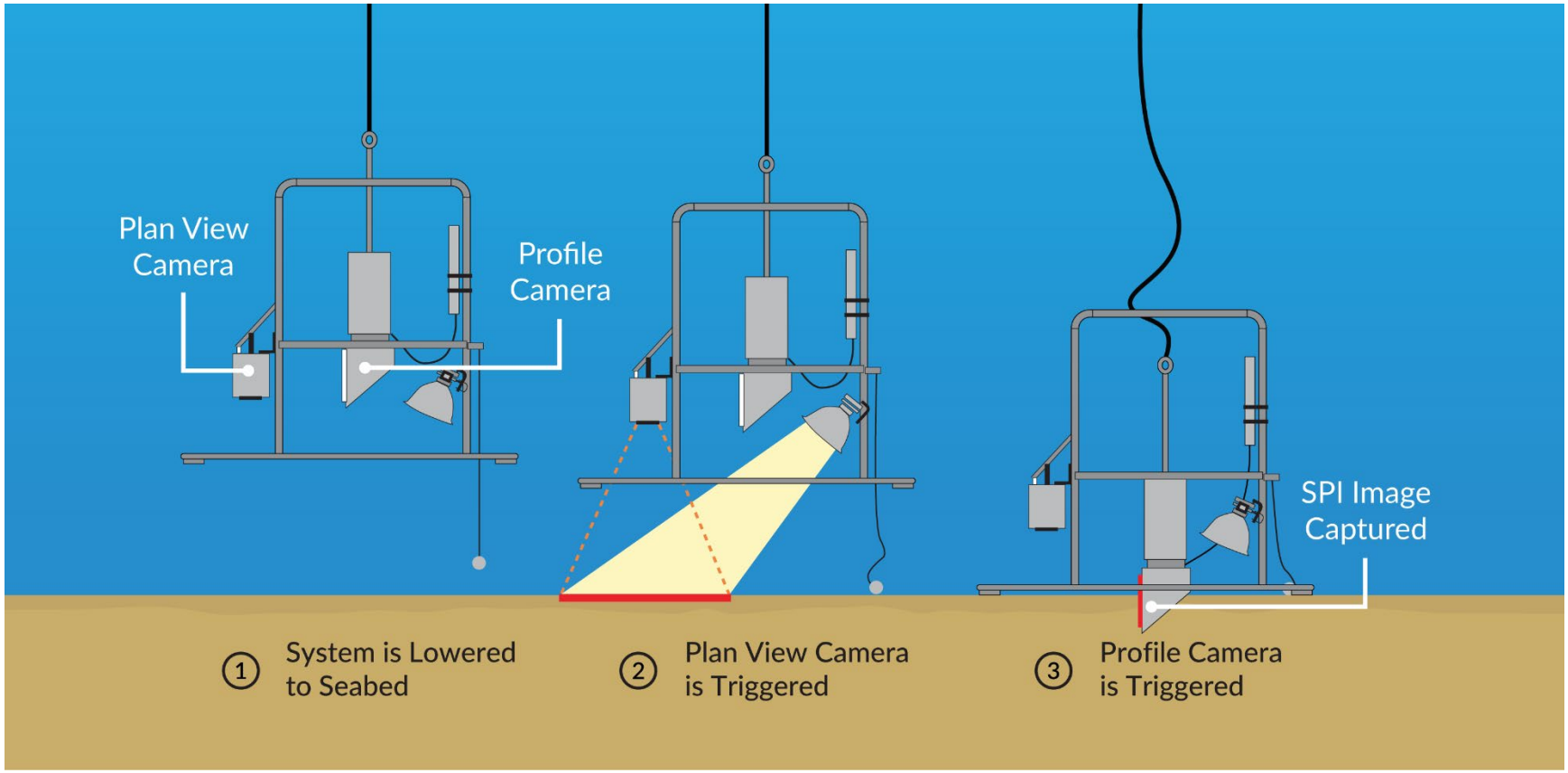

Figure 2-3. Schematic diagram of the operation of the sediment profile and plan view camera imaging system

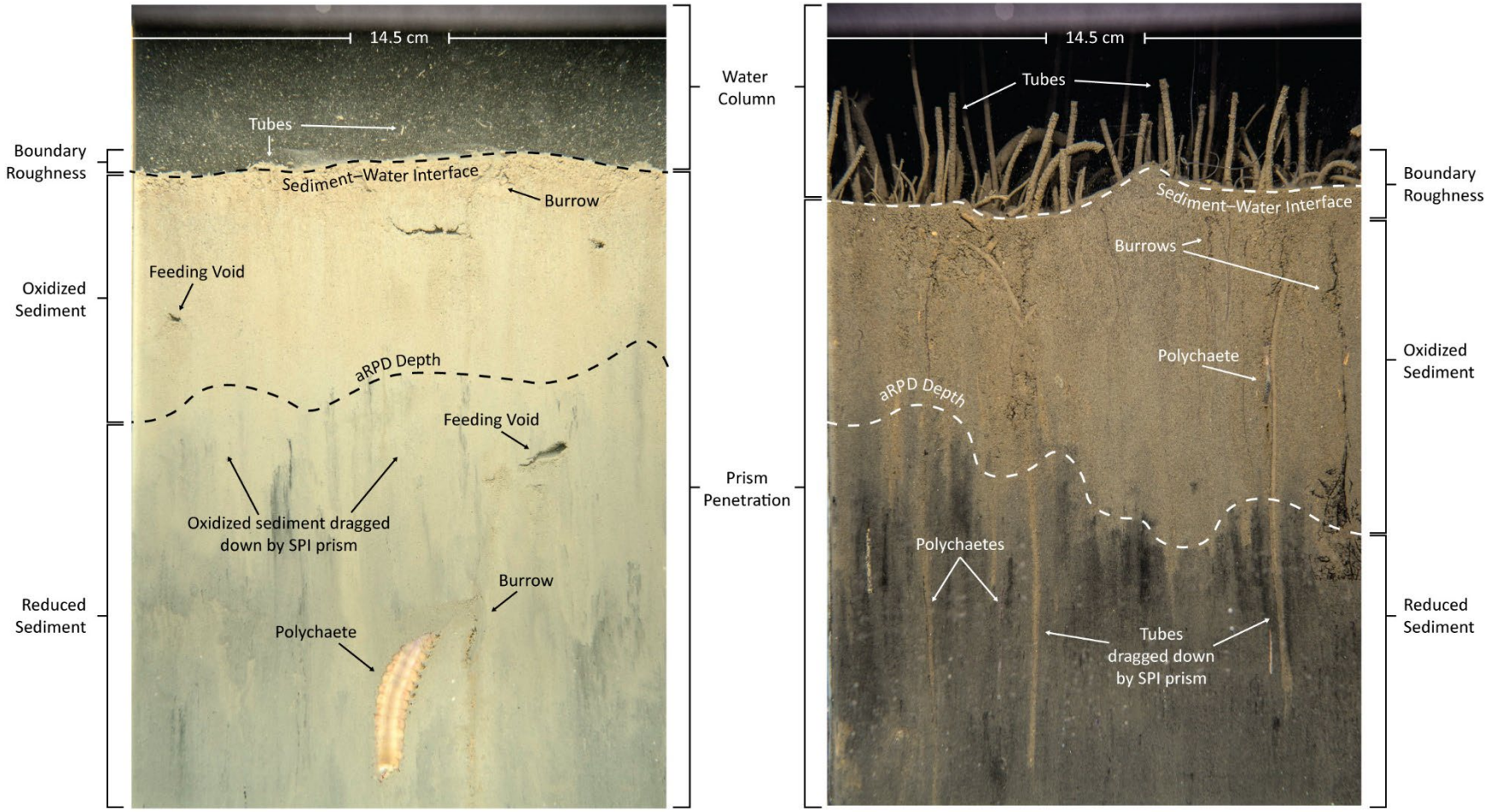

Figure 2-4. SPI images from soft bottom coastal and estuarine environments annotated with many standard variables derived from SPI images. The water column, depth of prism penetration, boundary roughness of the sediment–water interface, and zones of oxidized and reduced sediment are denoted with brackets. The apparent redox potential discontinuity (aRPD), the boundary between oxidized and reduced sediments, is marked with a dashed line. Infauna and related structures (tubes, burrows, feeding voids) are noted with arrows.

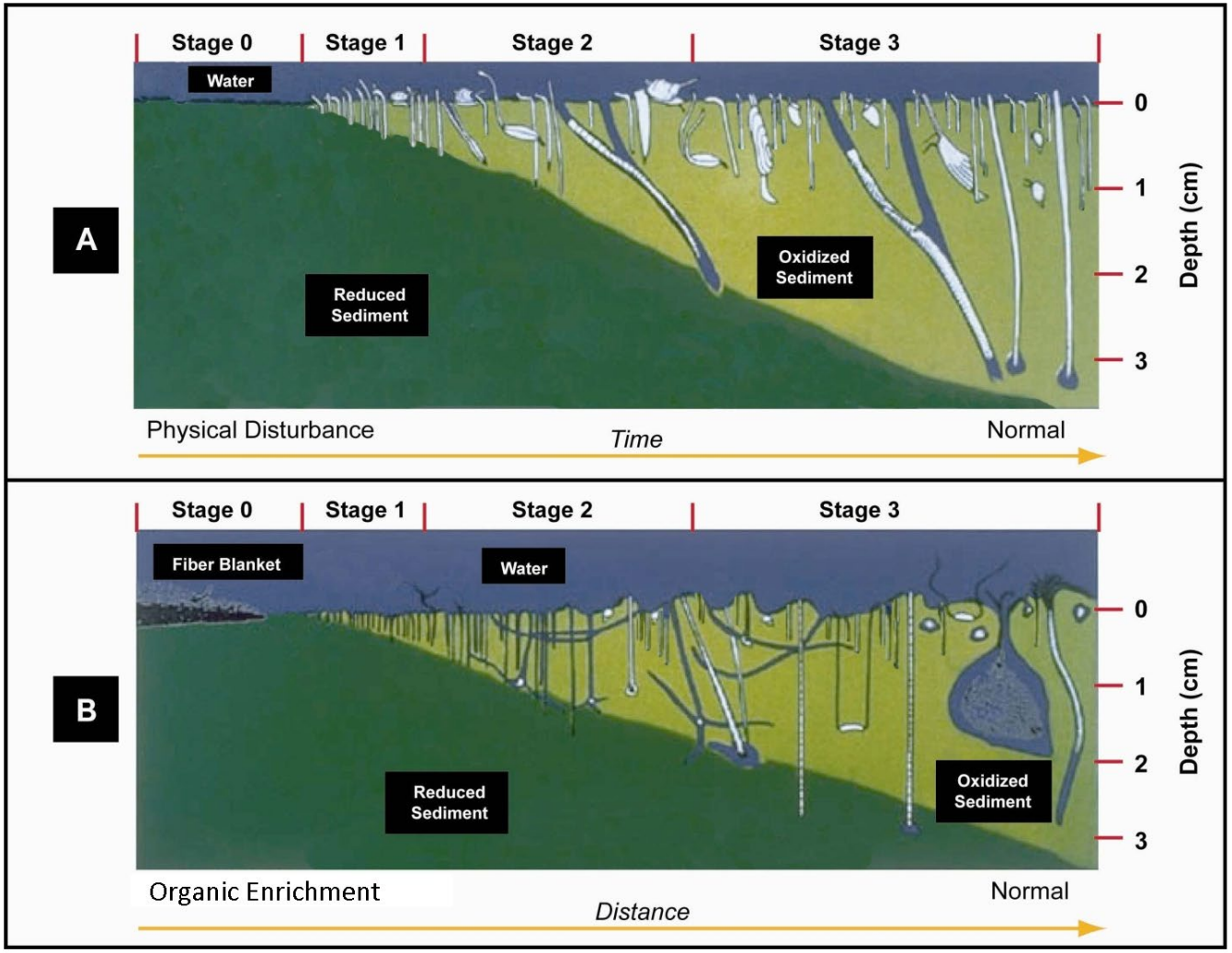

Figure 2-5. The stages of infaunal succession as a response of soft bottom benthic communities to (A) physical disturbance or (B) organic enrichment; from Rhoads and Germano (1982)

Figure 2-6. This representative plan view image shows the sampling relationship between plan view and sediment profile images. Note: plan view images differ between surveys and stations and the area covered by each plan view image may vary slightly between images and stations.

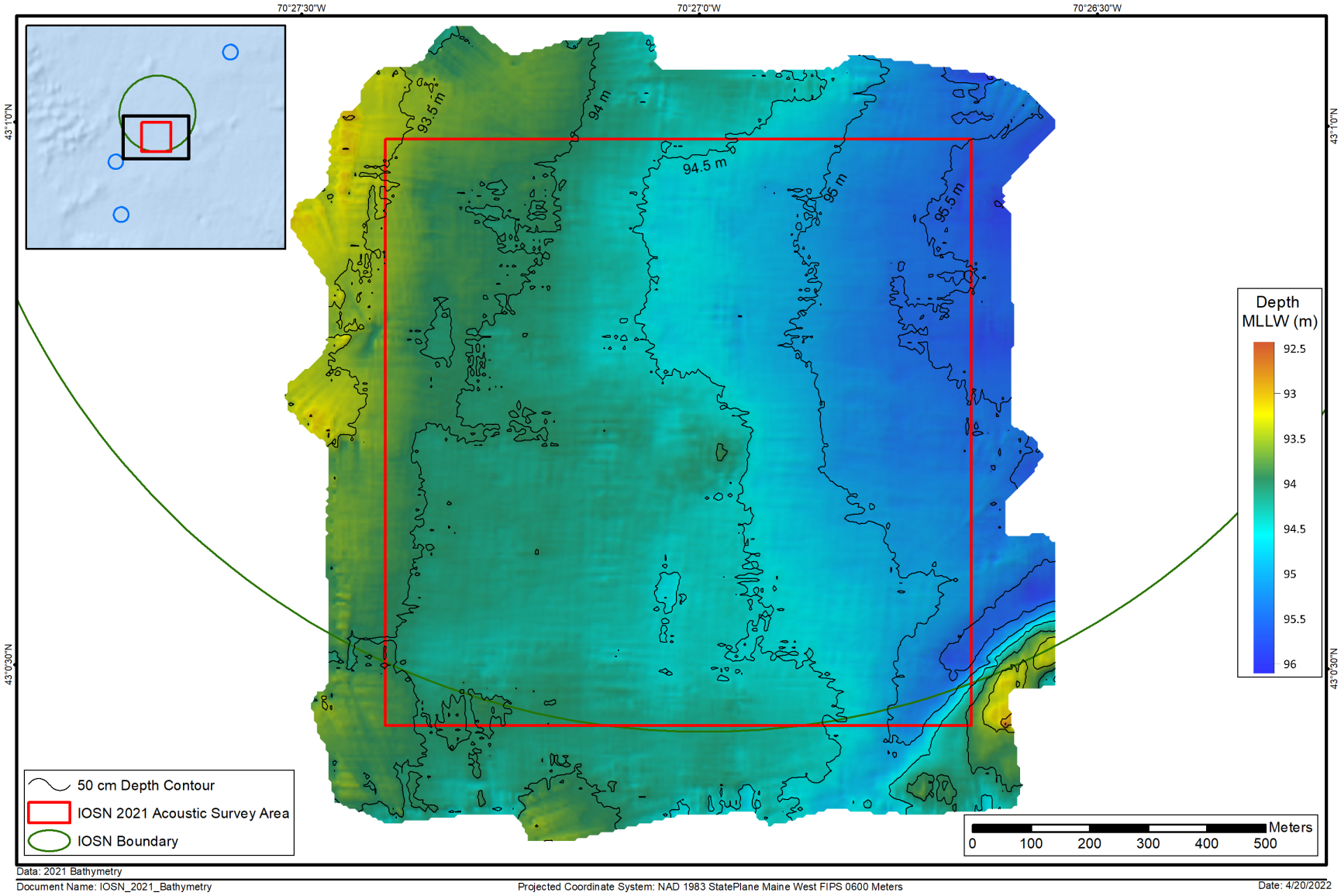

Figure 3-1. Bathymetric depth data over acoustic relief model of IOSN - October 2021

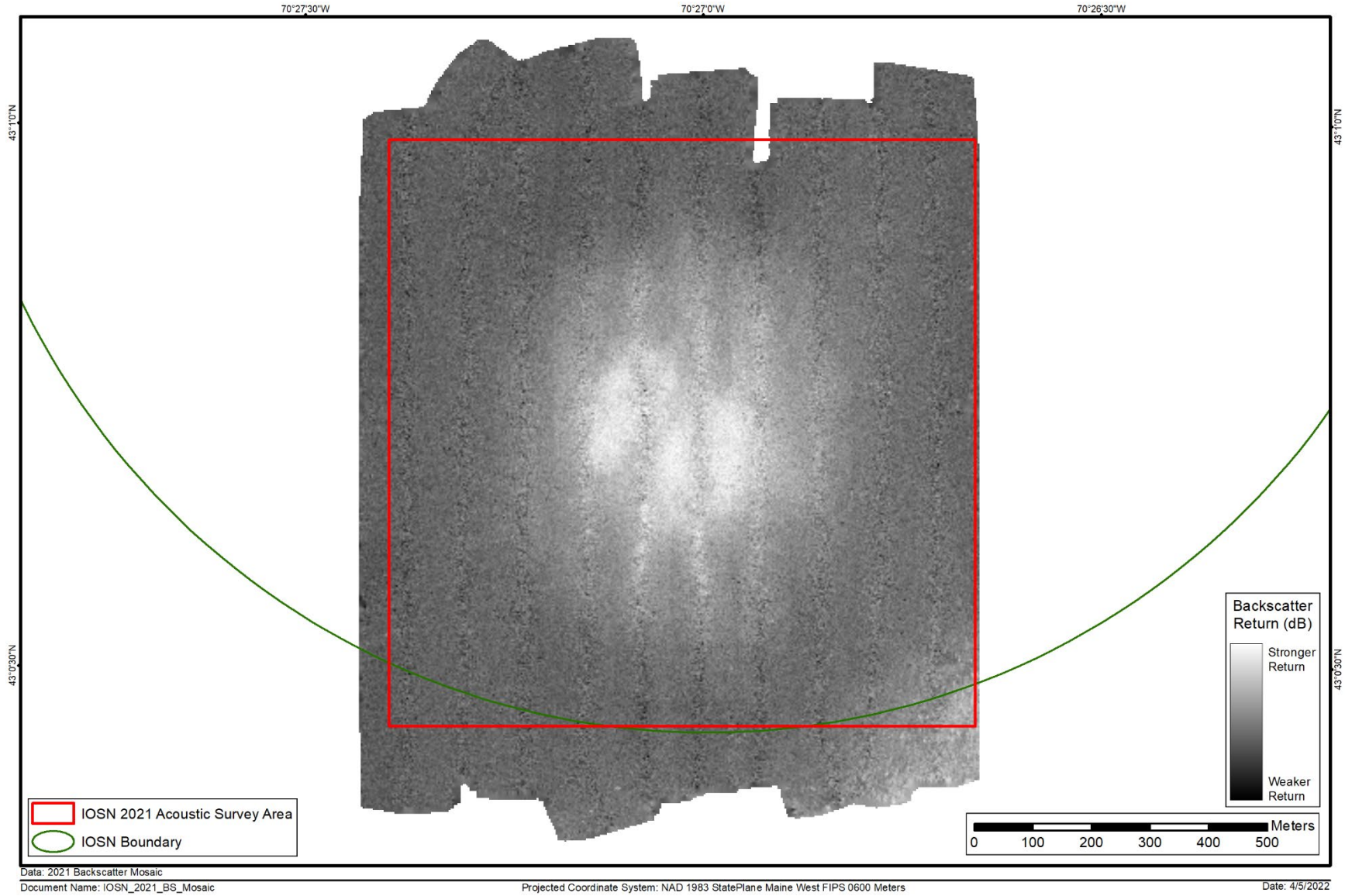

Figure 3-2. Mosaic of unfiltered backscatter data at IOSN - October 2021

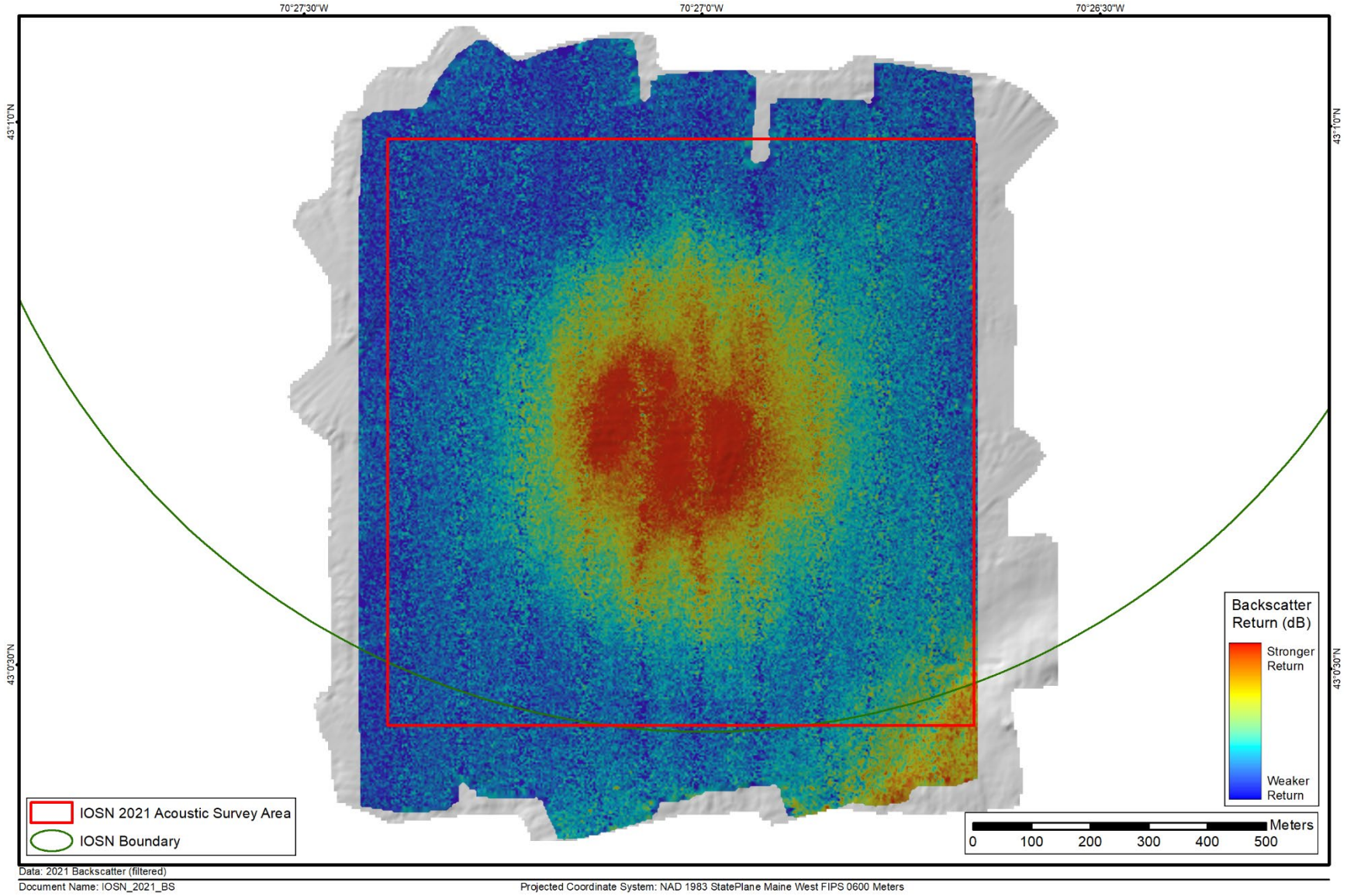

Figure 3-3. Filtered backscatter over acoustic relief model of IOSN - October 2021

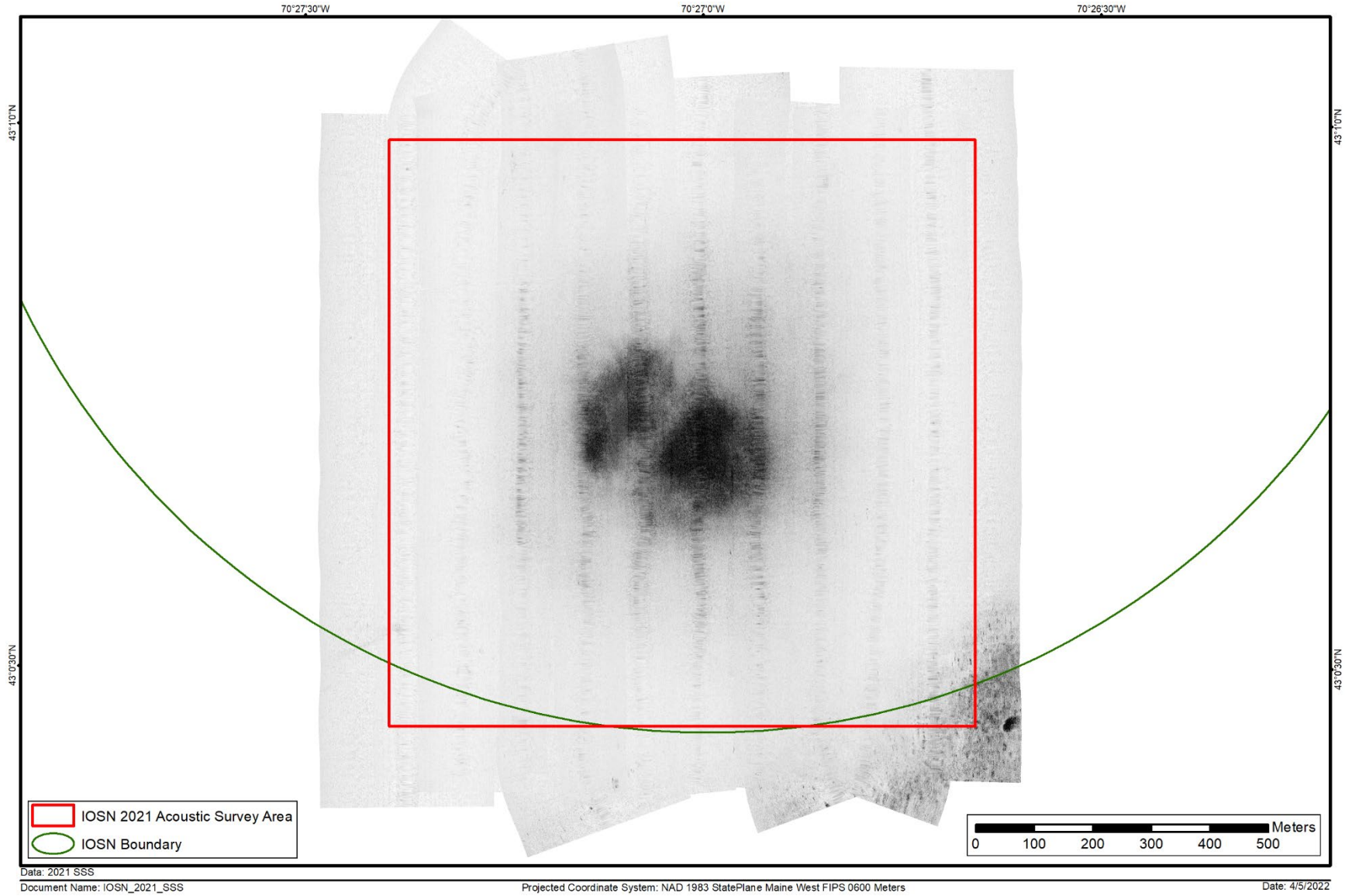

Figure 3-4. Side-scan sonar mosaic at IOSN - October 2021

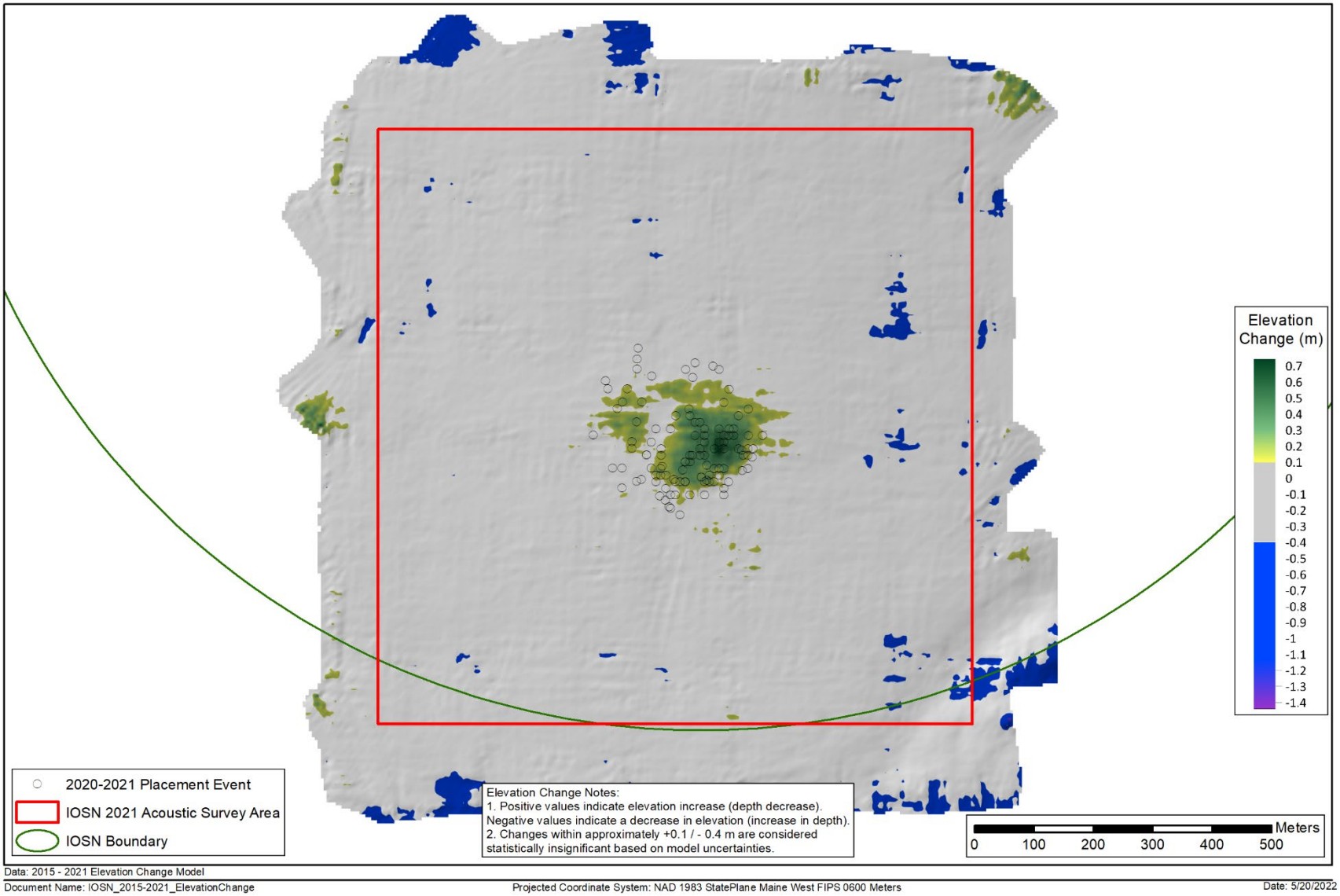

Figure 3-5. Elevation difference September 2015 (baseline) vs. October 2021

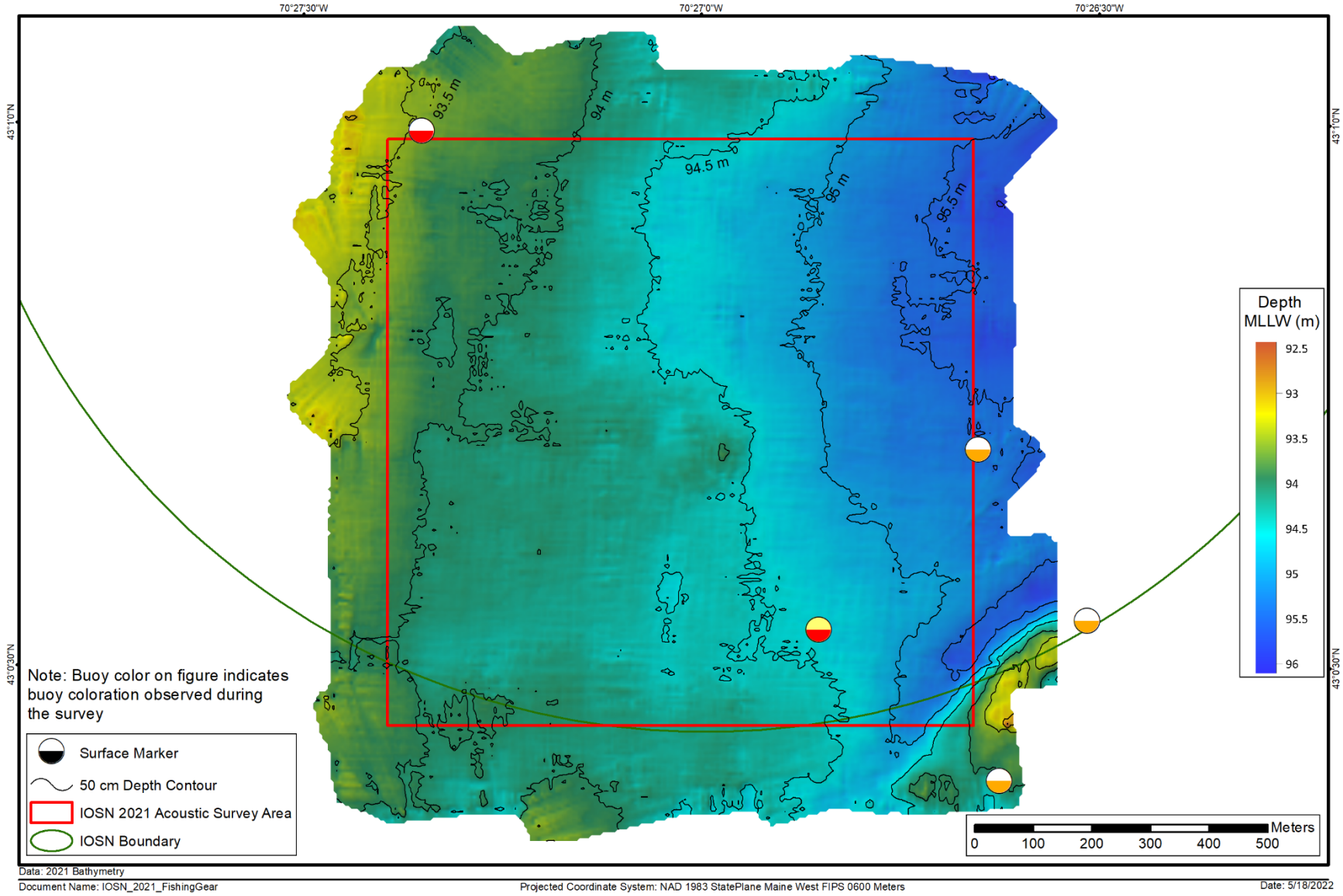

Figure 3-6. Fishing gear observation made by hydrographers during the MBES survey - October 2021

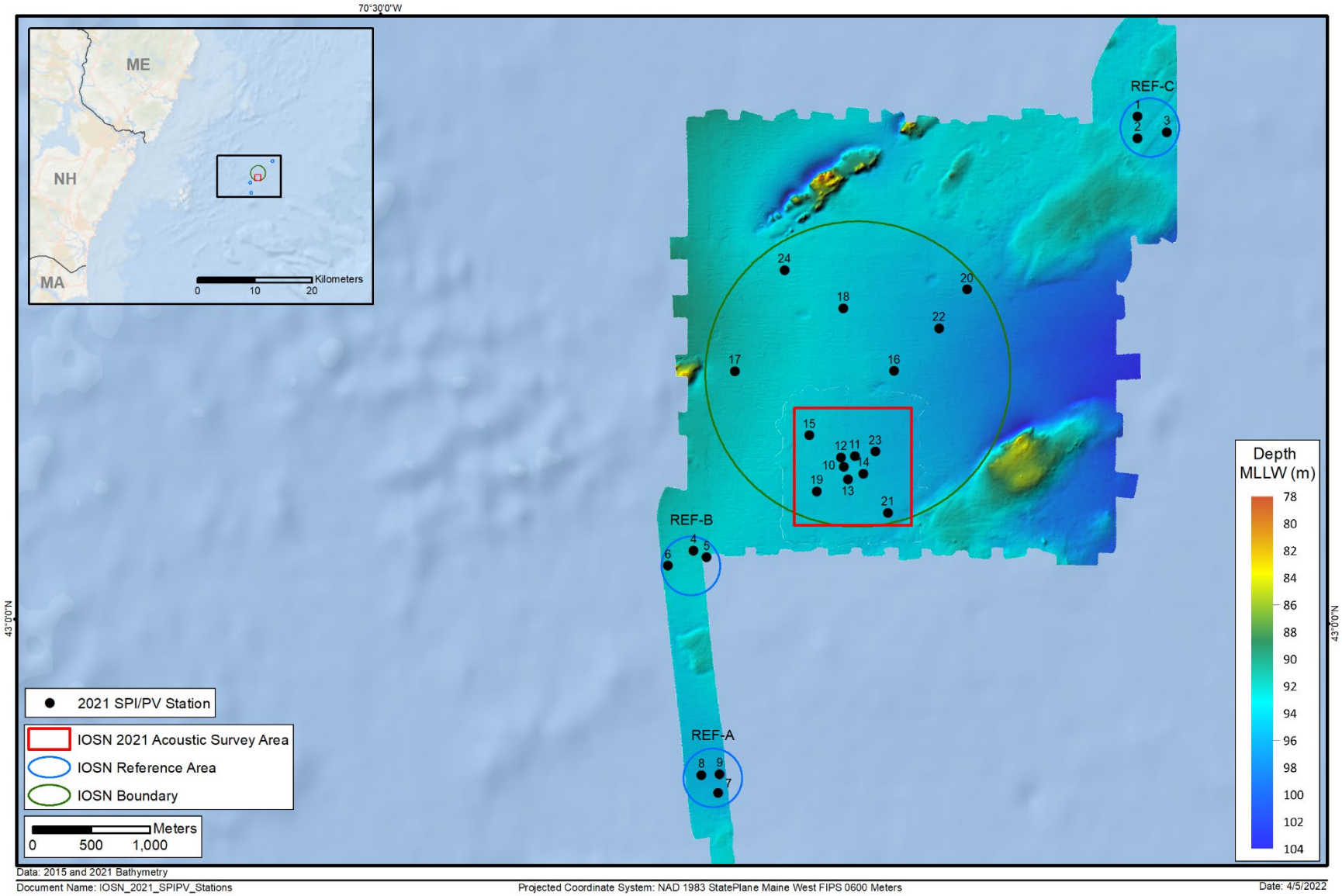

Figure 3-7. SPI/PV actual station locations at IOSN and reference areas

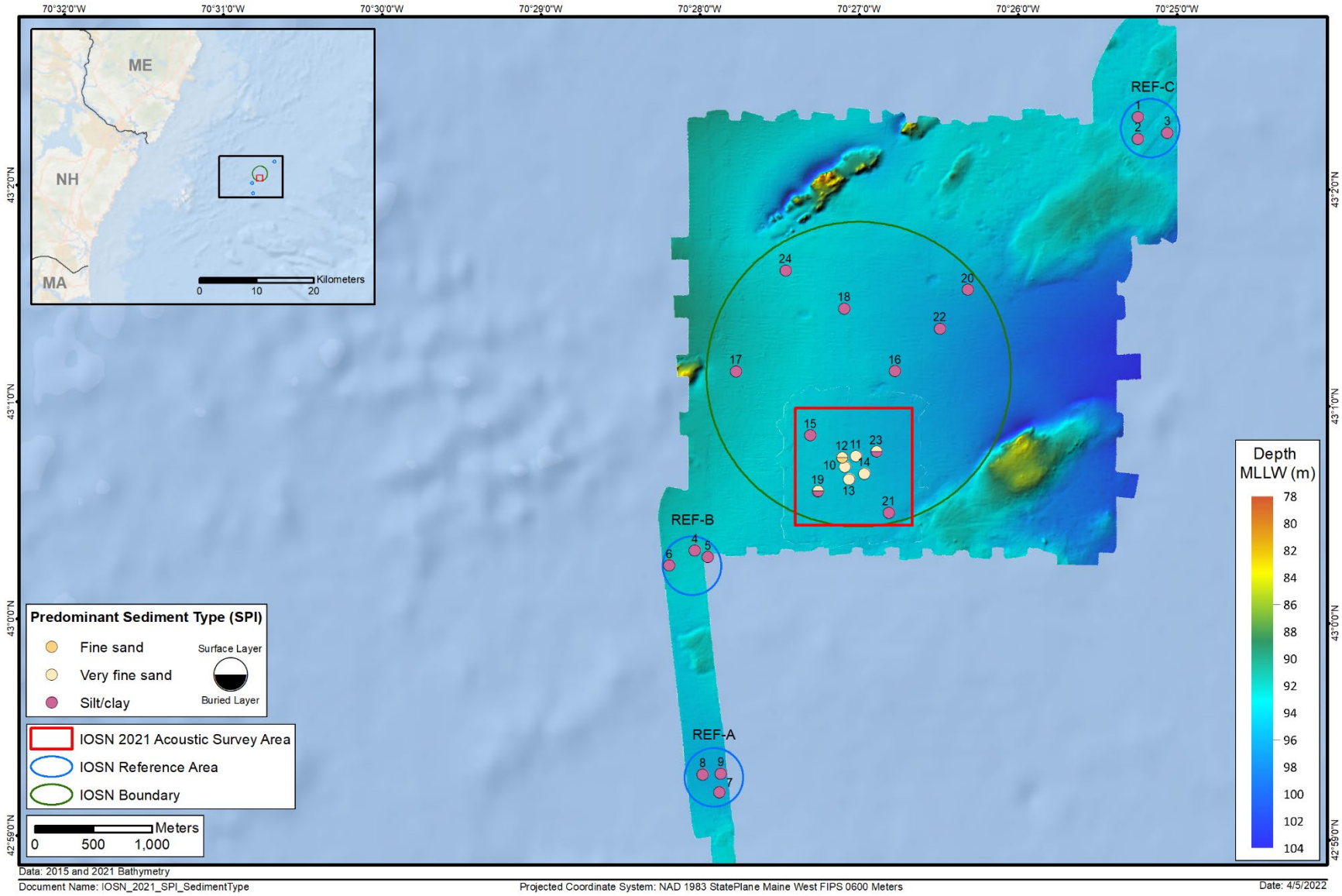

Figure 3-8. Predominant sediment grain size major mode (phi units) at IOSN and reference areas

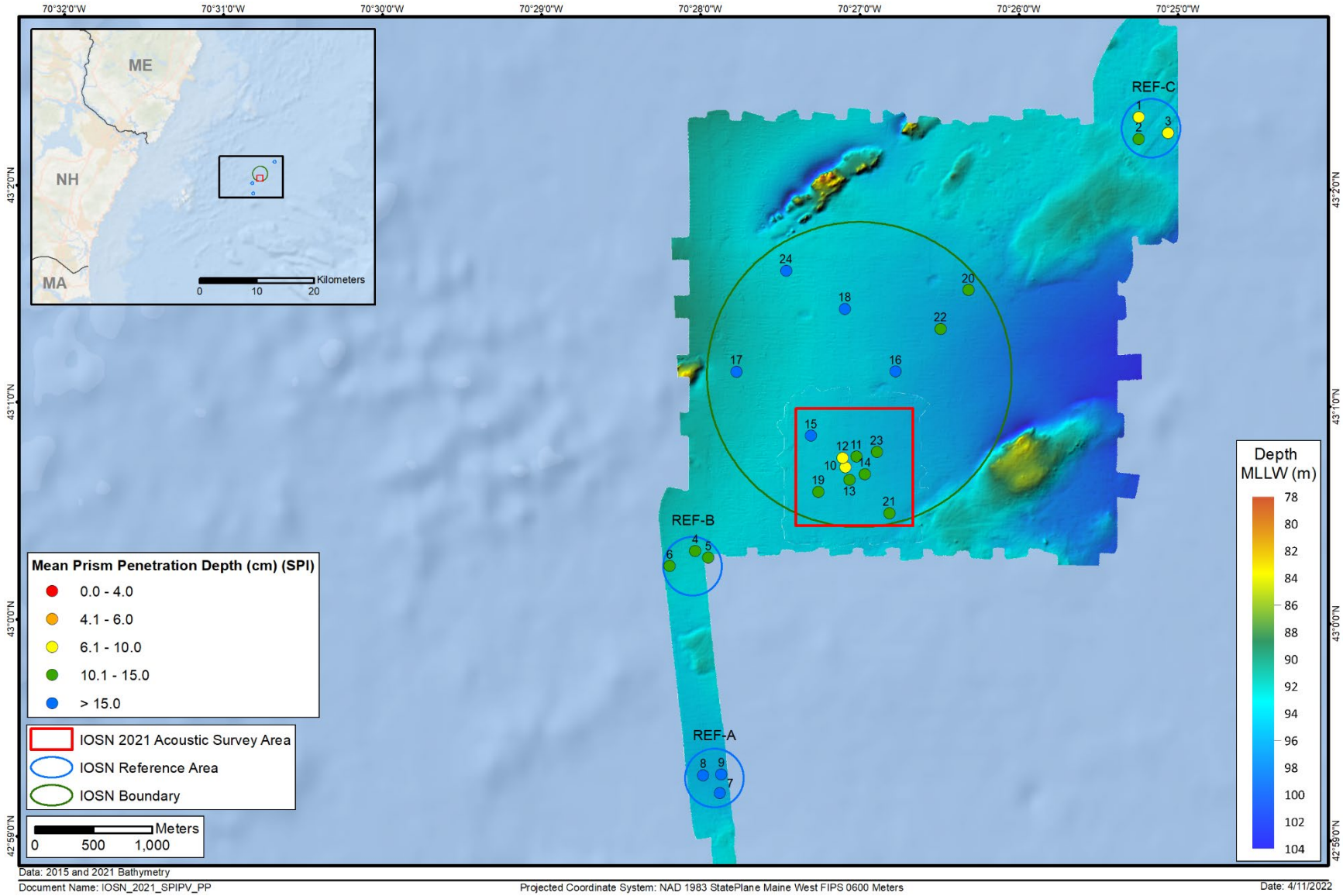

Figure 3-9. Mean station camera prism penetration depths (cm) at IOSN and reference areas

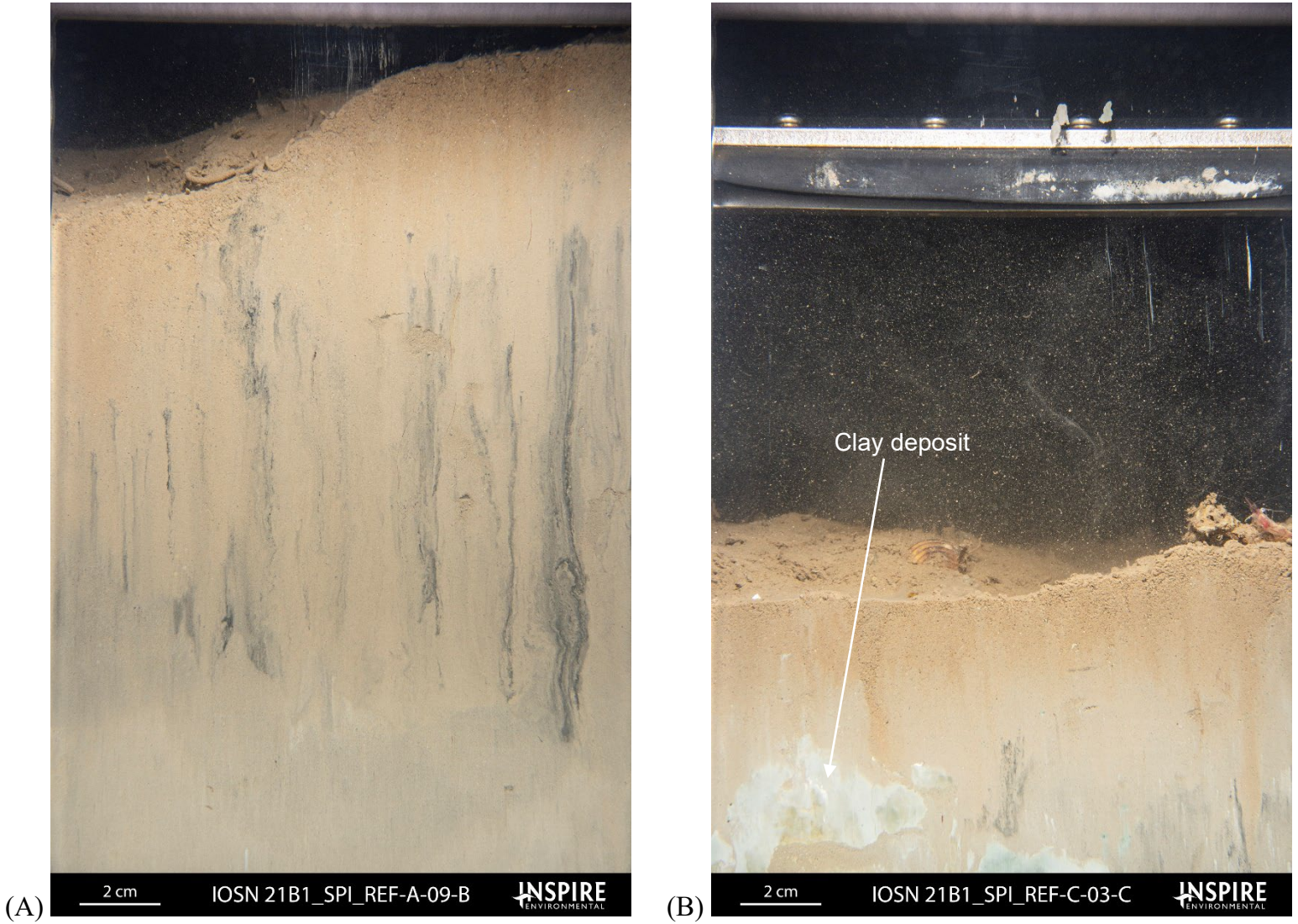

Figure 3-10. Profile images depicting sediment grain size and variation in penetration depth at reference areas; (A) silt/clay at REF-A-09 displaying deep camera penetration; and (B) silt/clay at REF-C-03 displaying shallow penetration (relative to other reference locations)

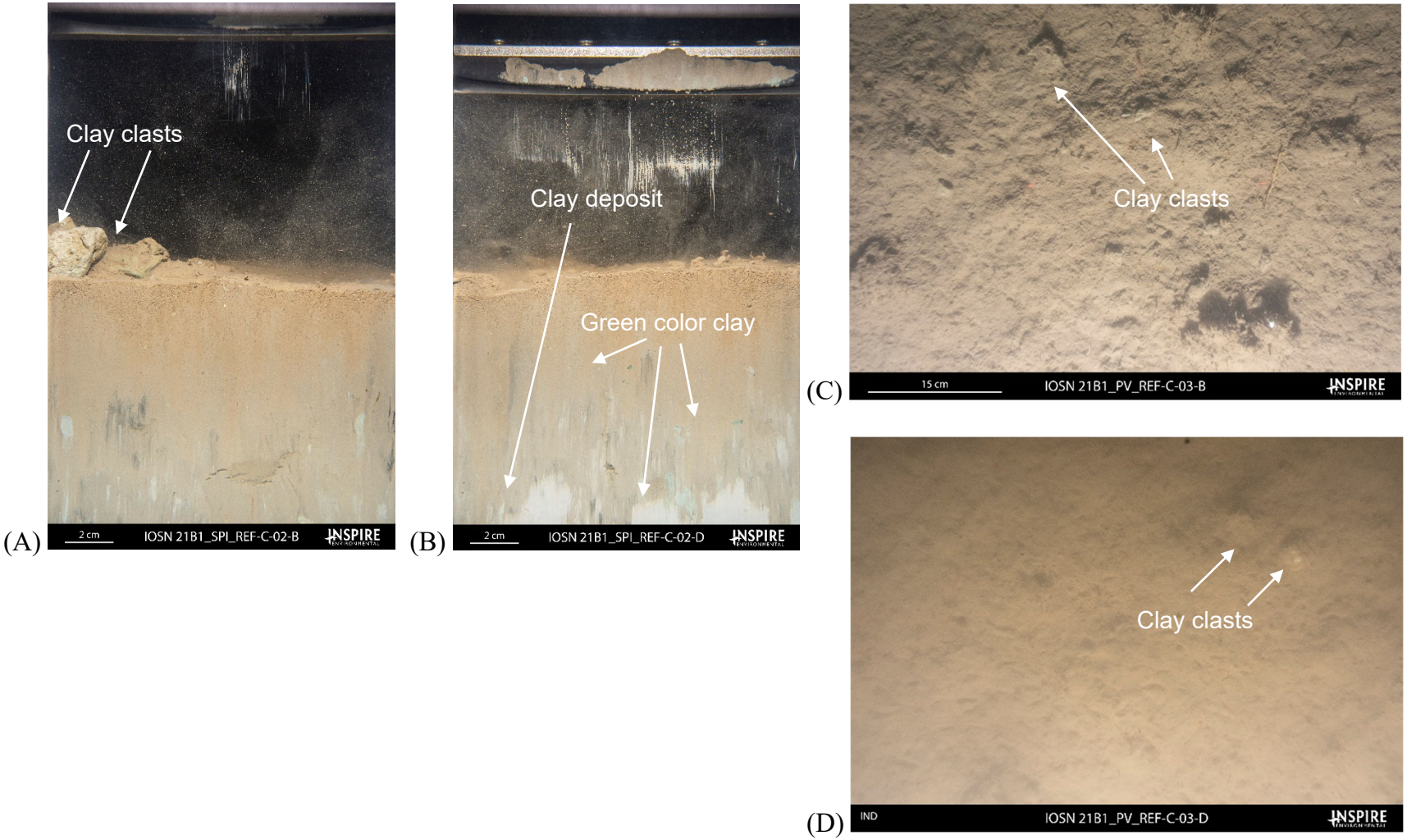

Figure 3-11. Profile images depicting clay clasts and subsurface clay deposits visible at Reference Area C: (A) clay clasts on the sediment surface and small clay deposits throughout the sediment column at REF-C-02; (B) subsurface clay deposits appearing to be green in color at depth at REF-C-02; and (C&D) plan view images displaying presence of clay clasts on the sediment surface at REF-C-03 B and D.

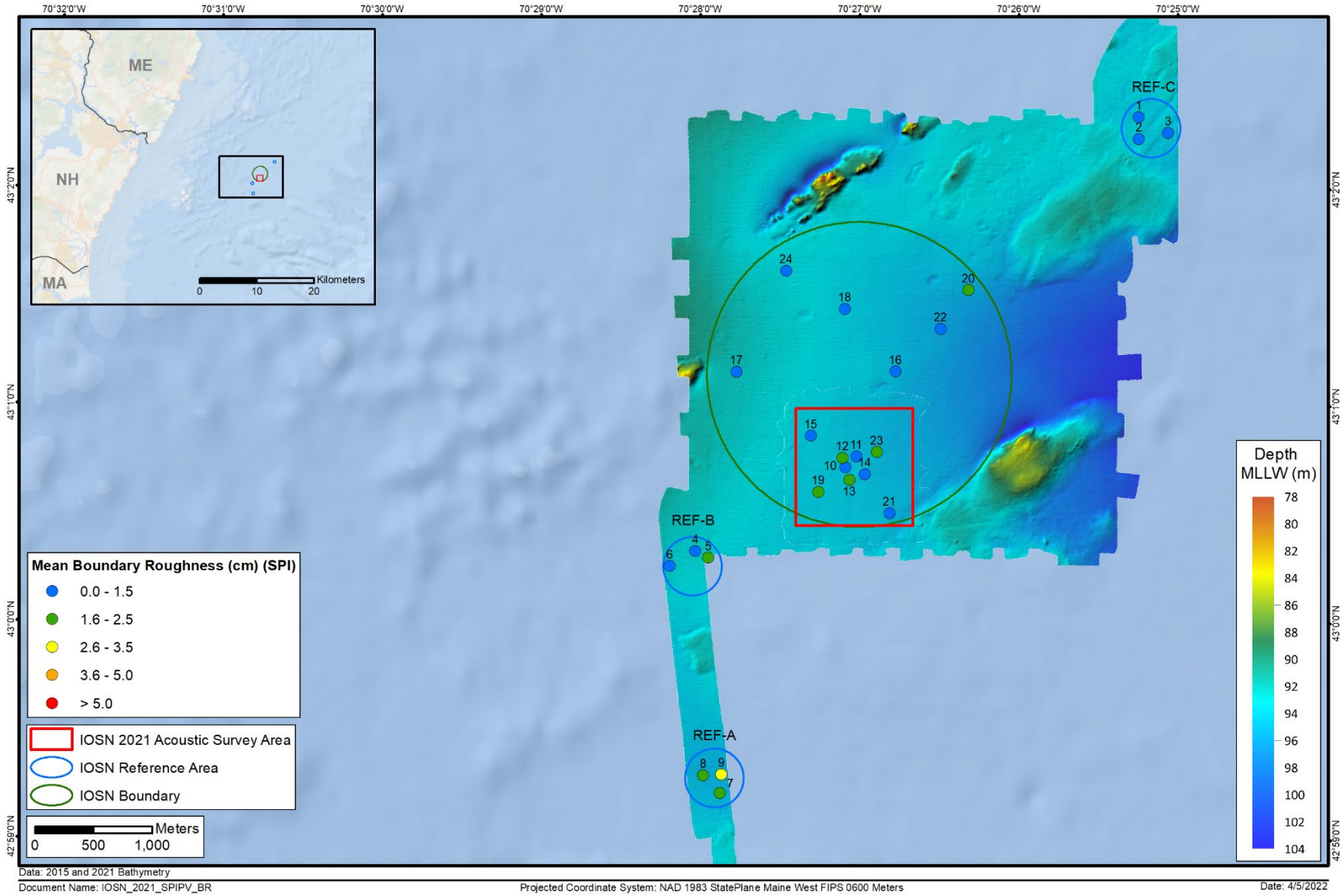

Figure 3-12. Mean station small-scale boundary roughness (cm) at IOSN and reference areas

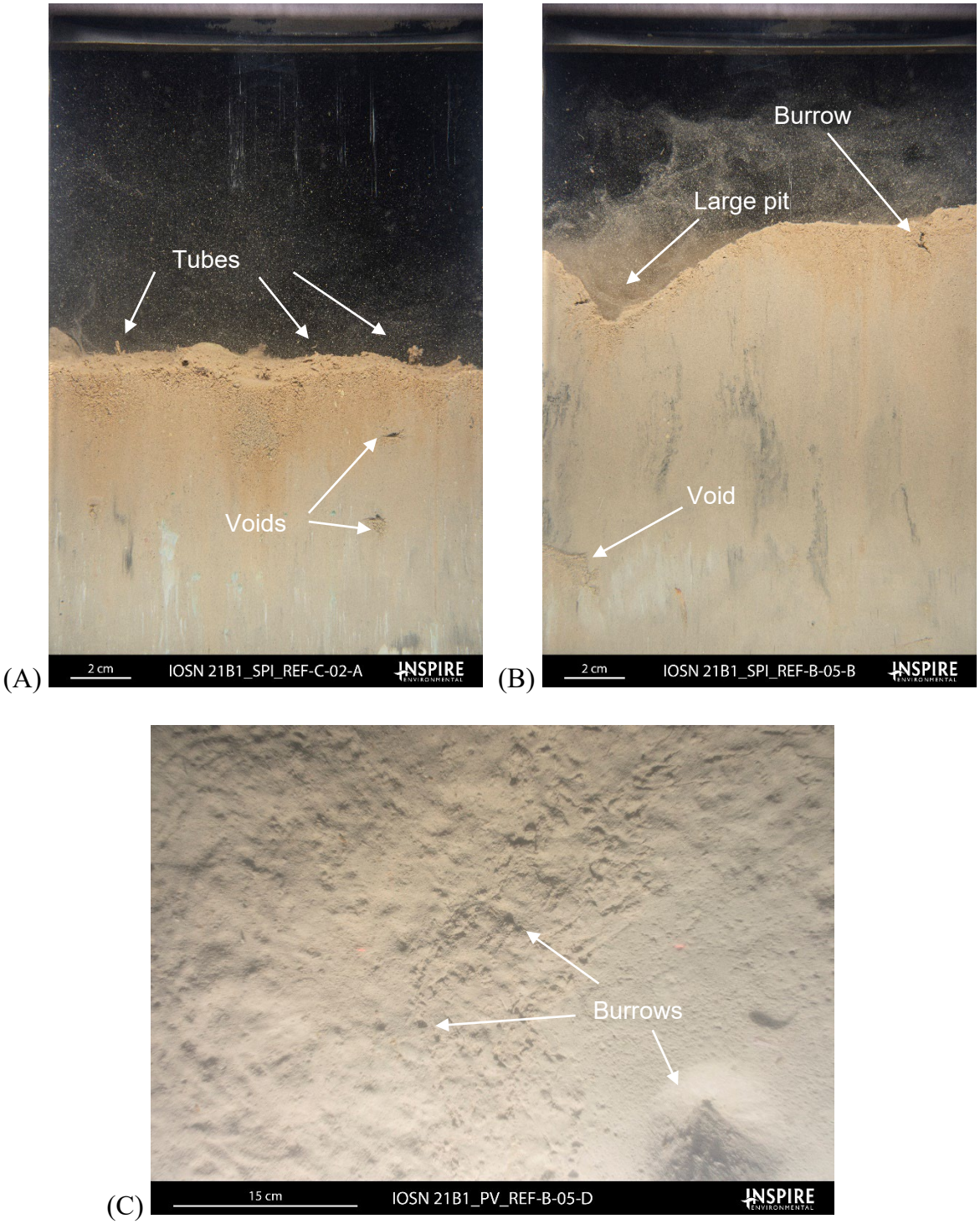

Figure 3-13. Profile and plan view images depicting range of boundary roughness and variation in biological contributors at reference areas; (A) reduced boundary roughness, some surficial tubes and smaller feeding voids at depth; (B) deep feeding void; and (C) PV image displaying burrow depressions on surface sediment

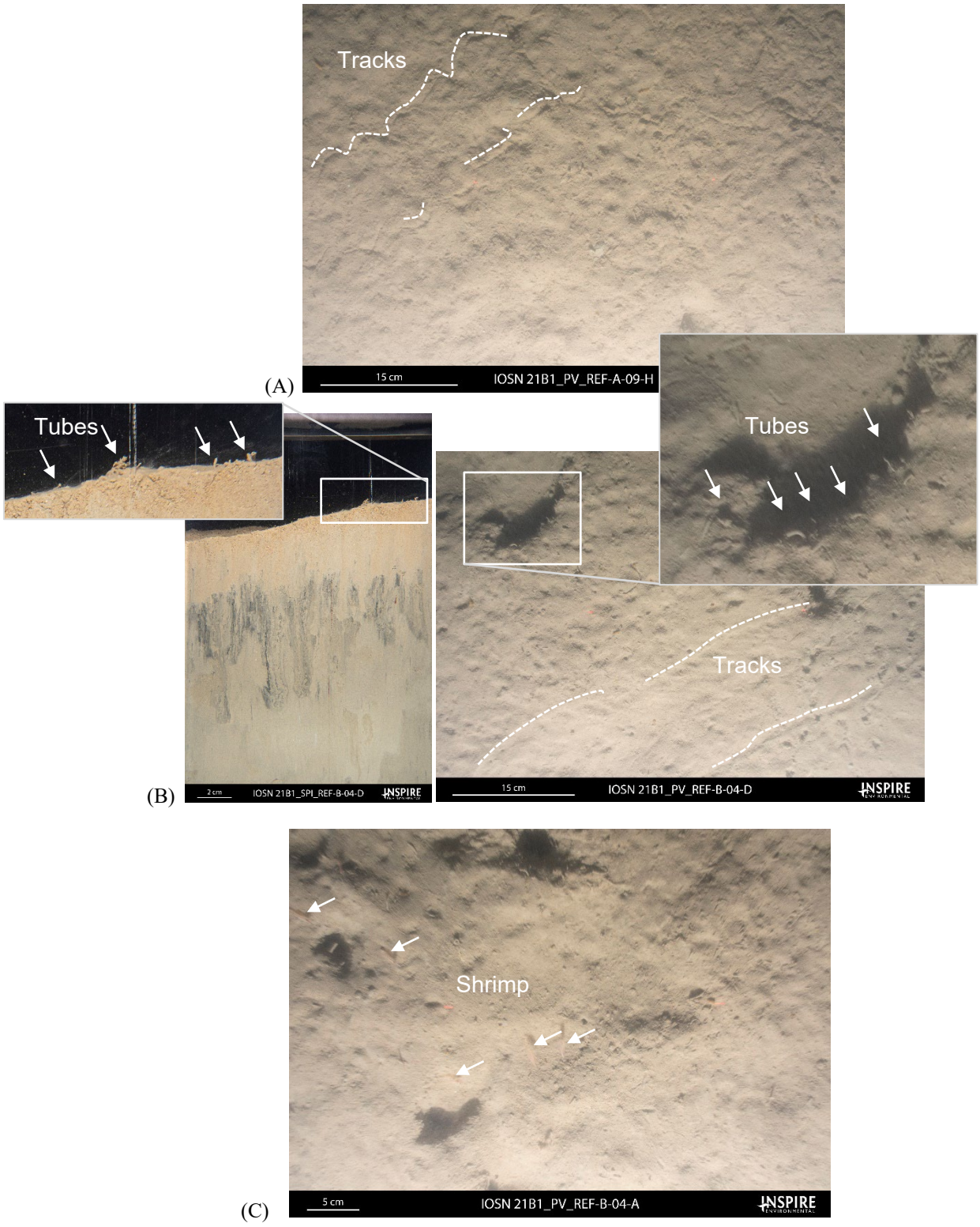

Figure 3-14. Profile and plan view images displaying surface sediment characteristics indicative of biological activity; (A) surface sediment tracks at REF-A-09; (B) surface tubes located at the sediment–water interface at REF-B-04; and (C) presence of shrimp at Reference Area B.

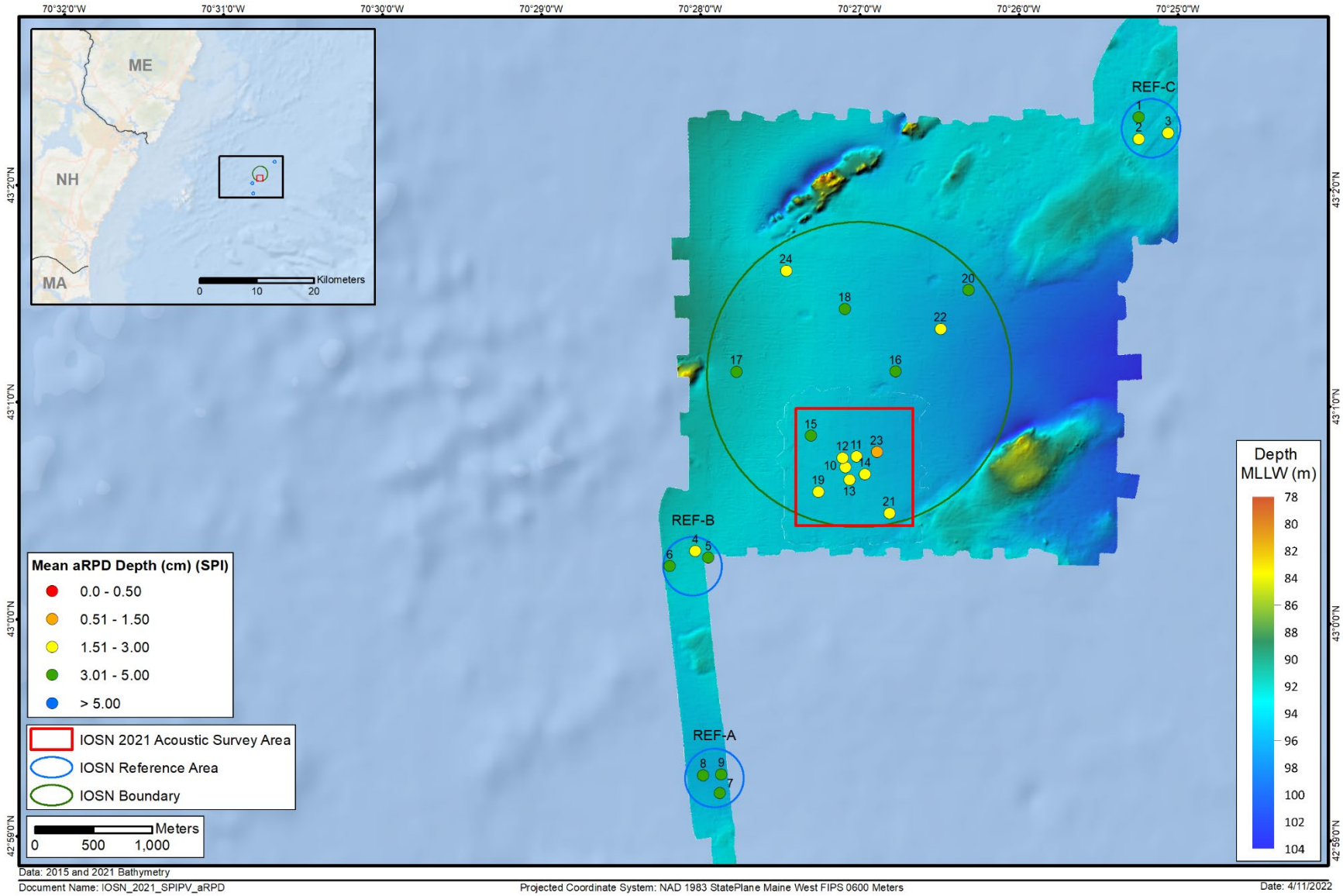

Figure 3-15. Mean station aRPD depth values (cm) at IOSN and reference areas

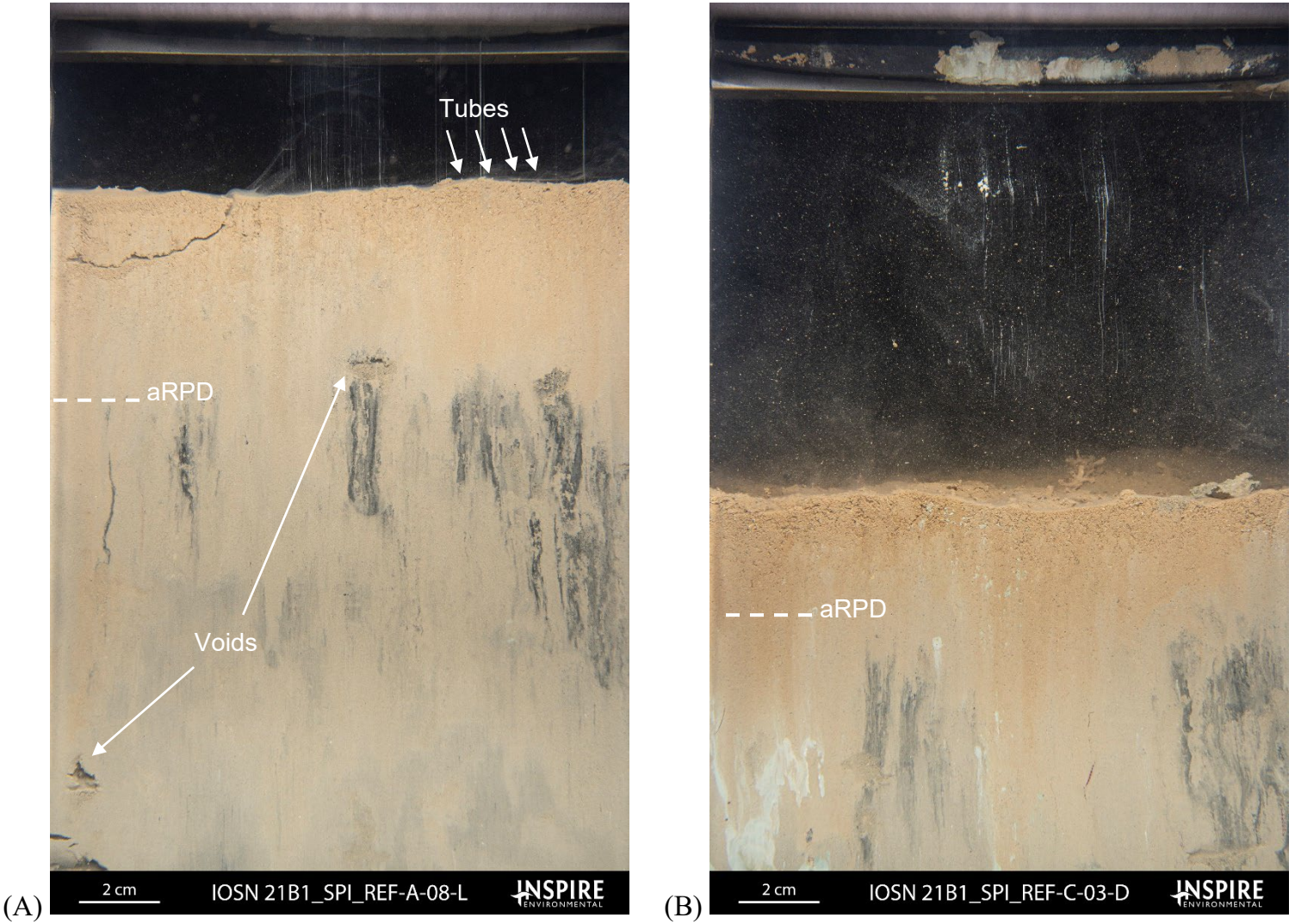

Figure 3-16. Profile images depicting a well-developed aRPD layer at the reference areas; (A) relatively deep aRPD depth at the surface over darker subsurface layer, as well as surficial tubes and feeding voids visible in image; and (B) relatively shallow aRPD depth at REF-C with evidence of clay clasts on the surface and subsurface clay deposits

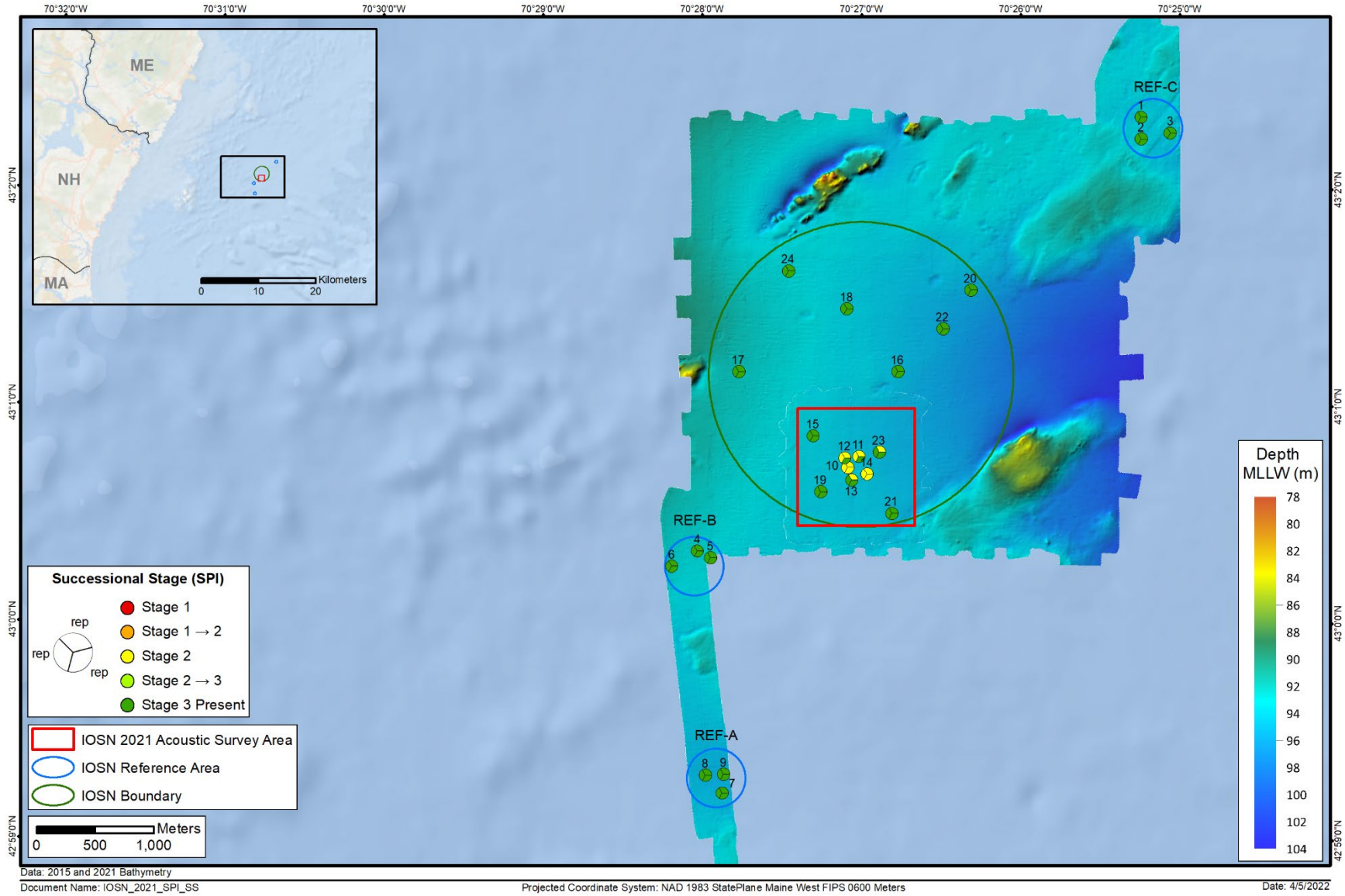

Figure 3-17. Infaunal successional stages at IOSN and reference areas. Results shown provide a value for each of three replicate images at each sampling station.

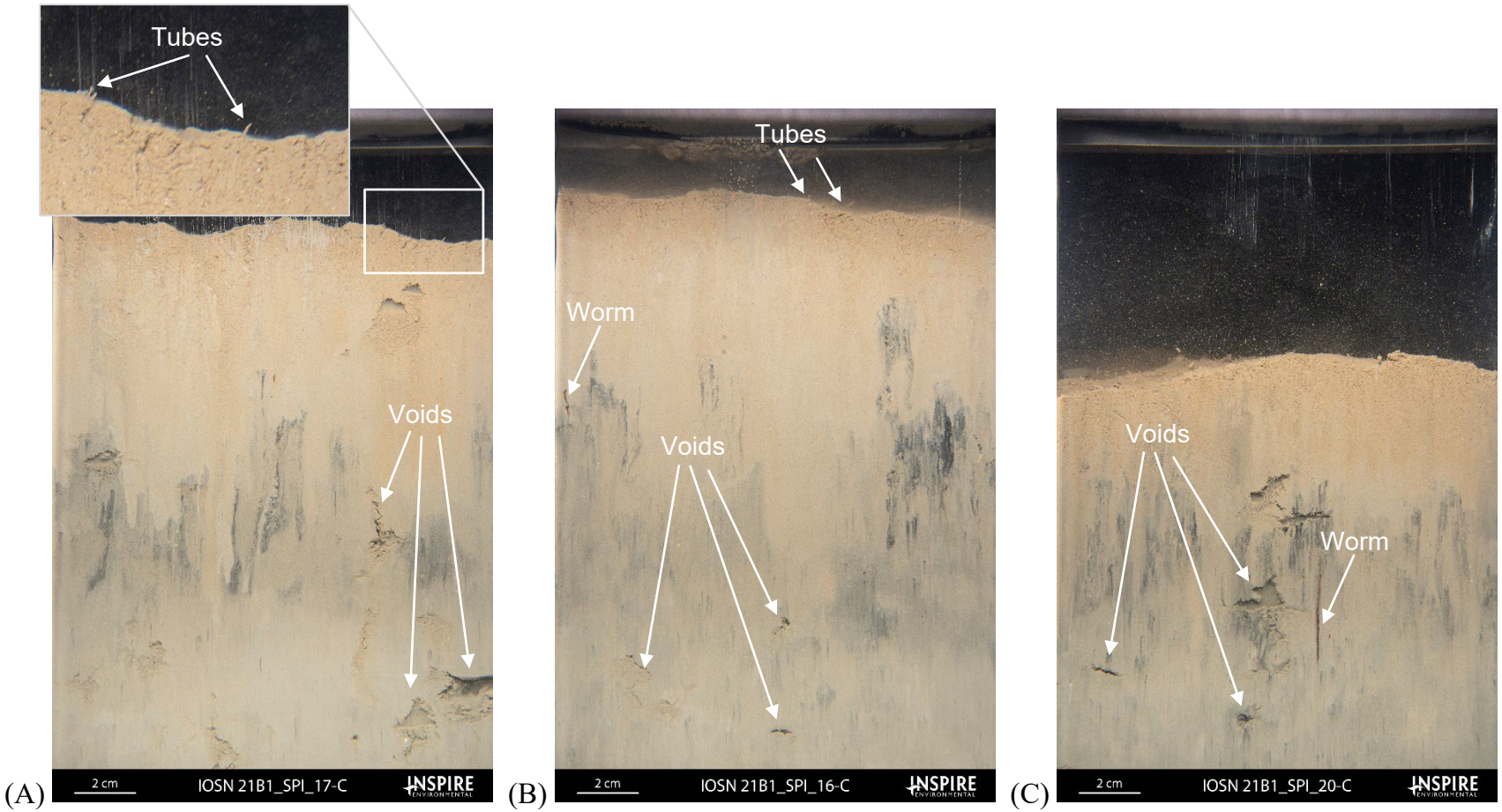

Figure 3-18. Profile images depicting successional stage characteristics at IOSN baseline stations; (A) deep feeding voids and tubes at the sediment–water interface (IOSN-17); (B) presence of Stage 3 organisms including deep feeding voids and polychaete worms at depth, tubes at the sediment–water interface (IOSN-16); and (C) presence of Stage 3 fauna, deep feeding voids, and large polychaete worm (IOSN-20)

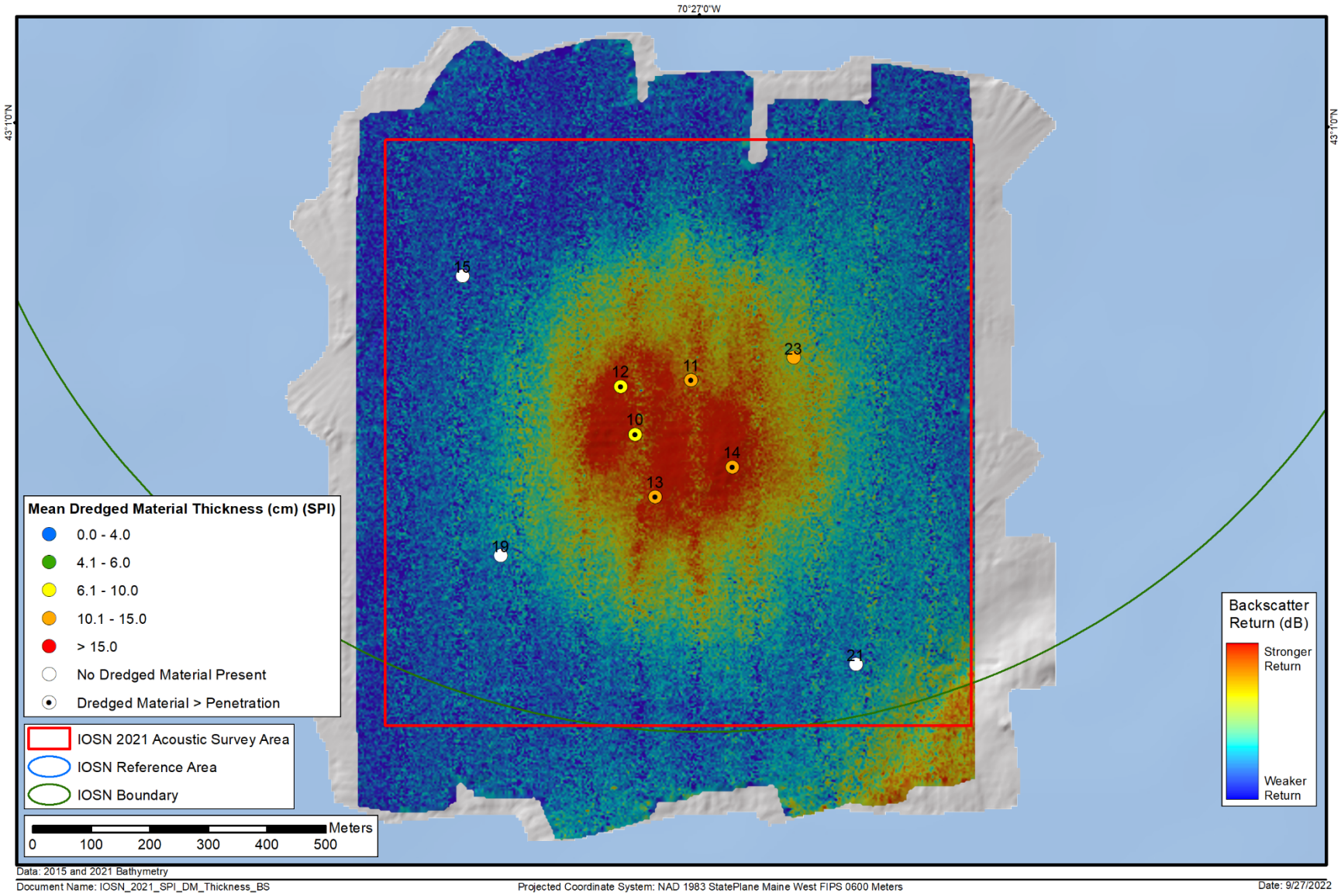

Figure 3-19. SPI/PV stations located within the active disposal area of IOSN, displaying DM thickness

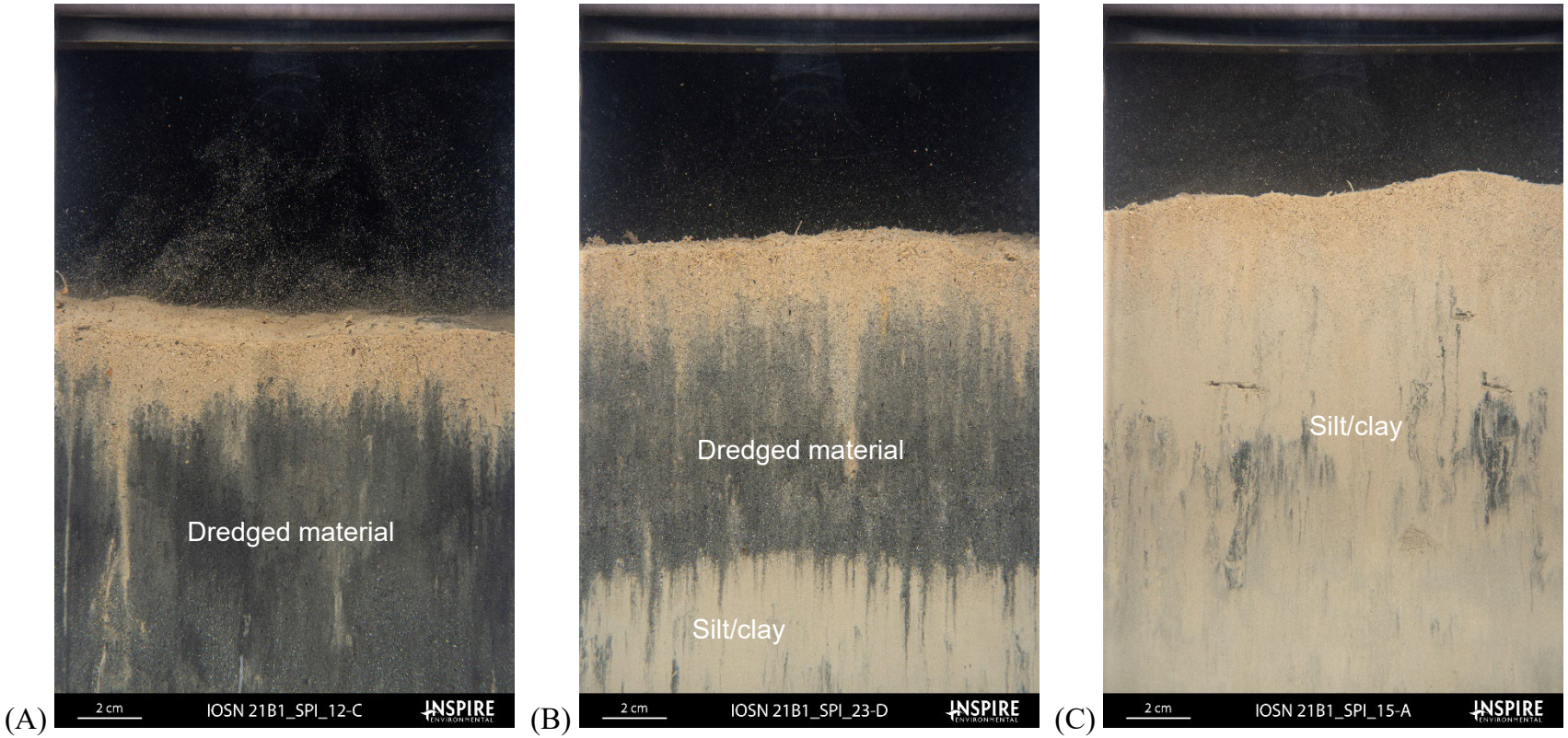

Figure 3-20. Profile images depicting grain size variation and dredged material presence at locations within the active IOSN site; (A) dredged material throughout, with reworked dredged material at the sediment–water interface; (B) light brown fine dredged material that becomes darker and more reduced over silt/clay layer; and (C) silt/clay layer throughout SPI image, outside of the dredged material footprint

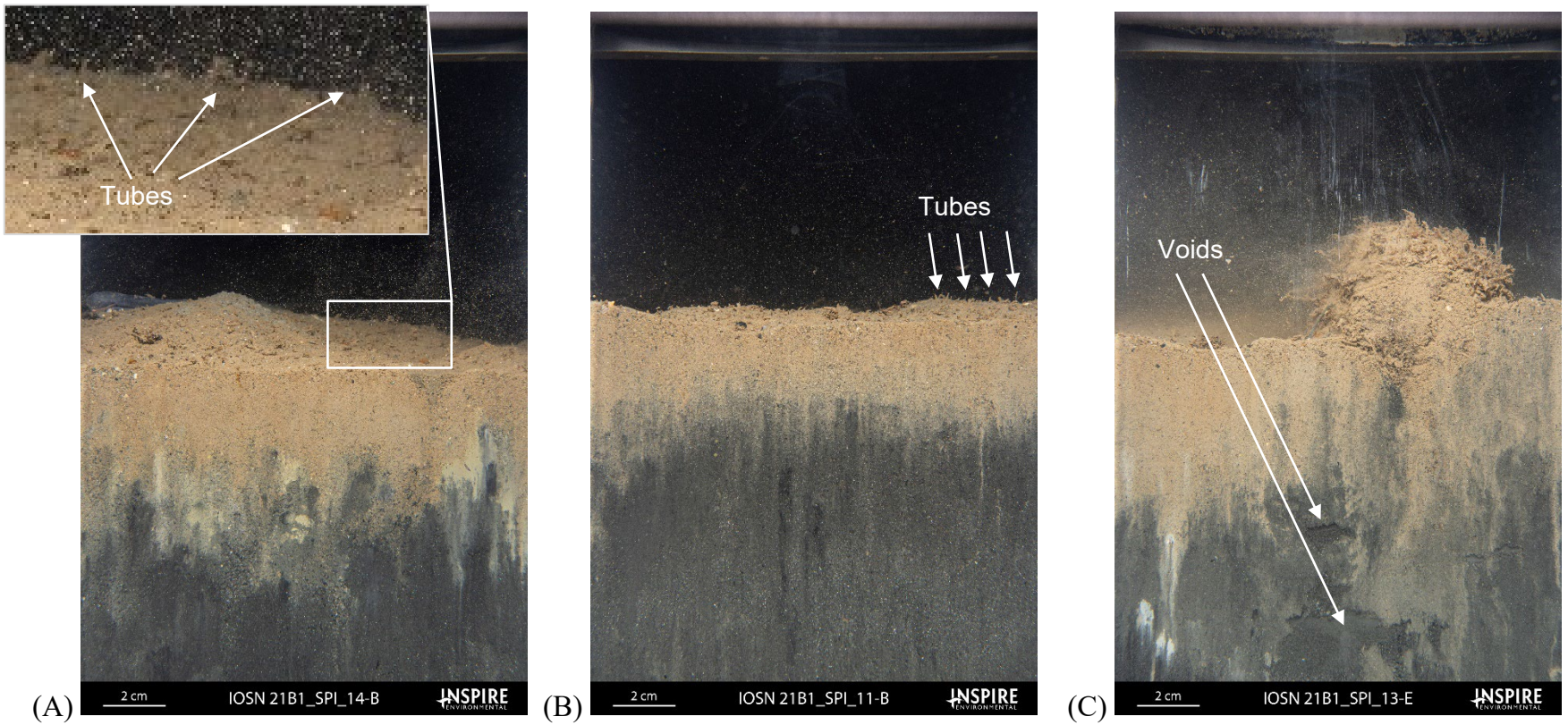

Figure 3-21. Profile images depicting different successional stages at the active disposal area; (A) Stage 2 tubes at the sediment–water interface; (B) Stage 2 organisms, tubes at the sediment–water interface located on the dredged material apron; and (C) Stage 2 on 3 succession with deep feeding voids located where dredged material was prominent based on disposal event logs and MBES data

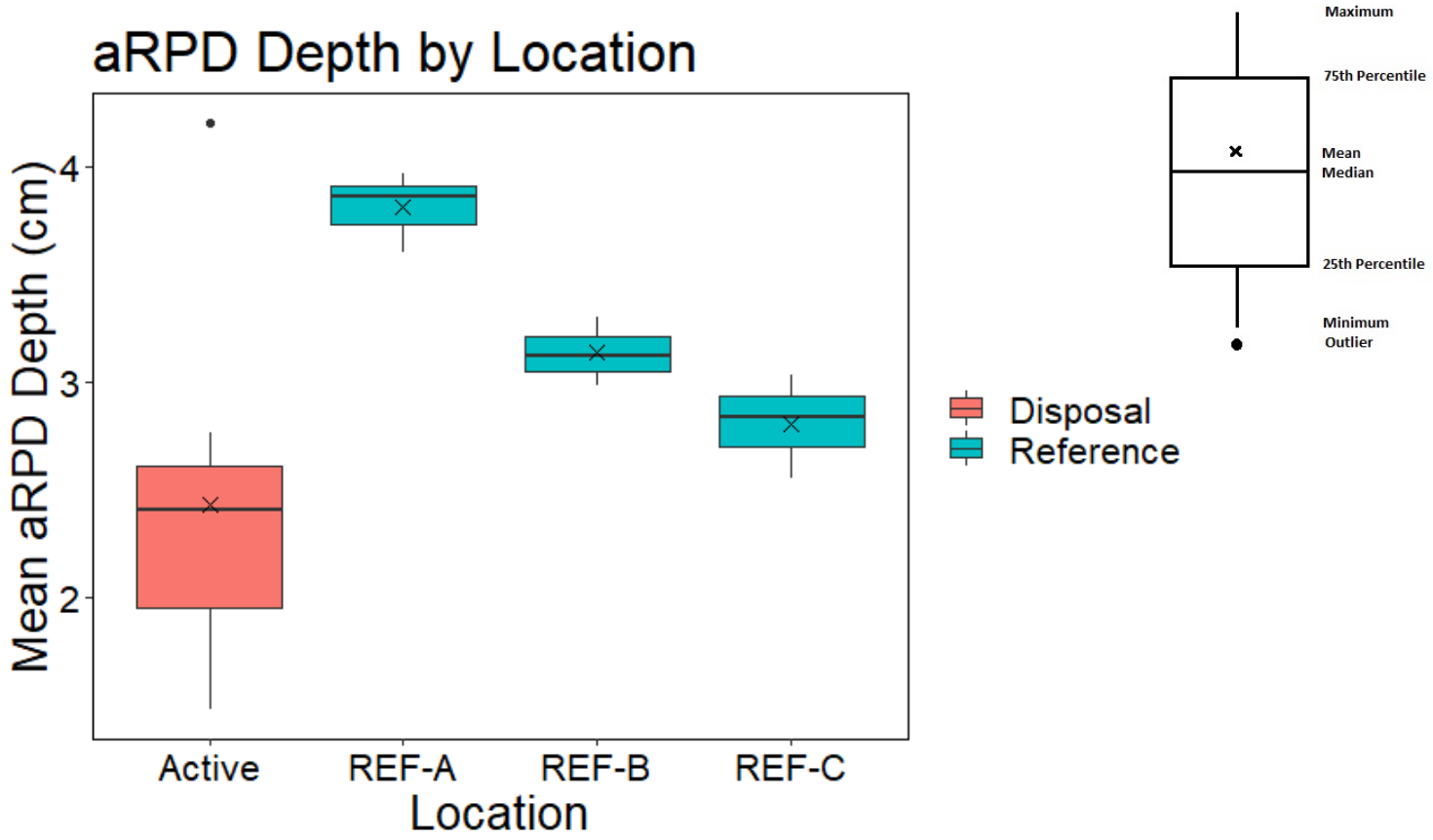

Figure 3-22. Distribution of aRPD depth measurements by sampling area at IOSN and reference areas

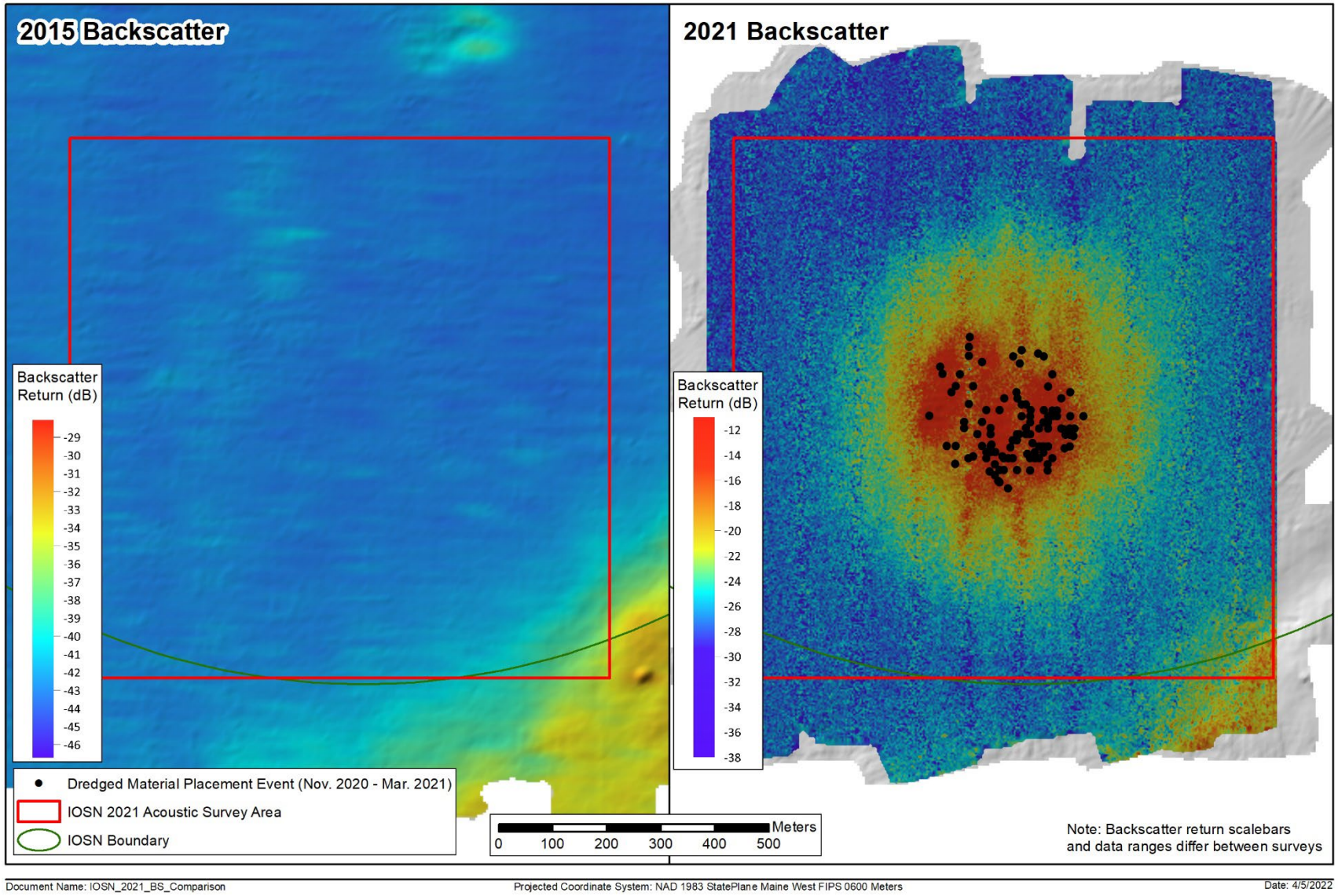

Figure 4-1. Comparison of 2015 and 2021 filtered backscatter with recent disposal events

MONITORING SURVEY AT THE
ISLES OF SHOALS NORTH DISPOSAL SITE
OCTOBER 2021

APPENDICES

CONTRIBUTION #214

September 2022

Contract No. W912WJ-19-D-0010
Delivery Order W912WJ21F0113

Funded and Managed by:
New England District
U.S. Army Corps of Engineers
696 Virginia Road
Concord, MA 01742-2751

Prepared by:
INSPIRE ENVIRONMENTAL
INSPIRE Environmental
513 Broadway
Newport, RI 02840

LIST OF APPENDICES

APPENDIX A - TABLE OF COMMON CONVERSIONS

APPENDIX A

TABLE OF COMMON CONVERSIONS

Metric Unit	**Conversion to English Unit**	**English Unit**	**Conversion to Metric Unit**
1 meter	3.2808 ft	1 foot	0.3048 m
1 m		1 ft	
1 square meter	10.7639 ft^2	1 square foot	0.0929 m^2
1 m^2		1 ft^2	
1 kilometer	0.6214 mi	1 mile	1.6093 km
1 km		1 mi	
1 cubic meter	1.3080 yd^3	1 cubic yard	0.7646 m^3
1 m^3		1 yd^3	
1 centimeter	0.3937 in	1 inch	2.54 cm
1 cm		1 in	

APPENDIX B - IOSN DISPOSAL LOG DATA, NOV 2020 - MARCH 2021

Notes:

Disposal Log Data provided by USACE NAE, February 2022

Project ID	Scow ID	Disposal Site	Load volume (m^3)	Load volume (yd^3)	Placement date/time	Placement latitude	Placement longitude	Permit Number*
Rye Harbor FNP	Barge 15	IOSN	316.9	414.5	21-Nov-20	43.01268	-70.45005	W912WJ-20-C-0016
Rye Harbor FNP	Barge 15	IOSN	69.0	90.2	22-Nov-20	43.01113	-70.45043	W912WJ-20-C-0016
Rye Harbor FNP	Barge 15	IOSN	98.9	129.3	25-Nov-20	43.0115	-70.45005	W912WJ-20-C-0016
Rye Harbor FNP	Barge 15	IOSN	69.5	90.9	25-Nov-20	43.01113	-70.4511	W912WJ-20-C-0016
Rye Harbor FNP	Barge 15	IOSN	492.0	643.5	26-Nov-20	43.0111	-70.4502	W912WJ-20-C-0016
Rye Harbor FNP	Barge 15	IOSN	522.0	682.7	26-Nov-20	43.0123	-70.4515	W912WJ-20-C-0016
Rye Harbor FNP	Barge 15	IOSN	453.8	593.6	27-Nov-20	43.0115	-70.451	W912WJ-20-C-0016
Rye Harbor FNP	Barge 15	IOSN	127.3	166.5	28-Nov-20	43.01117	-70.44987	W912WJ-20-C-0016
Rye Harbor FNP	Barge 15	IOSN	556.0	727.2	28-Nov-20	43.01117	-70.44987	W912WJ-20-C-0016
Rye Harbor FNP	Barge 15	IOSN	534.0	698.5	29-Nov-20	43.0113	-70.4494	W912WJ-20-C-0016
Rye Harbor FNP	Barge 15	IOSN	526.0	688	29-Nov-20	43.0115	-70.449	W912WJ-20-C-0016
Rye Harbor FNP	Barge 15	IOSN	579.6	758.1	4-Dec-20	43.0116	-70.4496	W912WJ-20-C-0016
Rye Harbor FNP	Barge 15	IOSN	548.8	717.8	4-Dec-20	43.01295	-70.4512	W912WJ-20-C-0016
Rye Harbor FNP	Barge 15	IOSN	548.8	717.8	4-Dec-20	43.0122	-70.45012	W912WJ-20-C-0016
Rye Harbor FNP	Barge 17	IOSN	547.9	716.6	4-Dec-20	43.0128	-70.4502	W912WJ-20-C-0016
Rye Harbor FNP	Barge 17	IOSN	361.0	472.2	5-Dec-20	43.01312	-70.45118	W912WJ-20-C-0016
Rye Harbor FNP	Barge 15	IOSN	479.8	627.6	7-Dec-20	43.01147	-70.44882	W912WJ-20-C-0016
Rye Harbor FNP	Barge 15	IOSN	490.6	641.7	7-Dec-20	43.0113	-70.4515	W912WJ-20-C-0016
Rye Harbor FNP	Barge 17	IOSN	472.6	618.1	7-Dec-20	43.01127	-70.44902	W912WJ-20-C-0016
Rye Harbor FNP	Barge 17	IOSN	431.6	564.5	7-Dec-20	43.01285	-70.44963	W912WJ-20-C-0016
Rye Harbor FNP	Barge 15	IOSN	292.7	382.9	8-Dec-20	43.01082	-70.4506	W912WJ-20-C-0016
Rye Harbor FNP	Barge 17	IOSN	490.7	641.8	8-Dec-20	43.01088	-70.45072	W912WJ-20-C-0016
Rye Harbor FNP	Barge 15	IOSN	495.3	647.8	10-Dec-20	43.0109	-70.4498	W912WJ-20-C-0016
Rye Harbor FNP	Barge 15	IOSN	577.2	754.9	10-Dec-20	43.0111	-70.4498	W912WJ-20-C-0016
Rye Harbor FNP	Barge 15	IOSN	583.6	763.3	11-Dec-20	43.0129	-70.45	W912WJ-20-C-0016
Rye Harbor FNP	Barge 17	IOSN	518.0	677.5	11-Dec-20	43.0111	-70.4502	W912WJ-20-C-0016
Rye Harbor FNP	Barge 15	IOSN	353.7	462.6	12-Dec-20	43.0118	-70.4494	W912WJ-20-C-0016
Rye Harbor FNP	Barge 15	IOSN	234.7	307	12-Dec-20	43.0115	-70.4507	W912WJ-20-C-0016
Rye Harbor FNP	Barge 17	IOSN	475.6	622.1	12-Dec-20	43.0128	-70.4495	W912WJ-20-C-0016
Rye Harbor FNP	Barge 17	IOSN	389.7	509.7	12-Dec-20	43.0111	-70.4508	W912WJ-20-C-0016
Rye Harbor FNP	Barge 17	IOSN	262.5	343.4	13-Dec-20	43.0123	-70.4511	W912WJ-20-C-0016
Rye Harbor FNP	Barge 15	IOSN	489.4	640.1	14-Dec-20	43.0118	-70.4492	W912WJ-20-C-0016
Rye Harbor FNP	Barge 15	IOSN	403.3	527.5	14-Dec-20	43.0112	-70.4507	W912WJ-20-C-0016
Rye Harbor FNP	Barge 17	IOSN	464.5	607.5	14-Dec-20	43.0115	-70.4501	W912WJ-20-C-0016
Rye Harbor FNP	Barge 17	IOSN	300.9	393.6	14-Dec-20	43.0106	-70.4503	W912WJ-20-C-0016
Rye Harbor FNP	Barge 15	IOSN	575.4	752.6	16-Dec-20	43.0115	-70.4499	W912WJ-20-C-0016
Rye Harbor FNP	Barge 15	IOSN	317.9	415.8	16-Dec-20	43.0116	-70.4513	W912WJ-20-C-0016
Rye Harbor FNP	Barge 17	IOSN	204.4	267.4	16-Dec-20	43.0116	-70.4494	W912WJ-20-C-0016
Rye Harbor FNP	Barge 17	IOSN	116.1	151.9	19-Dec-20	43.0125	-70.4518	W912WJ-20-C-0016
Rye Harbor FNP	Barge 15	IOSN	499.2	652.9	20-Dec-20	43.0128	-70.4512	W912WJ-20-C-0016
Rye Harbor FNP	Barge 15	IOSN	121.3	158.6	20-Dec-20	43.0118	-70.4493	W912WJ-20-C-0016
Rye Harbor FNP	Barge 17	IOSN	438.0	572.9	20-Dec-20	43.0122	-70.4516	W912WJ-20-C-0016

Project ID	Scow ID	Disposal Site	Load volume (m^3)	Load volume (yd^3)	Placement date/time	Placement latitude	Placement longitude	Permit Number*
Rye Harbor FNP	Barge 15	IOSN	299.4	391.6	21-Dec-20	43.0118		W912WJ-20-C-0016
Rye Harbor FNP	Barge 17	IOSN	287.0	375.4	21-Dec-20	43.0114		W912WJ-20-C-0016
Rye Harbor FNP	Barge 17	IOSN	331.1	433.1	21-Dec-20	43.0114		W912WJ-20-C-0016
Rye Harbor FNP	Barge 15	IOSN	421.5	551.3	22-Dec-20	43.0112		W912WJ-20-C-0016
Rye Harbor FNP	Barge 15	IOSN	421.6	551.4	22-Dec-20	43.0116		W912WJ-20-C-0016
Rye Harbor FNP	Barge 17	IOSN	381.8	499.4	22-Dec-20	43.0119		W912WJ-20-C-0016
Rye Harbor FNP	Barge 15	IOSN	310.6	406.2	23-Dec-20	43.0116		W912WJ-20-C-0016
Rye Harbor FNP	Barge 17	IOSN	300.9	393.5	23-Dec-20	43.0118		W912WJ-20-C-0016
Rye Harbor FNP	Barge 15	IOSN	353.7	462.6	27-Dec-20	43.0119		W912WJ-20-C-0016
Rye Harbor FNP	Barge 15	IOSN	411.0	537.6	28-Dec-20	43.0127		W912WJ-20-C-0016
Rye Harbor FNP	Barge 17	IOSN	379.8	496.8	28-Dec-20	43.0117		W912WJ-20-C-0016
Rye Harbor FNP	Barge 15	IOSN	454.9	595	29-Dec-20	43.0119		W912WJ-20-C-0016
Rye Harbor FNP	Barge 17	IOSN	420.0	549.3	29-Dec-20	43.0116		W912WJ-20-C-0016
Rye Harbor FNP	Barge 15	IOSN	313.8	410.5	30-Dec-20	43.0117		W912WJ-20-C-0016
Rye Harbor FNP	Barge 17	IOSN	362.9	474.7	30-Dec-20	43.0119		W912WJ-20-C-0016
Rye Harbor FNP	Barge 15	IOSN	345.4	451.8	1-Jan-21	43.0115		W912WJ-20-C-0016
Rye Harbor FNP	Barge 15	IOSN	386.0	504.9	1-Jan-21	43.0111		W912WJ-20-C-0016
Rye Harbor FNP	Barge 17	IOSN	400.4	523.7	1-Jan-21	43.0118		W912WJ-20-C-0016
Rye Harbor FNP	Barge 17	IOSN	382.1	499.8	1-Jan-21	43.0116		W912WJ-20-C-0016
Rye Harbor FNP	Barge 15	IOSN	364.2	476.4	7-Jan-21	43.0121	-70.4491	W912WJ-20-C-0016
Rye Harbor FNP	Barge 15	IOSN	412.7	539.8	8-Jan-21	43.01072	-70.45053	W912WJ-20-C-0016
Rye Harbor FNP	Barge 17	IOSN	393.4	514.6	8-Jan-21	43.0111	-70.4493	W912WJ-20-C-0016
Rye Harbor FNP	Barge 17	IOSN	167.4	218.9	8-Jan-21	43.0121	-70.4504	W912WJ-20-C-0016
Rye Harbor FNP	Barge 15	IOSN	303.8	397.4	9-Jan-21	43.0107	-70.4505	W912WJ-20-C-0016
Rye Harbor FNP	Barge 15	IOSN	475.9	622.5	10-Jan-21	43.0117	-70.4513	W912WJ-20-C-0016
Rye Harbor FNP	Barge 15	IOSN	461.0	603	10-Jan-21	43.0119	-70.4508	W912WJ-20-C-0016
Rye Harbor FNP	Barge 17	IOSN	462.1	604.4	10-Jan-21	43.0112	-70.4506	W912WJ-20-C-0016
Rye Harbor FNP	Barge 15	IOSN	507.6	663.9	11-Jan-21	43.0114	-70.4502	W912WJ-20-C-0016
Rye Harbor FNP	Barge 15	IOSN	424.4	555.1	11-Jan-21	43.012	-70.4499	W912WJ-20-C-0016
Rye Harbor FNP	Barge 17	IOSN	453.1	592.6	11-Jan-21	43.0109	-70.4494	W912WJ-20-C-0016
Rye Harbor FNP	Barge 17	IOSN	413.3	540.6	11-Jan-21	43.0111	-70.4502	W912WJ-20-C-0016
Rye Harbor FNP	Barge 15	IOSN	498.3	651.7	12-Jan-21	43.0113	-70.4507	W912WJ-20-C-0016
Rye Harbor FNP	Barge 17	IOSN	344.0	449.9	12-Jan-21	43.0115	-70.4489	W912WJ-20-C-0016
Rye Harbor FNP	Barge 17	IOSN	502.2	656.8	12-Jan-21	43.0109	-70.4501	W912WJ-20-C-0016
Rye Harbor FNP	Barge 15	IOSN	357.3	467.3	13-Jan-21	43.0117	-70.4498	W912WJ-20-C-0016
Rye Harbor FNP	Barge 15	IOSN	466.9	610.7	13-Jan-21	43.0115	-70.451	W912WJ-20-C-0016
Rye Harbor FNP	Barge 17	IOSN	406.3	531.4	13-Jan-21	43.0111	-70.4496	W912WJ-20-C-0016
Rye Harbor FNP	Barge 15	IOSN	627.5	820.8	14-Jan-21	43.0117	-70.4509	W912WJ-20-C-0016
Rye Harbor FNP	Barge 17	IOSN	506.1	661.9	14-Jan-21	43.0112	-70.4508	W912WJ-20-C-0016
Rye Harbor FNP	Barge 17	IOSN	352.7	461.3	15-Jan-21	43.0112	-70.4497	W912WJ-20-C-0016
Rye Harbor FNP	Barge 15	IOSN	536.1	701.2	20-Jan-21	43.0121	-70.4501	W912WJ-20-C-0016
Rye Harbor FNP	Barge 15	IOSN	421.5	551.3	20-Jan-21	43.0116	-70.4507	W912WJ-20-C-0016

Project ID	Scow ID	Disposal Site	Load volume (m^3)	Load volume (yd^3)	Placement date/time	Placement latitude	Placement longitude	Permit Number*
Rye Harbor FNP	Barge 17	IOSN	506.3	662.2	20-Jan-21	43.0119	-70.4495	W912WJ-20-C-0016
Rye Harbor FNP	Barge 17	IOSN	425.9	557.1	20-Jan-21	43.0113	-70.4495	W912WJ-20-C-0016
Rye Harbor FNP	Barge 17	IOSN	381.5	499	21-Jan-21	43.0122	-70.4489	W912WJ-20-C-0016
Rye Harbor FNP	Barge 15	IOSN	465.6	609	22-Jan-21	43.012	-70.4512	W912WJ-20-C-0016
Rye Harbor FNP	Barge 17	IOSN	416.5	544.8	22-Jan-21	43.0113	-70.4509	W912WJ-20-C-0016
Rye Harbor FNP	Barge 17	IOSN	254.9	333.4	25-Jan-21	43.012	-70.45	W912WJ-20-C-0016
Rye Harbor FNP	Barge 15	IOSN	553.2	723.5	26-Jan-21	43.011	-70.4494	W912WJ-20-C-0016
Rye Harbor FNP	Barge 17	IOSN	382.2	499.9	26-Jan-21	43.0118	-70.4521	W912WJ-20-C-0016
Rye Harbor FNP	Barge 17	IOSN	438.2	573.2	27-Jan-21	43.011	-70.4506	W912WJ-20-C-0016
Rye Harbor FNP	Barge 15	IOSN	500.5	654.6	28-Jan-21	43.011	-70.4515	W912WJ-20-C-0016
Rye Harbor FNP	Barge 17	IOSN	377.2	493.4	28-Jan-21	43.0113	-70.4517	W912WJ-20-C-0016
Rye Harbor FNP	Barge 17	IOSN	466.2	609.8	28-Jan-21	43.0111	-70.4503	W912WJ-20-C-0016
Rye Harbor FNP	Barge 15	IOSN	468.7	613.1	5-Feb-21	43.0109	-70.4505	W912WJ-20-C-0016
Rye Harbor FNP	Barge 17	IOSN	532.1	695.9	5-Feb-21	43.0111	-70.4504	W912WJ-20-C-0016
Rye Harbor FNP	Barge 15	IOSN	423.5	553.9	9-Feb-21	43.0125	-70.4493	W912WJ-20-C-0016
Rye Harbor FNP	Barge 17	IOSN	389.2	509.1	9-Feb-21	43.0113	-70.4489	W912WJ-20-C-0016
Rye Harbor FNP	Barge 17	IOSN	468.1	612.3	9-Feb-21	43.0111	-70.4512	W912WJ-20-C-0016
Rye Harbor FNP	Barge 15	IOSN	419.4	548.5037037	10-Feb-21	43.01112	-70.44975	W912WJ-20-C-0016
Rye Harbor FNP	Barge 17	IOSN	409.1	535.1	10-Feb-21	43.0118	-70.45	W912WJ-20-C-0016
Rye Harbor FNP	Barge 15	IOSN	393.8	515.0814815	11-Feb-21	43.01133	-70.45068	W912WJ-20-C-0016
Rye Harbor FNP	Barge 17	IOSN	520.5	680.8	11-Feb-21	43.0113	-70.4496	W912WJ-20-C-0016
Rye Harbor FNP	Barge 15	IOSN	399.8	522.9037037	12-Feb-21	43.01158	-70.44903	W912WJ-20-C-0016
Rye Harbor FNP	Barge 15	IOSN	426.2	557.4	17-Feb-21	43.0109	-70.4504	W912WJ-20-C-0016
Rye Harbor FNP	Barge 17	IOSN	394.6	516.1	18-Feb-21	43.0125	-70.4514	W912WJ-20-C-0016
Tom Bluoin Property	Barge 15	IOSN	507.4	663.6246914	26-Feb-21	43.01128	-70.45025	NAE-2016-2159
Tom Bluoin Property	Barge 15	IOSN	550.1	719.4864198	28-Feb-21	43.01262	-70.45185	NAE-2016-2159
Tom Bluoin Property	Barge 15	IOSN	505.2	660.7802469	3-Mar-21	43.01135	-70.44975	NAE-2016-2159
Tom Bluoin Property	Barge 17	IOSN	570.7	746.4	7-Mar-21	43.0123	-70.4494	NAE-2016-2159

* The FNP contract included dredging approximately 8,150 cubic yards from the Rye Harbor State Anchorage (permit number NAE-2019-02222) at 100% non-Federal cost through a Memorandum of Understating with the State of New Hampshire.

APPENDIX C - ACTUAL SPI/PV REPLICATE LOCATIONS

Category	Sample Type	Station ID	Replicate	Date	Time	X_MaineWestSP_m	Y_MaineWestSP_m	Latitude_NAD83_N	Longitude_NAD83_W	Depth (m)	Comments
Reference	SPI/PV	REF-A-07	A	10/6/2021	7:41:30	875723.91	17099.55	42.98687525	-70.46432963	97.84	
Reference	SPI/PV	REF-A-07	B	10/6/2021	7:42:50	875720.11	17099.51	42.98687477	-70.46437622	97.84	
Reference	SPI/PV	REF-A-07	C	10/6/2021	7:45:08	875730.28	17097.04	42.98685286	-70.46425141	97.84	
Reference	SPI/PV	REF-A-09	B	10/6/2021	7:53:33	875736.15	17259.65	42.98831681	-70.4641865	98.45	
Reference	SPI/PV	REF-A-09	C	10/6/2021	7:54:47	875732.17	17257.62	42.98829841	-70.46423521	98.45	
Reference	SPI/PV	REF-A-08	A	10/6/2021	8:02:51	875579.86	17250.73	42.98823151	-70.46610249	98.76	
Reference	SPI/PV	REF-A-08	E	10/6/2021	8:33:38	875582.62	17253.38	42.98825546	-70.46606876	98.76	
Reference	SPI/PV	REF-A-08	I	10/6/2021	9:05:06	875580.7	17252.01	42.98824306	-70.46609224	98.76	
Reference	SPI/PV	REF-A-08	J	10/6/2021	9:06:07	875583.23	17251.38	42.98823747	-70.4660612	98.76	
Reference	SPI/PV	REF-A-08	L	10/6/2021	9:08:25	875579.82	17256.11	42.98827994	-70.46610321	98.76	
Reference	SPI/PV	REF-A-07	E	10/6/2021	9:29:18	875725.86	17096.43	42.98684722	-70.46430558	97.84	
Reference	SPI/PV	REF-A-09	E	10/6/2021	9:36:25	875733.44	17257.73	42.98829944	-70.46421964	98.45	
Reference	SPI/PV	REF-B-06	A	10/6/2021	10:00:23	875294.24	19035.15	43.00428506	-70.46968358	95.4	
Reference	SPI/PV	REF-B-06	B	10/6/2021	10:02:03	875301.83	19036.82	43.00430034	-70.46959056	95.4	
Reference	SPI/PV	REF-B-06	C	10/6/2021	10:03:14	875299.26	19034.36	43.00427811	-70.46962198	95.4	
Reference	SPI/PV	REF-B-06	D	10/6/2021	10:04:33	875297.62	19040.54	43.00433369	-70.46964236	95.4	
Reference	SPI/PV	REF-B-05	A	10/6/2021	10:19:03	875624.88	19106.45	43.00493754	-70.46563144	84.43	
Reference	SPI/PV	REF-B-05	B	10/6/2021	10:20:31	875620.78	19103.48	43.00491067	-70.46568159	84.43	
Reference	SPI/PV	REF-B-05	D	10/6/2021	10:23:30	875618.65	19107.47	43.00494652	-70.46570789	84.43	
Reference	SPI/PV	REF-B-04	A	10/6/2021	10:29:33	875512.22	19165.74	43.00546763	-70.46701581	97.54	
Reference	SPI/PV	REF-B-04	B	10/6/2021	10:30:49	875511.67	19163.97	43.00545168	-70.46702248	97.54	
Reference	SPI/PV	REF-B-04	C	10/6/2021	10:32:11	875509.4	19164.7	43.00545818	-70.46705035	97.54	
Reference	SPI/PV	REF-B-04	D	10/6/2021	10:33:22	875509.38	19170.27	43.00550832	-70.46705084	97.54	
Active	SPI/PV	21	A	10/6/2021	10:52:29	877171.82	19484.31	43.0083869	-70.44667365	97.54	
Active	SPI/PV	21	B	10/6/2021	10:53:49	877166.77	19486.4	43.00840556	-70.44673567	97.54	
Active	SPI/PV	21	D	10/6/2021	10:56:23	877166.47	19480.53	43.00835271	-70.44673911	97.54	
Active	SPI/PV	19	A	10/6/2021	11:12:37	876565.84	19669.73	43.01003756	-70.4541142	96.93	
Active	SPI/PV	19	B	10/6/2021	11:14:05	876562.57	19670.83	43.01004736	-70.45415435	96.93	
Active	SPI/PV	19	D	10/6/2021	11:16:36	876564.91	19676.2	43.01009577	-70.45412588	96.93	
Active	SPI/PV	13	B	10/6/2021	11:27:04	876826.25	19776.18	43.01100376	-70.45092442	99.67	
Active	SPI/PV	13	C	10/6/2021	11:28:30	876831.33	19775.18	43.01099492	-70.45086207	99.67	
Active	SPI/PV	13	D	10/6/2021	11:30:02	876829.41	19769.5	43.01094373	-70.45088538	99.67	
Active	SPI/PV	14	A	10/6/2021	11:36:22	876960.92	19820.63	43.01140798	-70.44927436	99.06	
Active	SPI/PV	14	B	10/6/2021	11:37:56	876956.66	19826.28	43.01145871	-70.44932685	99.06	
Active	SPI/PV	14	C	10/6/2021	11:39:18	876959	19825.98	43.01145608	-70.44929813	99.06	
Active	SPI/PV	10	A	10/6/2021	11:48:39	876794.85	19876.43	43.01190522	-70.45131375	99.36	
Active	SPI/PV	10	C	10/6/2021	11:51:31	876794.79	19881.54	43.01195122	-70.4513147	99.36	Hypack crashed on Drop D.
Active	SPI/PV	10	E	10/6/2021	11:55:07	876798.83	19877.97	43.01191921	-70.45126499	99.36	
Active	SPI/PV	12	A	10/6/2021	12:02:07	876770.87	19955.46	43.01261589	-70.45161118	99.36	
Active	SPI/PV	12	B	10/6/2021	12:03:31	876770.36	19958.04	43.0126391	-70.45161755	99.36	
Active	SPI/PV	12	C	10/6/2021	12:04:58	876772.07	19955.27	43.01261422	-70.45159646	99.36	
Active	SPI/PV	12	D	10/6/2021	12:06:23	876765.65	19960.88	43.01266452	-70.45167544	99.36	
Active	SPI/PV	11	A	10/6/2021	12:19:59	876890.15	19969.05	43.01274186	-70.45014859	99.36	
Active	SPI/PV	11	B	10/6/2021	12:21:16	876879.23	19971.61	43.01276457	-70.45028265	99.36	
Active	SPI/PV	11	C	10/6/2021	12:22:37	876883.88	19972.53	43.01277299	-70.45022565	99.36	
Active	SPI/PV	23	A	10/6/2021	12:30:01	877065.62	20007.59	43.01309409	-70.44799776	99.97	
Active	SPI/PV	23	B	10/6/2021	12:31:21	877067.23	20012.83	43.01314131	-70.44797823	99.97	
Active	SPI/PV	23	C	10/6/2021	12:32:42	877066.42	20008.82	43.01310519	-70.447988	99.97	

Category	Sample Type	Station ID	Replicate	Date	Time	X_MaineWestSP_m	Y_MaineWestSP_m	Latitude_NAD83_N	Longitude_NAD83_W	Depth (m)	Comments
Active	SPI/PV	23	D	10/6/2021	12:34:03	877071.52	20011.82	43.01313235	-70.44792556	99.97	
Active	SPI/PV	15	A	10/6/2021	12:46:55	876500.23	20146.8	43.01432996	-70.45493906	98.76	
Active	SPI/PV	15	B	10/6/2021	12:48:07	876501.73	20149.72	43.01435629	-70.45492078	98.76	
Active	SPI/PV	15	C	10/6/2021	12:49:16	876502.3	20151.73	43.0143744	-70.45491387	98.76	
Active	SPI/PV	15	D	10/6/2021	12:50:36	876492.81	20149.89	43.01435754	-70.45503021	98.76	
Baseline	SPI/PV	17	A	10/6/2021	13:22:05	875872.47	20694.54	43.01924086	-70.46266339	96.32	
Baseline	SPI/PV	17	B	10/6/2021	13:23:28	875866.33	20693.6	43.0192322	-70.46273867	96.32	
Baseline	SPI/PV	17	C	10/6/2021	13:24:53	875870.98	20689.75	43.01919769	-70.46268146	96.32	SPI bounced off bottom; redo.
Baseline	SPI/PV	17	D	10/6/2021	13:26:01	875877.36	20693.61	43.01923264	-70.46260336	96.32	
Baseline	SPI/PV	24	A	10/6/2021	13:44:18	876290.79	21551.94	43.02697202	-70.45756794	96.93	
Baseline	SPI/PV	24	B	10/6/2021	13:45:41	876288.17	21549.69	43.02695168	-70.45759999	96.93	
Baseline	SPI/PV	24	D	10/6/2021	13:48:00	876285.22	21547.98	43.0269362	-70.45763611	96.93	SPI bounced off bottom.
Baseline	SPI/PV	18	A	10/6/2021	14:00:01	876788.93	21229.16	43.02408184	-70.45144263	97.54	
Baseline	SPI/PV	18	B	10/6/2021	14:01:07	876784.57	21234.45	43.02412933	-70.45149634	97.54	
Baseline	SPI/PV	18	D	10/6/2021	14:03:41	876791.43	21237.87	43.02416032	-70.45141232	97.54	
Baseline	SPI/PV	22	A	10/6/2021	14:17:38	877608.65	21058.34	43.02256876	-70.44137877	99.36	
Baseline	SPI/PV	22	B	10/6/2021	14:19:09	877612.59	21061.82	43.0226002	-70.44133057	99.36	
Baseline	SPI/PV	22	D	10/6/2021	14:22:01	877615.01	21065.79	43.02263601	-70.44130104	99.36	
Baseline	SPI/PV	16	A	10/6/2021	14:32:17	877223.48	20694.02	43.01927784	-70.44608936	98.45	
Baseline	SPI/PV	16	B	10/6/2021	14:33:37	877221.53	20693.57	43.01927373	-70.44611327	98.45	
Baseline	SPI/PV	16	C	10/6/2021	14:34:46	877219.43	20691.31	43.01925333	-70.44613894	98.45	
Baseline	SPI/PV	20	A	10/6/2021	14:51:26	877847.02	21388.87	43.02555106	-70.43846744	99.06	
Baseline	SPI/PV	20	B	10/6/2021	14:52:45	877846.5	21390.93	43.02556959	-70.4384739	99.06	
Baseline	SPI/PV	20	C	10/6/2021	14:53:57	877845.39	21387.57	43.02553931	-70.43848739	99.06	
Reference	SPI/PV	REF-C-02	A	10/6/2021	15:21:14	879299.62	22677.67	43.03719332	-70.42069313	97.23	
Reference	SPI/PV	REF-C-02	B	10/6/2021	15:22:18	879296.11	22678.74	43.03720286	-70.42073624	97.23	
Reference	SPI/PV	REF-C-02	C	10/6/2021	15:23:23	879298.02	22675.65	43.0371751	-70.42071269	97.23	
Reference	SPI/PV	REF-C-02	D	10/6/2021	15:24:23	879294	22679.94	43.0372136	-70.42076218	97.23	
Reference	SPI/PV	REF-C-03	A	10/6/2021	15:30:03	879546.76	22727.88	43.03765199	-70.4176622	97.23	
Reference	SPI/PV	REF-C-03	B	10/6/2021	15:31:27	879548.85	22729.91	43.03767032	-70.41763662	97.23	
Reference	SPI/PV	REF-C-03	C	10/6/2021	15:32:29	879549.5	22727.71	43.03765053	-70.41762857	97.23	
Reference	SPI/PV	REF-C-03	D	10/6/2021	15:33:29	879553.25	22727.71	43.03765063	-70.41758255	97.23	
Reference	SPI/PV	REF-C-01	A	10/6/2021	15:40:41	879298.39	22863.19	43.03886327	-70.42071511	96.62	
Reference	SPI/PV	REF-C-01	B	10/6/2021	15:41:45	879296.72	22863.03	43.03886179	-70.4207356	96.62	
Reference	SPI/PV	REF-C-01	C	10/6/2021	15:42:49	879294.37	22864.88	43.03887838	-70.4207645	96.62	
Reference	SPI/PV	REF-C-01	E	10/6/2021	15:44:41	879295.32	22867.51	43.03890208	-70.42075294	96.62	One of the replicates bounced, redo.
Active	SPI/PV	13	E	10/6/2021	16:32:26	876828.74	19776.85	43.01100987	-70.45089391	99.67	
Active	SPI/PV	13	F	10/6/2021	16:33:25	876826.95	19774.03	43.01098443	-70.45091574	99.67	
Reference	SPI/PV	REF-A-09	H	10/6/2021	16:51:11	875732.22	17261.72	42.98833532	-70.46423478	98.45	

APPENDIX D - SEDIMENT PROFILE IMAGE ANALYSIS RESULTS

Notes:

IND=Indeterminate

N/A=Not Applicable

SWI=Sediment–water interface

Grain Size: "/" indicates layer of one phi size range over another.

Successional Stage: "on" indicates one Stage is found on top of another Stage (i.e., 1 on 3).

Station ID	Replicate	Water Depth (m)	Date	Time	Image Width (cm)	Grain Size Major Mode (phi)	Grain Size Minimum (phi)	Grain Size Maximum (phi)	Grain Size Range (phi)	Penetration Mean (cm)	Penetration Minimum (cm)	Penetration Maximum (cm)	Over-penetration?	Boundary Roughness (cm)	Boundary Roughness Type	aRPD Mean (cm)	aRPD > Pen	Mud Clast Number	Mud Clast State
REF-C-01	A	96.62	10/6/2021	15:40:56	14.71	>4	>4	3	>4 to 3	10.01	9.68	10.47	No	0.78	Biological	3.70	No	1	Oxidized
REF-C-01	B	96.62	10/6/2021	15:42:03	14.71	>4	>4	3	>4 to 3	9.87	8.92	10.32	No	1.40	Biological	2.36	No	1	Oxidized
REF-C-01	E	96.62	10/6/2021	15:44:57	14.71	>4	>4	3	>4 to 3	9.48	9.07	10.02	No	0.95	Biological	IND	No	5	Reduced/ Oxidized
REF-C-02	A	97.23	10/6/2021	15:21:30	14.71	>4	>4	3	>4 to 3	9.60	9.19	10.01	No	0.82	Biological	2.58	No	2	Oxidized
REF-C-02	B	97.23	10/6/2021	15:22:35	14.71	>4	>4	3	>4 to 3	10.13	9.85	10.42	No	0.57	Biological	2.81	No	3	Reduced
REF-C-02	D	97.23	10/6/2021	15:24:39	14.71	>4	>4	3	>4 to 3	10.53	9.73	11.00	No	1.27	Biological	3.12	No	0	None
REF-C-03	A	97.23	10/6/2021	15:30:18	14.71	>4	>4	3	>4 to 3	9.00	8.61	9.26	No	0.65	Biological	2.84	No	4	Oxidized
REF-C-03	C	97.23	10/6/2021	15:32:44	14.71	>4	>4	3	>4 to 3	7.38	6.77	8.34	No	1.57	Biological	2.42	No	0	None
REF-C-03	D	97.23	10/6/2021	15:33:45	14.71	>4	>4	3	>4 to 3	9.45	9.14	9.70	No	0.56	Biological	2.40	No	0	None
REF-B-04	B	97.54	10/6/2021	10:31:05	14.71	>4	>4	3	>4 to 3	13.81	13.55	14.39	No	0.84	Biological	3.49	No	0	None
REF-B-04	C	97.54	10/6/2021	10:32:27	14.71	>4	>4	3	>4 to 3	14.80	14.35	15.53	No	1.18	Biological	2.68	No	0	None
REF-B-04	D	97.54	10/6/2021	10:33:38	14.71	>4	>4	3	>4 to 3	15.73	14.40	17.02	No	2.62	Biological	2.77	No	0	None
REF-B-05	A	84.43	10/6/2021	10:19:19	14.71	>4	>4	3	>4 to 3	11.58	10.84	12.16	No	1.32	Biological	3.10	No	0	None
REF-B-05	B	84.43	10/6/2021	10:20:48	14.71	>4	>4	3	>4 to 3	13.67	11.25	14.66	No	3.41	Biological	2.67	No	0	None
REF-B-05	D	84.43	10/6/2021	10:23:46	14.71	>4	>4	3	>4 to 3	13.22	12.51	13.77	No	1.25	Biological	3.59	No	0	None
REF-B-06	A	95.4	10/6/2021	10:00:38	14.71	>4	>4	3	>4 to 3	14.18	13.93	14.41	No	0.48	Biological	3.70	No	0	None
REF-B-06	B	95.4	10/6/2021	10:02:19	14.71	>4	>4	3	>4 to 3	13.94	13.50	14.40	No	0.89	Biological	2.68	No	0	None
REF-B-06	C	95.4	10/6/2021	10:03:31	14.71	>4	>4	3	>4 to 3	15.14	13.71	15.45	No	1.74	Biological	3.52	No	0	None

Station ID	Replicate	Water Depth (m)	Date	Time	Image Width (cm)	Grain Size Major Mode (phi)	Grain Size Minimum (phi)	Grain Size Maximum (phi)	Grain Size Range (phi)	Penetration Mean (cm)	Penetration Minimum (cm)	Penetration Maximum (cm)	Over-penetration?	Boundary Roughness (cm)	Boundary Roughness Type	aRPD Mean (cm)	aRPD > Pen	Mud Clast Number	Mud Clast State
REF-A-07	A	97.84	10/6/2021	7:41:45	14.71	>4	>4	3	>4 to 3	17.81	17.32	18.26	No	0.94	Biological	3.68	No	0	None
REF-A-07	B	97.84	10/6/2021	7:43:05	14.71	>4	>4	3	>4 to 3	18.98	16.63	19.82	No	3.19	Biological	4.05	No	0	None
REF-A-07	E	97.84	10/6/2021	9:29:31	14.71	>4	>4	3	>4 to 3	15.33	12.43	15.57	No	3.14	Biological	3.06	No	0	None
REF-A-08	I	98.76	10/6/2021	9:05:19	14.71	>4	>4	3	>4 to 3	14.24	13.50	15.11	No	1.61	Biological	4.29	No	0	None
REF-A-08	J	98.76	10/6/2021	9:06:21	14.71	>4	>4	3	>4 to 3	17.08	14.67	18.45	No	3.78	Biological	3.96	No	0	None
REF-A-08	L	98.76	10/6/2021	9:08:40	14.71	>4	>4	3	>4 to 3	17.31	17.12	17.60	No	0.49	Biological	3.63	No	0	None
REF-A-09	B	98.45	10/6/2021	7:53:47	14.71	>4	>4	3	>4 to 3	19.09	15.63	21.31	No	5.68	Biological	2.70	No	0	None
REF-A-09	C	98.45	10/6/2021	7:55:01	14.71	>4	>4	3	>4 to 3	19.22	18.36	20.19	No	1.83	Biological	3.48	No	0	None
REF-A-09	E	98.45	10/6/2021	9:36:42	14.71	>4	>4	3	>4 to 3	14.91	14.28	15.79	No	1.51	Biological	5.41	No	0	None
10	A	99.36	10/6/2021	11:48:56	14.71	4 to 3/>4	>4	1	>4 to 1	8.90	8.02	9.81	No	1.79	Biological	2.43	No	0	None
10	C	99.36	10/6/2021	11:51:49	14.71	4 to 3	>4	2	>4 to 2	8.56	8.08	9.15	No	1.06	Biological	3.07	No	0	None
10	E	99.36	10/6/2021	11:55:24	14.71	4 to 3	>4	2	>4 to 2	8.93	8.63	9.44	No	0.81	Biological	2.77	No	1	Oxidized
11	A	99.36	10/6/2021	12:20:13	14.71	4 to 3	>4	2	>4 to 2	11.22	11.01	11.49	No	0.49	Biological	2.45	No	0	None
11	B	99.36	10/6/2021	12:21:31	14.71	4 to 3	>4	2	>4 to 2	11.88	11.46	12.51	No	1.06	Biological	2.28	No	0	None

Station ID	Replicate	Water Depth (m)	Date	Time	Image Width (cm)	Grain Size Major Mode (phi)	Grain Size Minimum (phi)	Grain Size Maximum (phi)	Grain Size Range (phi)	Penetration Mean (cm)	Penetration Minimum (cm)	Penetration Maximum (cm)	Over-penetration?	Boundary Roughness (cm)	Boundary Roughness Type	aRPD Mean (cm)	aRPD > Pen	Mud Clast Number	Mud Clast State
11	C	99.36	10/6/2021	12:22:53	14.71	4 to 3	>4	2	>4 to 2	10.16	9.74	10.36	No	0.62	Biological	1.62	No	1	Oxidized
12	B	99.36	10/6/2021	12:03:47	14.71	4 to 3	>4	2	>4 to 2	5.49	3.97	6.50	No	2.53	Biological	2.17	No	0	None
12	C	99.36	10/6/2021	12:05:14	14.71	4 to 3/3 to 2	>4	2	>4 to 2	11.47	9.02	11.83	No	2.81	Biological	1.45	No	0	None
12	D	99.36	10/6/2021	12:06:39	14.71	4 to 3/3 to 2	>4	-5	>4 to -5	8.38	7.74	8.87	No	1.14	Biological	1.87	No	0	None
13	D	99.67	10/6/2021	11:30:18	14.71	4 to 3	>4	2	>4 to 2	11.46	11.03	11.99	No	0.96	Biological	2.98	No	0	None
13	E	99.67	10/6/2021	16:32:42	14.71	4 to 3	>4	2	>4 to 2	11.61	10.93	12.65	No	1.71	Biological	2.23	No	0	None
13	F	99.67	10/6/2021	16:33:42	14.71	4 to 3	>4	2	>4 to 2	9.93	8.15	10.56	No	2.41	Biological	2.63	No	0	None
14	A	99.06	10/6/2021	11:36:38	14.71	4 to 3	>4	2	>4 to 2	10.47	10.04	11.02	No	0.98	Biological	2.55	No	0	None
14	B	99.06	10/6/2021	11:38:12	14.71	4 to 3	>4	2	>4 to 2	10.30	10.06	10.53	No	0.47	Biological	2.22	No	0	None
14	C	99.06	10/6/2021	11:39:34	14.71	4 to 3	>4	2	>4 to 2	9.80	9.31	10.28	No	0.98	Biological	1.09	No	0	None
15	A	98.76	10/6/2021	12:47:11	14.71	>4	>4	3	>4 to 3	16.07	15.36	16.68	No	1.31	Biological	4.35	No	0	None
15	C	98.76	10/6/2021	12:49:32	14.71	>4	>4	3	>4 to 3	17.39	15.97	17.98	No	2.00	Biological	4.88	No	0	None
15	D	98.76	10/6/2021	12:50:53	14.71	>4	>4	3	>4 to 3	14.36	13.97	14.94	No	0.97	Biological	3.37	No	0	None

Station ID	Replicate	Water Depth (m)	Date	Time	Image Width (cm)	Grain Size Major Mode (phi)	Grain Size Minimum (phi)	Grain Size Maximum (phi)	Grain Size Range (phi)	Penetration Mean (cm)	Penetration Minimum (cm)	Penetration Maximum (cm)	Over-penetration?	Boundary Roughness (cm)	Boundary Roughness Type	aRPD Mean (cm)	aRPD > Pen	Mud Clast Number	Mud Clast State
16	A	98.45	10/6/2021	14:32:34	14.71	>4	>4	3	>4 to 3	15.03	14.74	15.30	No	0.56	Biological	4.83	No	0	None
16	B	98.45	10/6/2021	14:33:54	14.71	>4	>4	3	>4 to 3	15.67	15.01	16.32	No	1.31	Biological	4.97	No	0	None
16	C	98.45	10/6/2021	14:35:02	14.71	>4	>4	3	>4 to 3	18.84	19.09	19.36	No	0.26	Biological	4.40	No	0	None
17	B	96.32	10/6/2021	13:23:45	14.71	>4	>4	3	>4 to 3	16.82	15.96	17.44	No	1.48	Biological	4.33	No	0	None
17	C	96.32	10/6/2021	13:25:09	14.71	>4	>4	3	>4 to 3	18.03	17.52	18.65	No	1.13	Biological	4.29	No	0	None
17	D	96.32	10/6/2021	13:26:17	14.71	>4	>4	3	>4 to 3	15.96	15.54	16.46	No	0.92	Biological	4.44	No	0	None
18	A	97.54	10/6/2021	14:00:17	14.71	>4	>4	3	>4 to 3	16.01	15.13	16.58	No	1.45	Biological	3.59	No	0	None
18	B	97.54	10/6/2021	14:01:24	14.71	>4	>4	3	>4 to 3	13.36	12.56	14.36	No	1.79	Biological	3.30	No	0	None
18	D	97.54	10/6/2021	14:03:57	14.71	>4	>4	3	>4 to 3	18.27	17.56	18.71	No	1.15	Biological	4.68	No	0	None
19	A	96.93	10/6/2021	11:12:53	14.71	4 to 3/>4	>4	2	>4 to 2	14.25	13.86	14.69	No	0.83	Biological	2.24	No	0	None
19	B	96.93	10/6/2021	11:14:20	14.71	4 to 3/>4	>4	2	>4 to 2	12.45	11.33	13.07	No	1.74	Biological	2.88	No	0	None
19	D	96.93	10/6/2021	11:16:53	14.71	4 to 3/>4	>4	2	>4 to 2	13.73	12.68	15.06	No	2.38	Biological	2.11	No	0	None
20	A	99.06	10/6/2021	14:51:42	14.71	>4	>4	3	>4 to 3	13.46	11.39	13.90	No	2.51	Biological	3.40	No	0	None
20	B	99.06	10/6/2021	14:53:01	14.71	>4	>4	3	>4 to 3	14.53	13.88	15.04	No	1.16	Biological	3.62	No	0	None
20	C	99.06	10/6/2021	14:54:14	14.71	>4	>4	3	>4 to 3	13.30	12.30	13.84	No	1.54	Biological	3.04	No	0	None

Station ID	Replicate	Water Depth (m)	Date	Time	Image Width (cm)	Grain Size Major Mode (phi)	Grain Size Minimum (phi)	Grain Size Maximum (phi)	Grain Size Range (phi)	Penetration Mean (cm)	Penetration Minimum (cm)	Penetration Maximum (cm)	Over-penetration?	Boundary Roughness (cm)	Boundary Roughness Type	aRPD Mean (cm)	aRPD > Pen	Mud Clast Number	Mud Clast State
21	A	97.54	10/6/2021	10:52:45	14.71	>4	>4	3	>4 to 3	15.70	15.12	16.04	No	0.92	Biological	3.21	No	0	None
21	B	97.54	10/6/2021	10:54:05	14.71	>4	>4	3	>4 to 3	14.39	13.91	15.04	No	1.13	Biological	2.42	No	0	None
21	D	97.54	10/6/2021	10:56:38	14.71	>4	>4	3	>4 to 3	12.81	12.24	13.29	No	1.06	Biological	1.89	No	0	None
22	A	99.36	10/6/2021	14:17:54	14.71	>4	>4	3	>4 to 3	14.86	14.36	15.25	No	0.89	Biological	1.87	No	0	None
22	B	99.36	10/6/2021	14:19:24	14.71	>4	>4	3	>4 to 3	15.11	14.54	15.63	No	1.08	Biological	2.39	No	0	None
22	D	99.36	10/6/2021	14:22:17	14.71	>4	>4	3	>4 to 3	13.41	13.01	13.85	No	0.84	Biological	2.49	No	0	None
23	A	99.97	10/6/2021	12:30:16	14.71	4 to 3/>4	>4	2	>4 to 2	13.94	12.81	15.39	No	2.58	Biological	0.89	No	0	None
23	B	99.97	10/6/2021	12:31:37	14.71	4 to 3/>4	>4	2	>4 to 2	12.10	11.01	12.50	No	1.49	Biological	2.12	No	0	None
23	D	99.97	10/6/2021	12:34:19	14.71	4 to 3/>4	>4	2	>4 to 2	14.16	13.74	14.47	No	0.74	Biological	1.43	No	0	None
24	A	96.93	10/6/2021	13:44:34	14.71	>4	>4	3	>4 to 3	15.00	14.50	15.43	No	0.92	Biological	2.21	No	0	None
24	B	96.93	10/6/2021	13:45:57	14.71	>4	>4	3	>4 to 3	15.70	15.04	16.24	No	1.19	Biological	2.44	No	0	None
24	D	96.93	10/6/2021	13:48:19	14.71	>4	>4	3	>4 to 3	18.12	17.10	18.69	No	1.59	Biological	2.78	No	0	None

Station ID	Replicate	Sediment Feature Anomalies	Dredged Material Present?	Dredged Material Layer Mean Thickness (cm)	Dredged Material Layer Minimum Thickness (cm)	Dredged Material Layer Maximum Thickness (cm)	Mean Dredged Material Depth (cm)	Buried Dredged Material?	Dredged Material > Pen	Dredged Material Notes
REF-C-01	A	Cohesive white clay surficial clast(s), and buried patchy layers	No	N/A	N/A	N/A	N/A	N/A	No	
REF-C-01	B	Cohesive white clay surficial clast(s), and buried patchy layers	No	N/A	N/A	N/A	N/A	N/A	No	
REF-C-01	E	Cohesive white clay surficial clast(s), and buried patchy layers	No	N/A	N/A	N/A	N/A	N/A	No	
REF-C-02	A	Cohesive white clay surficial clast(s), and buried patchy layers	No	N/A	N/A	N/A	N/A	N/A	No	
REF-C-02	B	Cohesive white clay surficial clast(s), and buried patchy layers	No	N/A	N/A	N/A	N/A	N/A	No	
REF-C-02	D	Cohesive white clay buried patchy layers	No	N/A	N/A	N/A	N/A	N/A	No	
REF-C-03	A	Cohesive white clay surficial clast(s), and buried patchy layers	No	N/A	N/A	N/A	N/A	N/A	No	
REF-C-03	C	Cohesive white clay buried patchy layers	No	N/A	N/A	N/A	N/A	N/A	No	
REF-C-03	D	Cohesive white clay surficial clast(s), and buried patchy layers	No	N/A	N/A	N/A	N/A	N/A	No	
REF-B-04	B		No	N/A	N/A	N/A	N/A	N/A	No	
REF-B-04	C		No	N/A	N/A	N/A	N/A	N/A	No	
REF-B-04	D		No	N/A	N/A	N/A	N/A	N/A	No	
REF-B-05	A		No	N/A	N/A	N/A	N/A	N/A	No	
REF-B-05	B	Trace white clay	No	N/A	N/A	N/A	N/A	N/A	No	
REF-B-05	D		No	N/A	N/A	N/A	N/A	N/A	No	
REF-B-06	A		No	N/A	N/A	N/A	N/A	N/A	No	
REF-B-06	B	Trace white clay	No	N/A	N/A	N/A	N/A	N/A	No	
REF-B-06	C		No	N/A	N/A	N/A	N/A	N/A	No	

Station ID	Replicate	Sediment Feature Anomalies	Dredged Material Present?	Dredged Material Layer Mean Thickness (cm)	Dredged Material Layer Minimum Thickness (cm)	Dredged Material Layer Maximum Thickness (cm)	Mean Dredged Material Depth (cm)	Buried Dredged Material?	Dredged Material > Pen	Dredged Material Notes
REF-A-07	A	Trace white clay	No	N/A	N/A	N/A	N/A	N/A	No	
REF-A-07	B	Trace white clay	No	N/A	N/A	N/A	N/A	N/A	No	
REF-A-07	E	Trace white clay	No	N/A	N/A	N/A	N/A	N/A	No	
REF-A-08	I		No	N/A	N/A	N/A	N/A	N/A	No	
REF-A-08	J		No	N/A	N/A	N/A	N/A	N/A	No	
REF-A-08	L		No	N/A	N/A	N/A	N/A	N/A	No	
REF-A-09	B		No	N/A	N/A	N/A	N/A	N/A	No	
REF-A-09	C		No	N/A	N/A	N/A	N/A	N/A	No	
REF-A-09	E		No	N/A	N/A	N/A	N/A	N/A	No	
10	A		Yes	8.90	8.02	9.87	0.00	No	Yes	DM is present from top to bottom of image and is coarser than native sediment. Black debris scattered throughout image, with darker, more reduced, silt/clay nearing bottom.
10	C		Yes	8.56	8.08	9.21	0.00	No	Yes	DM is present from top to bottom of image and is coarser than native sediment. Black debris scattered throughout image, with darker, more reduced sediments nearing bottom.
10	E		Yes	8.93	8.63	9.50	0.00	No	Yes	DM is present from top to bottom of image and is coarser than native sediment. Black debris scattered throughout image, with darker, more reduced sediments nearing bottom. Large clast along right of image at SWI.
11	A		Yes	11.22	11.01	11.55	0.00	No	Yes	DM is present from top to bottom of image and is coarser than native sediment. Black debris scattered throughout image, with darker, more reduced sediments nearing bottom.
11	B		Yes	11.88	11.46	12.57	0.00	No	Yes	DM is present from top to bottom of image and is coarser than native sediment. Black debris scattered throughout image, with darker, more reduced sediments nearing bottom.

Station ID	Replicate	Sediment Feature Anomalies	Dredged Material Present?	Dredged Material Layer Mean Thickness (cm)	Dredged Material Layer Minimum Thickness (cm)	Dredged Material Layer Maximum Thickness (cm)	Mean Dredged Material Depth (cm)	Buried Dredged Material?	Dredged Material > Pen	Dredged Material Notes
11	C		Yes	10.16	9.74	10.42	0.00	No	Yes	DM is present from top to bottom of image and is coarser than native sediment. Black debris scattered throughout image, with darker, more reduced sediments nearing bottom.
12	B		Yes	5.49	3.97	6.50	0.00	No	Yes	DM is present from top to bottom of image and is coarser than native sediment. Black debris scattered throughout image, with darker, more reduced sediments nearing bottom.
12	C		Yes	11.47	9.02	11.89	0.00	No	Yes	DM is present from top to bottom of image and is coarser than native sediment. Black debris scattered throughout image, with darker, more reduced sediments nearing bottom.
12	D		Yes	8.38	7.74	8.93	0.00	No	Yes	DM is present from top to bottom of image and is coarser than native sediment. Multiple clasts present at SWI and in background. Black debris scattered throughout image, with darker, more reduced sediments nearing bottom.
13	D		Yes	11.47	11.03	12.05	0.00	No	Yes	DM is present from top to bottom of image and is coarser than native sediment. Black debris scattered throughout image, with darker, more reduced sediments nearing bottom.
13	E		Yes	11.61	10.93	12.71	0.00	No	Yes	DM is present from top to bottom of image and is coarser than native sediment. Large clast with heavy tube growth at SWI. Black debris scattered throughout image, with darker, more reduced sediments nearing bottom.
13	F		Yes	9.93	8.15	10.62	0.00	No	Yes	DM is present from top to bottom of image and is coarser than native sediment. Small, reduced clast and man-made debris at SWI. Black debris scattered throughout image, with darker, more reduced sediments nearing bottom.
14	A		Yes	10.47	10.04	11.08	0.00	No	Yes	DM is present from top to bottom of image and is coarser than native sediment. Black debris scattered throughout image, with darker, more reduced sediments nearing bottom.
14	B		Yes	10.30	10.06	10.59	0.00	No	Yes	DM is present from top to bottom of image and is coarser than native sediment. Black debris scattered throughout image, with darker, more reduced sediments nearing bottom, with some clays mixed in.
14	C		Yes	9.80	9.31	10.34	0.00	No	Yes	DM is present from top to bottom of image and is coarser than native sediment. Black debris scattered throughout image, with darker, more reduced sediments nearing bottom, with some clays mixed in.
15	A		No	N/A	N/A	N/A	N/A	N/A	No	
15	C		No	N/A	N/A	N/A	N/A	N/A	No	
15	D		No	N/A	N/A	N/A	N/A	N/A	No	

Station ID	Replicate	Sediment Feature Anomalies	Dredged Material Present?	Dredged Material Layer Mean Thickness (cm)	Dredged Material Layer Minimum Thickness (cm)	Dredged Material Layer Maximum Thickness (cm)	Mean Dredged Material Depth (cm)	Buried Dredged Material?	Dredged Material > Pen	Dredged Material Notes
16	A		No	N/A	N/A	N/A	N/A	N/A	No	
16	B		No	N/A	N/A	N/A	N/A	N/A	No	
16	C		No	N/A	N/A	N/A	N/A	N/A	No	
17	B		No	N/A	N/A	N/A	N/A	N/A	No	
17	C		No	N/A	N/A	N/A	N/A	N/A	No	
17	D		No	N/A	N/A	N/A	N/A	N/A	No	
18	A		No	N/A	N/A	N/A	N/A	N/A	No	
18	B		No	N/A	N/A	N/A	N/A	N/A	No	
18	D		No	N/A	N/A	N/A	N/A	N/A	No	
19	A		No	N/A	N/A	N/A	N/A	N/A	No	
19	B		No	N/A	N/A	N/A	N/A	N/A	No	
19	D		No	N/A	N/A	N/A	N/A	N/A	No	
20	A		No	N/A	N/A	N/A	N/A	N/A	No	
20	B		No	N/A	N/A	N/A	N/A	N/A	No	
20	C		No	N/A	N/A	N/A	N/A	N/A	No	

Station ID	Replicate	Sediment Feature Anomalies	Dredged Material Present?	Dredged Material Layer Mean Thickness (cm)	Dredged Material Layer Minimum Thickness (cm)	Dredged Material Layer Maximum Thickness (cm)	Mean Dredged Material Depth (cm)	Buried Dredged Material?	Dredged Material > Pen	Dredged Material Notes
21	A		No	N/A	N/A	N/A	N/A	N/A	No	
21	B		No	N/A	N/A	N/A	N/A	N/A	No	
21	D		No	N/A	N/A	N/A	N/A	N/A	No	
22	A		No	N/A	N/A	N/A	N/A	N/A	No	
22	B		No	N/A	N/A	N/A	N/A	N/A	No	
22	D		No	N/A	N/A	N/A	N/A	N/A	No	
23	A		Yes	10.20	8.85	11.72	0.00	No	No	DM is present in majority of image and is coarser than native sediment. Black debris scattered throughout image, with tan, silt/clay sediments nearing bottom.
23	B		Yes	10.49	7.50	10.18	0.00	No	No	DM is present in majority of image and is coarser than native sediment. Black debris scattered throughout image, with tan, silt/clay sediments nearing bottom.
23	D		Yes	9.70	8.62	11.13	0.00	No	No	DM is present in majority of image and is coarser than native sediment. Black debris scattered throughout image, with tan, silt/clay sediments nearing bottom.
24	A		No	N/A	N/A	N/A	N/A	N/A	No	
24	B		No	N/A	N/A	N/A	N/A	N/A	No	
24	D		No	N/A	N/A	N/A	N/A	N/A	No	

Station ID	Replicate	Methane Present?	Low DO Present?	Sediment Oxygen Demand	Beggiatoa Present?	Beggiatoa Type/Extent	Voids Present?	Maximum Bioturbation Depth (cm)	Successional Stage	Comment
REF-C-01	A	No	No	Low	No	None	Yes	7.88	2 on 3	Light brown sediment. Large clast with tube growth present at surface. Several voids and tubes at SWI present as well.
REF-C-01	B	No	No	Low	No	None	Yes	9.57	2 on 3	Light brown sediment. Small clast with sediment deposition on top present in background at SWI. One void and several tubes present as well.
REF-C-01	E	No	No	Low	No	None	Yes	9.01	2 on 3	Light brown sediment. Several small clasts with sediment deposition on top present in background at SWI. One large void and tubes at SWI present as well.
REF-C-02	A	No	No	Low	No	None	Yes	8.00	2 on 3	Light brown sediment. Clasts with sediment deposition on top present in background at SWI. Several small voids and tubes at SWI present as well.
REF-C-02	B	No	No	Low	No	None	Yes	9.89	2 on 3	Light brown sediment. Clasts with light sediment deposition on top present in background at SWI. One large void and tubes at SWI present as well
REF-C-02	D	No	No	Low	No	None	Yes	10.58	2 on 3	Light brown sediment. Multiple voids present, with tubes at SWI.
REF-C-03	A	No	No	Low	No	None	Yes	9.06	2 on 3	Light brown sediment. Clasts with heavy sediment deposition and tube growth on top present in background on right at SWI. Several voids and tubes present as well.
REF-C-03	C	No	No	Low	No	None	Yes	7.04	2 on 3	Light brown sediment. Clasts with heavy sediment deposition and tube growth on top present in background on right at SWI. Several voids and tubes present as well. Shrimp and clam shell present at SWI as well.
REF-C-03	D	No	No	Low	No	None	Yes	9.50	2 on 3	Light brown sediment that tapers off into some darker, more reduced sediment. Tubes present at surface, while worms and voids apparent below SWI.
REF-B-04	B	No	No	Low	No	None	Yes	9.45	1 on 3	Light brown sediment, mixed with darker more reduced sediment below the aRPD. Various worms present below SWI, with small tubes located at surface.
REF-B-04	C	No	No	Low	No	None	Yes	14.81	1 on 3	Light brown sediment, mixed with darker more reduced sediment below the aRPD. Various worms and numerous feeding voids present below SWI, with small tubes located at surface.
REF-B-04	D	No	No	Low	No	None	Yes	15.15	1 on 3	Light brown sediment, mixed with darker more reduced sediment below the aRPD. Numerous worms and several feeding voids present below SWI, with small tubes apparent at surface.
REF-B-05	A	No	No	Low	No	None	Yes	11.55	1 on 3	Light brown sediment, mixed with darker more reduced sediment below the aRPD. Worm located along right side of image, with several feeding voids also present below SWI and small tubes in background at surface.
REF-B-05	B	No	No	Low	No	None	Yes	14.31	1 on 3	Light brown sediment, mixed with darker more reduced sediment below the aRPD. Worm located along the bottom left of image, with several feeding voids also present below SWI and small tubes in background at surface.
REF-B-05	D	No	No	Low	No	None	Yes	10.17	1 on 3	Light brown sediment, mixed with darker more reduced sediment below the aRPD. Multiple worms present below surface, in addition to a large feeding void. Small tubes located in background at SWI.
REF-B-06	A	No	No	Low	No	None	Yes	14.10	1 on 3	Light brown sediment, mixed with darker more reduced sediment below the aRPD. Multiple feeding voids present below surface, in addition large voids nearing the bottom of image. Small tubes located at SWI.
REF-B-06	B	No	No	Low	No	None	Yes	13.01	1 on 3	Light brown sediment, mixed with darker more reduced sediment below the aRPD. Multiple feeding voids and worms present below surface. Small tubes located at SWI.
REF-B-06	C	No	No	Low	No	None	Yes	13.76	1 on 3	Light brown sediment, mixed with darker more reduced sediment below the aRPD. Multiple feeding voids and worms present below surface. Small tubes located at SWI.

Station ID	Replicate	Methane Present?	Low DO Present?	Sediment Oxygen Demand	Beggiatoa Present?	Beggiatoa Type/Extent	Voids Present?	Maximum Bioturbation Depth (cm)	Successional Stage	Comment
REF-A-07	A	No	No	Low	No	None	Yes	14.90	1 on 3	Light brown sediment, mixed with darker more reduced sediment below the aRPD. Feeding void present along SWI in top right of image, with a worm present near center. Small tubes located at SWI.
REF-A-07	B	No	No	Low	No	None	Yes	18.16	2 on 3	Light brown sediment, mixed with darker more reduced sediment below the aRPD. Feeding voids present near SWI and close to bottom of image , with worms present near void closest to surface. Larger tubes located at along right at SWI.
REF-A-07	E	No	No	Low	No	None	Yes	15.35	1 on 3	Light brown sediment, mixed with darker more reduced sediment below the aRPD. Feeding voids present throughout image , with worms present near void closest to surface. Small tubes located at SWI.
REF-A-08	I	No	No	Low	No	None	No	9.97	1 on 3	Light brown sediment, mixed with darker more reduced sediment below the aRPD. Worms present throughout image with small tubes located at SWI.
REF-A-08	J	No	No	Low	No	None	Yes	16.69	2 on 3	Light brown sediment, mixed with darker more reduced sediment below the aRPD. Feeding voids present closer to bottom of image , with worms located towards the image center. Larger tube located on right at SWI.
REF-A-08	L	No	No	Low	No	None	Yes	17.20	1 on 3	Light brown sediment, mixed with darker more reduced sediment below the aRPD. Feeding voids present throughout image, the largest in the bottom left. Worms present near void near image center and small tubes located at SWI.
REF-A-09	B	No	No	Low	No	None	Yes	17.46	1 on 3	Light brown sediment, mixed with darker more reduced sediment below the aRPD. Feeding voids and worm present throughout image. Various sized tubes located at SWI.
REF-A-09	C	No	No	Low	No	None	Yes	18.62	1 on 3	Light brown sediment, mixed with darker more reduced sediment below the aRPD. Large feeding voids and several worm present throughout image. Small tubes located at SWI.
REF-A-09	E	No	No	Low	No	None	Yes	14.90	1 on 3	Light brown sediment, mixed with darker more reduced sediment below the aRPD. Large feeding void in center and several worms present throughout image. Small tubes located at SWI.
10	A	No	No	Medium	No	None	No	8.76	2	Light brown fine sand over much darker silt/clay DM. Shell hash and debris present in background at SWI. Worms present and small tubes located at SWI.
10	C	No	No	Medium	No	None	No	6.31	2	Light brown fine sand over much darker fines. Small worms and debris scattered throughout image, with small tubes present at SWI.
10	E	No	No	Medium	No	None	No	6.34	2	Light brown fine sand over much darker fines. Small worms and debris scattered throughout image, with the addition of a void near the bottom right. small tubes present at SWI, but larger tubes located both on and near clasts in background.
11	A	No	No	Medium	No	None	No	8.38	2	Light brown fine sand over much darker fines. Small worms and debris scattered throughout image, with small tubes present at SWI.
11	B	No	No	Medium	No	None	No	5.48	2	Light brown fine sand over much darker fines. Debris scattered throughout image, with larger tubes present at SWI.

Station ID	Replicate	Methane Present?	Low DO Present?	Sediment Oxygen Demand	Beggiatoa Present?	Beggiatoa Type/Extent	Voids Present?	Maximum Bioturbation Depth (cm)	Successional Stage	Comment
11	C	No	No	Medium	No	None	Yes	7.28	2 on 3	Light brown fine sand over much darker fines. Debris and worms scattered throughout image, with larger tubes present in background at SWI and a large void in the center.
12	B	No	No	Medium	No	None	No	4.64	2	Light brown fine sand over much darker fines. Debris and few smaller worms scattered throughout image.
12	C	No	No	Medium	No	None	No	11.22	2 on 3	Light brown fine sand over much darker fines. Large worm located along bottom of image and small tubes scattered across SWI. Debris is also present throughout image.
12	D	No	No	Medium	No	None	No	4.43	2	Light brown fine sand over much darker fines, with few small worms scattered throughout image. Large clasts in background at SWI supporting larger tubes.
13	D	No	No	Medium	No	None	No	7.59	2	Light brown fine sand over much darker fines, with a feeding void present along the right side of the image. Small tubes located along surface.
13	E	No	No	Medium	No	None	Yes	10.20	2 on 3	Light brown fine sand over much darker fines. Debris and worms scattered throughout image, with large tubes present at SWI (mainly located on large clast). Several voids present throughout image, with the largest being along the bottom.
13	F	No	No	Medium	No	None	Yes	7.21	2 on 3	Light brown fine sand over much darker fines, with a feeding void present along the left side of the image. Small tubes located along surface. Worms found just under SWI, with mud clast and human debris above SWI.
14	A	No	No	Medium	No	None	No	5.10	2	Light brown fine sand over much darker fines, with a feeding void present along the left side of the image. Small tubes located along surface, and worms found just under SWI,
14	B	No	No	Medium	No	None	No	9.96	2	Light brown fine sand over much darker fines, with a feeding void present along the bottom of the image. Small tubes located along surface.
14	C	No	No	Medium	No	None	No	9.17	2	Light brown fine sand over much darker fines, with a small feeding void present along the bottom of the image. Small tubes located along surface.
15	A	No	No	Low	No	None	Yes	11.73	1 on 3	Light brown sediment, mixed with darker more reduced sediment below the aRPD. Multiple feeding voids present below surface with small tubes located at SWI.
15	C	No	No	Low	No	None	Yes	11.81	2 on 3	Light brown sediment, mixed with darker more reduced sediment below the aRPD. Multiple feeding voids present below surface with larger tube located along left at SWI.
15	D	No	No	Low	No	None	Yes	10.84	1 on 3	Light brown sediment, mixed with darker more reduced sediment below the aRPD. Multiple feeding voids present below surface with smaller tubes along SWI.

Station ID	Replicate	Methane Present?	Low DO Present?	Sediment Oxygen Demand	Beggiatoa Present?	Beggiatoa Type/Extent	Voids Present?	Maximum Bioturbation Depth (cm)	Successional Stage	Comment
16	A	No	No	Low	No	None	Yes	13.91	1 on 3	Light brown sediment, mixed with darker more reduced sediment below the aRPD. Multiple feeding voids present below surface with smaller tubes along SWI.
16	B	No	No	Low	No	None	Yes	15.40	1 on 3	Light brown sediment, mixed with darker more reduced sediment below the aRPD. Multiple feeding voids present below surface with smaller tubes along SWI.
16	C	No	No	Low	No	None	Yes	18.00	1 on 3	Light brown sediment, mixed with darker more reduced sediment below the aRPD. Multiple larger feeding voids located along bottom portion of image, with worms present throughout image center. Tubes in background of SWI.
17	B	No	No	Low	No	None	Yes	16.14	1 on 3	Light brown sediment, mixed with darker more reduced sediment below the aRPD. Multiple larger feeding voids located throughout the image, with a worm present along the image bottom. Smaller tubes located along SWI.
17	C	No	No	Low	No	None	Yes	17.84	1 on 3	Light brown sediment, mixed with darker more reduced sediment below the aRPD. Multiple larger feeding voids located throughout the image, with one present along the image bottom and a worm located in the center. Small tubes located along SWI.
17	D	No	No	Low	No	None	Yes	15.15	1 on 3	Light brown sediment, mixed with darker more reduced sediment below the aRPD. Multiple feeding voids and worms scattered throughout the image. Small tubes located along SWI.
18	A	No	No	Low	No	None	Yes	17.90	1 on 3	Light brown sediment, mixed with darker more reduced sediment below the aRPD. Multiple feeding voids scattered throughout the image. Small tubes located along SWI.
18	B	No	No	Low	No	None	Yes	13.64	1 on 3	Light brown sediment, mixed with darker more reduced sediment below the aRPD. Multiple feeding voids along with numerous worms scattered throughout the image. Small tubes located along SWI.
18	D	No	No	Low	No	None	Yes	16.00	1 on 3	Light brown sediment, mixed with darker more reduced sediment below the aRPD. Multiple feeding voids scattered throughout the image. Large worm present nearing bottom of the image. Small tubes located along SWI.
19	A	No	No	Low	No	None	Yes	12.87	2 on 3	Light brown sediment, mixed with darker more reduced sediment below the aRPD. Multiple feeding voids scattered throughout the image, with worms present throughout center. Large tube present along the center of the SWI.
19	B	No	No	Low	No	None	Yes	12.62	2 on 3	Light brown sediment, mixed with darker more reduced sediment below the aRPD. Multiple large feeding voids scattered throughout the image, with the largest being at the bottom. Larger tubes present along the left side of the SWI.
19	D	No	No	Low	No	None	Yes	13.75	2 on 3	Light brown sediment, mixed with darker more reduced sediment below the aRPD. Multiple feeding voids present throughout image, with a large worm present mid-image and another near the SWI. Larger tubes present along the SWI.
20	A	No	No	Low	No	None	Yes	12.46	2 on 3	Light brown sediment, mixed with darker more reduced sediment below the aRPD. Multiple feeding voids present throughout image, with a worm present near the SWI along right.
20	B	No	No	Low	No	None	Yes	14.62	1 on 3	Light brown sediment, mixed with darker more reduced sediment below the aRPD. Multiple feeding voids present throughout image and worm along the right side of image. Small tubes present along SWI.
20	C	No	No	Low	No	None	Yes	12.31	1 on 3	Light brown sediment, mixed with darker more reduced sediment below the aRPD. Multiple large feeding voids present throughout image and worms located in center and along left. Small tubes present along SWI.

Station ID	Replicate	Methane Present?	Low DO Present?	Sediment Oxygen Demand	Beggiatoa Present?	Beggiatoa Type/Extent	Voids Present?	Maximum Bioturbation Depth (cm)	Successional Stage	Comment
21	A	No	No	Low	No	None	Yes	15.19	1 on 3	Light brown sediment, mixed with darker more reduced sediment below the aRPD. Multiple feeding voids and worms scattered throughout the image. Small tubes present along SWI.
21	B	No	No	Low	No	None	Yes	14.93	1 on 3	Light brown sediment, mixed with darker more reduced sediment below the aRPD. Multiple feeding voids present, with several worms also located throughout the image. Smaller tubes present along SWI.
21	D	No	No	Low	No	None	Yes	13.09	1 on 3	Light brown sediment, mixed with darker more reduced sediment below the aRPD. Multiple large feeding voids present and numerous worms also located throughout the image and along bottom of image. Smaller tubes present along SWI.
22	A	No	No	Low	No	None	Yes	15.07	1 on 3	Light brown sediment, mixed with darker more reduced sediment below the aRPD. Multiple large feeding voids present and numerous worms also located throughout the image. Smaller tubes present along SWI.
22	B	No	No	Low	No	None	Yes	8.33	1 on 3	Light brown sediment, mixed with darker more reduced sediment below the aRPD. Several feeding voids present and numerous worms also located throughout the image, but are aggregated along the right size of the image. Smaller tubes present along SWI.
22	D	No	No	Low	No	None	Yes	13.46	1 on 3	Light brown sediment, mixed with darker more reduced sediment below the aRPD. Numerous feeding voids and worms located throughout the image. Smaller tubes present along SWI.
23	A	No	No	Medium	No	None	Yes	12.35	2 on 3	Light brown fine DM that becomes darker and more reduced, that taper off into silt/clay below the reduced portion. Voids located mainly along the left side of image. Worm present in image center, with larger tubes present above SWI.
23	B	No	No	Medium	No	None	Yes	11.93	2 on 3	Light brown fine DM that becomes darker and more reduced, that taper off into silt/clay below the reduced portion. Two voids present; along right and left sides of image. Small worms scattered just under SWI, with larger tubes present above SWI.
23	D	No	No	Medium	No	None	No	11.64	2	Light brown fine DM that becomes darker and more reduced, that taper off into silt/clay below the reduced portion. Small worms located mid-image, with larger tubes present in background at SWI.
24	A	No	No	Low	No	None	Yes	12.87	1 on 3	Light brown sediment, mixed with darker more reduced sediment below the aRPD. Numerous feeding voids throughout image, with worms located along the left. Smaller tubes present along SWI.
24	B	No	No	Low	No	None	Yes	10.12	2 on 3	Light brown sediment, mixed with darker more reduced sediment below the aRPD. Large void present along the left. Larger tubes present along SWI.
24	D	No	No	Low	No	None	Yes	17.51	2 on 3	Light brown sediment, mixed with darker more reduced sediment below the aRPD. Numerous worms and voids present throughout image. Larger tube present in center of image.

APPENDIX E - PLAN VIEW IMAGE ANALYSIS RESULTS

Notes:

IND=Indeterminate

N/A=Not Applicable

SAV=Submerged Aquatic Vegetation

Station ID	Replicate	Water Depth (m)	Date	Time	Image Width (cm)	Image Height (cm)	Field of View (m2)	Sediment Type	Surface Oxidation	Bedforms	Beggiatoa Present?	Beggiatoa Type/Extent	Dredged Material Present?	Dredged Material Notes	Debris	Tube Abundance
REF-C-01	A	96.62	10/6/2021	15:40:34	65.08	43.39	0.28	Silt/Clay	Oxidized	None	No	None	No		None	Present (10-25%)
REF-C-01	B	96.62	10/6/2021	15:41:41	58.41	38.94	0.23	Silt/Clay	Oxidized	None	No	None	No		None	Present (10-25%)
REF-C-01	C	96.62	10/6/2021	15:42:44	65.46	43.64	0.29	Silt/Clay	Oxidized	None	No	None	No		None	Present (10-25%)
REF-C-02	A	97.23	10/6/2021	15:21:11	62.05	41.37	0.26	Silt/Clay	Oxidized	None	No	None	No		None	Present (10-25%)
REF-C-02	C	97.23	10/6/2021	15:23:19	57.61	38.40	0.22	Silt/Clay	Oxidized	None	No	None	No		None	Present (10-25%)
REF-C-02	D	97.23	10/6/2021	15:24:20	58.30	38.86	0.23	Silt/Clay	Oxidized	None	No	None	No		None	Present (10-25%)
REF-C-03	A	97.23	10/6/2021	15:29:58	63.00	42.00	0.26	Silt/Clay	Oxidized	None	No	None	No		None	Sparse (<10%)
REF-C-03	B	97.23	10/6/2021	15:31:24	61.78	41.19	0.25	Silt/Clay	Oxidized	None	No	None	No		None	Abundant (25-75%)
REF-C-03	D	97.23	10/6/2021	15:33:25	IND	IND	IND	Silt/Clay	Oxidized	None	No	None	No		None	Present (10-25%)
REF-B-04	A	97.54	10/6/2021	10:29:30	52.05	34.70	0.18	Silt/Clay	Oxidized	None	No	None	No		None	Abundant (25-75%)
REF-B-04	C	97.54	10/6/2021	10:32:07	IND	IND	IND	Silt/Clay	Oxidized	None	IND	IND	IND		IND	Present (10-25%)
REF-B-04	D	97.54	10/6/2021	10:33:18	59.75	39.83	0.24	Silt/Clay	Oxidized	None	No	None	No		None	Abundant (25-75%)
REF-B-05	A	84.43	10/6/2021	10:19:00	58.12	38.75	0.23	Silt/Clay	Oxidized	None	No	None	No		None	Present (10-25%)
REF-B-05	B	84.43	10/6/2021	10:20:28	IND	IND	IND	Silt/Clay	Oxidized	None	IND	IND	IND		None	IND
REF-B-05	D	84.43	10/6/2021	10:23:24	55.75	37.17	0.21	Silt/Clay	Oxidized	None	No	None	No		None	Present (10-25%)
REF-B-06	A	95.4	10/6/2021	10:00:17	56.50	37.67	0.21	Silt/Clay	Oxidized	None	No	None	No		None	Sparse (<10%)
REF-B-06	B	95.4	10/6/2021	10:02:00	57.61	38.40	0.22	Silt/Clay	Oxidized	None	No	None	No		None	Present (10-25%)
REF-B-06	D	95.4	10/6/2021	10:04:29	55.75	37.17	0.21	Silt/Clay	Oxidized	None	No	None	No		None	Present (10-25%)
REF-A-07	A	97.84	10/6/2021	7:41:24	84.69	56.46	0.48	Silt/Clay	Oxidized	None	No	None	No		None	Present (10-25%)
REF-A-07	C	97.84	10/6/2021	7:45:03	81.68	54.45	0.44	Silt/Clay	Oxidized	None	No	None	No		None	Sparse (<10%)
REF-A-07	E	97.84	10/6/2021	9:29:12	57.40	38.26	0.22	Silt/Clay	Oxidized	None	No	None	No		None	Present (10-25%)
REF-A-08	A	98.76	10/6/2021	8:02:48	77.77	51.84	0.40	Silt/Clay	Oxidized	None	No	None	No		None	Present (10-25%)
REF-A-08	E	98.76	10/6/2021	8:33:34	74.86	49.90	0.37	Silt/Clay	Oxidized	None	No	None	No		None	Abundant (25-75%)

Station ID	Replicate	Water Depth (m)	Date	Time	Image Width (cm)	Image Height (cm)	Field of View (m2)	Sediment Type	Surface Oxidation	Bedforms	Beggiatoa Present?	Beggiatoa Type/Extent	Dredged Material Present?	Dredged Material Notes	Debris	Tube Abundance
REF-A-08	I	98.76	10/6/2021	9:04:58	51.28	34.19	0.18	Silt/Clay	Oxidized	None	No	None	No		None	Abundant (25-75%)
REF-A-09	B	98.45	10/6/2021	7:53:27	83.16	55.44	0.46	Silt/Clay	Oxidized	None	No	None	No		None	Present (10-25%)
REF-A-09	E	98.45	10/6/2021	9:36:22	54.41	36.27	0.20	Silt/Clay	Oxidized	None	No	None	No		None	Present (10-25%)
REF-A-09	H	98.45	10/6/2021	16:51:07	59.29	39.53	0.23	Silt/Clay	Oxidized	None	No	None	No		None	Present (10-25%)
10	A	99.36	10/6/2021	11:48:37	58.91	39.27	0.23	Silt/Clay	Oxidized	None	No	None	Yes	Rock along left side of image	None	Present (10-25%)
10	C	99.36	10/6/2021	11:51:28	60.61	40.40	0.24	Silt/Clay	Oxidized	None	No	None	No		None	Present (10-25%)
10	E	99.36	10/6/2021	11:55:03	67.42	44.94	0.30	Silt/Clay	Oxidized	None	No	None	Yes	Clasts scattered with varying degrees of growth on top. Rock in top right corner of image.	None	Abundant (25-75%)
11	A	99.36	10/6/2021	12:19:54	62.98	41.99	0.26	Silt/Clay	Oxidized	None	No	None	Yes	Clast with growth located to the left of image center.	Gastropod shells	Present (10-25%)
11	B	99.36	10/6/2021	12:21:10	51.90	34.60	0.18	Silt/Clay	Oxidized	None	No	None	Yes	Large rock with heavy epifaunal growth along right of image.	None	Abundant (25-75%)
11	C	99.36	10/6/2021	12:22:34	57.78	38.52	0.22	Silt/Clay	Oxidized	None	No	None	No		None	Abundant (25-75%)
12	A	99.36	10/6/2021	12:02:02	63.96	42.64	0.27	Silt/Clay	Oxidized	None	No	None	Yes	Small clasts, rock, and debris.	Gastropod shells, rope	Abundant (25-75%)
12	B	99.36	10/6/2021	12:03:27	68.06	45.38	0.31	Silt/Clay	Oxidized	None	No	None	Yes	Small clasts and rocks.	None	Present (10-25%)
12	C	99.36	10/6/2021	12:04:53	62.95	41.97	0.26	Silt/Clay	Oxidized	None	No	None	Yes	Various sized clasts scattered throughout image, some with settled sediment on top.	None	Present (10-25%)
13	B	99.67	10/6/2021	11:27:01	63.96	42.64	0.27	Silt/Clay	Oxidized	None	No	None	No		Rope	Present (10-25%)
13	C	99.67	10/6/2021	11:28:23	59.77	39.85	0.24	Silt/Clay	Oxidized	None	No	None	No		None	Present (10-25%)
13	E	99.67	10/6/2021	16:32:23	58.67	39.11	0.23	Silt/Clay	Oxidized	None	No	None	Yes	Wood debris	Wood	Present (10-25%)
14	A	99.06	10/6/2021	11:36:18	63.13	42.09	0.27	Silt/Clay	Oxidized	None	No	None	Yes	Small clasts scattered throughout image, some with settled sediment on top.	Fish vertebrae	Present (10-25%)
14	B	99.06	10/6/2021	11:37:53	61.95	41.30	0.26	Silt/Clay	Oxidized	None	No	None	Yes	Small clasts and rocks scattered throughout image.	None	Present (10-25%)
14	C	99.06	10/6/2021	11:39:12	60.65	40.44	0.25	Silt/Clay	Oxidized	None	No	None	No		None	Present (10-25%)
15	A	98.76	10/6/2021	12:46:52	69.52	46.35	0.32	Silt/Clay	Oxidized	None	No	None	No		None	Present (10-25%)
15	B	98.76	10/6/2021	12:48:03	59.05	39.36	0.23	Silt/Clay	Oxidized	None	No	None	No		None	Present (10-25%)
15	D	98.76	10/6/2021	12:50:29	58.54	39.02	0.23	Silt/Clay	Oxidized	None	No	None	No		None	Present (10-25%)
16	A	98.45	10/6/2021	14:32:14	57.52	38.35	0.22	Silt/Clay	Oxidized	None	No	None	No		None	Present (10-25%)

Station ID	Replicate	Water Depth (m)	Date	Time	Image Width (cm)	Image Height (cm)	Field of View (m2)	Sediment Type	Surface Oxidation	Bedforms	Beggiatoa Present?	Beggiatoa Type/Extent	Dredged Material Present?	Dredged Material Notes	Debris	Tube Abundance
16	B	98.45	10/6/2021	14:33:32	52.47	34.98	0.18	Silt/Clay	Oxidized	None	No	None	No		None	Abundant (25-75%)
16	C	98.45	10/6/2021	14:34:43	44.52	29.68	0.13	Silt/Clay	Oxidized	None	No	None	No		None	Abundant (25-75%)
17	A	96.32	10/6/2021	13:22:01	59.32	39.54	0.23	Silt/Clay	Oxidized	None	No	None	No		None	Sparse (<10%)
17	B	96.32	10/6/2021	13:23:25	52.58	35.05	0.18	Silt/Clay	Oxidized	None	No	None	No		None	Sparse (<10%)
17	C	96.32	10/6/2021	13:24:47	51.84	34.56	0.18	Silt/Clay	Oxidized	None	No	None	No		None	Present (10-25%)
18	A	97.54	10/6/2021	13:59:55	55.97	37.32	0.21	Silt/Clay	Oxidized	None	No	None	No		None	Present (10-25%)
18	B	97.54	10/6/2021	14:01:04	60.42	40.28	0.24	Silt/Clay	Oxidized	None	No	None	No		None	Present (10-25%)
18	D	97.54	10/6/2021	14:03:38	59.20	39.47	0.23	Silt/Clay	Oxidized	None	No	None	No		None	Present (10-25%)
19	A	96.93	10/6/2021	11:12:32	64.54	43.03	0.28	Silt/Clay	Oxidized	None	No	None	No		None	Present (10-25%)
19	B	96.93	10/6/2021	11:13:58	61.68	41.12	0.25	Silt/Clay	Oxidized	None	No	None	No		None	Abundant (25-75%)
19	D	96.93	10/6/2021	11:16:32	61.27	40.85	0.25	Silt/Clay	Oxidized	None	No	None	No		None	Abundant (25-75%)
20	A	99.06	10/6/2021	14:51:22	54.36	36.24	0.20	Silt/Clay	Oxidized	None	No	None	No		None	Present (10-25%)
20	B	99.06	10/6/2021	14:52:40	56.69	37.79	0.21	Silt/Clay	Oxidized	None	No	None	No		None	Abundant (25-75%)
20	C	99.06	10/6/2021	14:53:54	53.94	35.96	0.19	Silt/Clay	Oxidized	None	No	None	No		None	Abundant (25-75%)
21	A	97.54	10/6/2021	10:52:25	59.88	39.92	0.24	Silt/Clay	Oxidized	None	No	None	No		None	Present (10-25%)
21	B	97.54	10/6/2021	10:53:45	55.16	36.78	0.20	Silt/Clay	Oxidized	None	No	None	No		None	Present (10-25%)
22	A	99.36	10/6/2021	14:17:33	60.12	40.08	0.24	Silt/Clay	Oxidized	None	No	None	No		None	Present (10-25%)
22	B	99.36	10/6/2021	14:19:04	58.93	39.29	0.23	Silt/Clay	Oxidized	None	No	None	No		None	Present (10-25%)
22	D	99.36	10/6/2021	14:21:54	52.79	35.19	0.19	Silt/Clay	Oxidized	None	No	None	No		None	Present (10-25%)
23	A	99.97	10/6/2021	12:29:56	65.99	43.99	0.29	Silt/Clay	Oxidized	None	No	None	No		None	Abundant (25-75%)
23	B	99.97	10/6/2021	12:31:18	62.25	41.50	0.26	Silt/Clay	Oxidized	None	No	None	No		None	Abundant (25-75%)
23	C	99.97	10/6/2021	12:32:38	IND	IND	IND	Silt/Clay	Oxidized	IND	IND	IND	IND		IND	IND
24	A	96.93	10/6/2021	13:44:13	56.79	37.86	0.22	Silt/Clay	Oxidized	None	No	None	No		None	Present (10-25%)
24	B	96.93	10/6/2021	13:45:36	63.47	42.31	0.27	Silt/Clay	Oxidized	None	No	None	No		None	Present (10-25%)
24	D	96.93	10/6/2021	13:47:56	46.64	31.09	0.14	Silt/Clay	Oxidized	None	No	None	No		None	Present (10-25%)

Station ID	Replicate	Burrow Abundance	Track Abundance	Epifauna	Macroalgae and/or SAV	Number of Fish	Comment
REF-C-01	A	Sparse (<10%)	Present (10-25%)	Shrimp	None	0	Soft, silty, light brown sediment with burrows, tubes, and tracks scattered throughout. Shrimp located just right of top center.
REF-C-01	B	Sparse (<10%)	Present (10-25%)	Shrimp	None	0	Soft, silty, light brown sediment with burrows, tubes, and tracks throughout. Shrimp and mud clasts also scattered within image.
REF-C-01	C	Sparse (<10%)	Sparse (<10%)	Shrimp	None	0	Soft, silty, light brown sediment with burrows, tubes, and tracks throughout. Shrimp present. Small mud clasts also scattered throughout image.
REF-C-02	A	None	Present (10-25%)	Shrimp	None	0	Soft, silty, light brown sediment with tubes, and tracks throughout. Shrimp and mud clasts also scattered within image.
REF-C-02	C	Sparse (<10%)	Abundant (25-75%)	Shrimp	None	0	Soft, silty, light brown sediment with tubes scattered throughout image. Numerous tracks present in top left corner, with scattered shrimp (top right) and mud clasts (top left and center).
REF-C-02	D	Sparse (<10%)	Abundant (25-75%)	Shrimp	None	0	Soft, silty, light brown sediment with tubes and shrimp scattered throughout image. Numerous tracks present in top left corner, with mud clasts along bottom and right side of image.
REF-C-03	A	Sparse (<10%)	Present (10-25%)	Crab, Shrimp	None	0	Soft, silty, and brown sediment with shrimp in center and Jonah crab along right side of image. Mud clasts located in center, with tracks scattered throughout image.
REF-C-03	B	Sparse (<10%)	Sparse (<10%)	Hydroids, Shrimp	Yes	0	Soft, silty, light brown sediment with tubes located mainly on top of clasts and shrimp located along top center. Frond present along right center of image.
REF-C-03	D	Sparse (<10%)	Present (10-25%)	Shrimp	None	0	Soft, silty, light brown sediment with clasts along top right and shrimp in top left. Some of image is not able to be interpreted.
REF-B-04	A	Present (10-25%)	Sparse (<10%)	Shrimp	None	0	Soft, silty, light brown sediment with several large clasts, shrimp, and numerous tubes scattered throughout image.
REF-B-04	C	IND	IND	IND	IND	1	Soft, silty, light brown sediment, but most of image is not viewable due to sediment cloud.
REF-B-04	D	Present (10-25%)	Abundant (25-75%)	None	None	0	Soft, silty, light brown sediment with burrows and tubes scattered throughout. Large fish track present along right side of image.
REF-B-05	A	Sparse (<10%)	Present (10-25%)	Shrimp	None	0	Soft, silty, light brown sediment with tubes scattered throughout and tracks mainly in top left corner. Shrimp present in bottom center of image.
REF-B-05	B	IND	IND	IND	None	1	Soft, silty, light brown sediment, but most of image details are not viewable due to sediment cloud.
REF-B-05	D	Present (10-25%)	Abundant (25-75%)	None	None	1	Soft, silty, light brown sediment with burrows and tubes scattered throughout. Tracks are abundant through center of image.
REF-B-06	A	Sparse (<10%)	Present (10-25%)	None	None	0	Soft, silty, light brown sediment with tracks abundant throughout image.
REF-B-06	B	Sparse (<10%)	Abundant (25-75%)	None	None	0	Soft, silty, light brown sediment with tracks abundant throughout image.
REF-B-06	D	Sparse (<10%)	Sparse (<10%)	Shrimp	None	0	Soft, silty, light brown sediment with shrimp present in top left corner tubes scattered throughout image.
REF-A-07	A	Present (10-25%)	Abundant (25-75%)	Shrimp	None	1	Soft, silty, light brown sediment with tracks and tubes scattered throughout image. Large burrow located to the right of image center. Hake in lower left, mostly off camera.
REF-A-07	C	Present (10-25%)	Abundant (25-75%)	None	None	0	Soft, silty, light brown sediment with tracks scattered throughout image. Large burrow located in the top left of image.
REF-A-07	E	Sparse (<10%)	Present (10-25%)	Shrimp	None	1	Soft, silty, light brown sediment with tracks and tubes scattered throughout image. Multiple shrimp present.
REF-A-08	A	Present (10-25%)	Abundant (25-75%)	Shrimp	None	0	Soft, silty, light brown sediment and abundant tracks, with tubes scattered throughout image. Large burrow located in top right of image.
REF-A-08	E	Sparse (<10%)	IND	None	None	0	Soft, silty, light brown sediment with abundant tube growth. Disturbed Seafloor due to prior prism penetration.

Station ID	Replicate	Burrow Abundance	Track Abundance	Epifauna	Macroalgae and/or SAV	Number of Fish	Comment
REF-A-08	I	Sparse (<10%)	IND	None	None	0	Soft, silty, light brown sediment with abundant tube growth. Disturbed Seafloor due to prior prism penetration.
REF-A-09	B	Sparse (<10%)	Abundant (25-75%)	None	None	0	Soft, silty, light brown sediment and abundant tracks, with tubes and burrows scattered throughout image.
REF-A-09	E	Sparse (<10%)	Sparse (<10%)	Shrimp	None	0	Soft, silty, light brown sediment with tubes and a few shrimp scattered throughout image.
REF-A-09	H	Sparse (<10%)	Abundant (25-75%)	Shrimp	None	0	Soft, silty, light brown sediment with tubes and numerous tracks scattered throughout image.
10	A	Present (10-25%)	Abundant (25-75%)	None	None	0	Soft, silty, light brown sediment with larger burrows and numerous tracks scattered throughout image. Rock in center of image with growth on it.
10	C	Present (10-25%)	Present (10-25%)	Gastropod	None	2	Soft, silty, light brown sediment with burrows and numerous tracks scattered throughout image. Fish and snail both located along right side of image.
10	E	Present (10-25%)	Present (10-25%)	Hermit Crab	None	0	Soft, silty, light brown sediment with clasts in a clump at the image center and also scattered throughout image. Multiple burrows present with hermit crab along right-side of image,
11	A	None	Abundant (25-75%)	None	None	0	Soft, silty, light brown sediment with clast at the image center, with numerous tracks scattered throughout image.
11	B	None	Present (10-25%)	Hermit Crab, Shrimp	None	0	Soft, silty, light brown sediment with clast supporting heavy tube growth at the image center.
11	C	None	Abundant (25-75%)	None	None	0	Soft, silty, light brown sediment with numerous tracks scattered throughout image.
12	A	Sparse (<10%)	Abundant (25-75%)	Gastropod	None	0	Soft, silty, light brown sediment with numerous tracks and small clasts scattered throughout image. Rope located in bottom left corner of image.
12	B	None	Abundant (25-75%)	Shrimp	None	0	Soft, silty, light brown sediment with numerous tracks and clasts of various sized scattered throughout image.
12	C	None	Abundant (25-75%)	Shrimp	None	0	Soft, silty, light brown sediment with tubes, numerous tracks, and clasts of various sized scattered throughout image.
13	B	Sparse (<10%)	Present (10-25%)	Shrimp	None	0	Soft, silty, light brown sediment with tubes, burrows, and tracks scattered throughout image. Debris present to left of image center.
13	C	Present (10-25%)	Abundant (25-75%)	Shrimp	None	0	Soft, silty, light brown sediment with numerous tracks throughout image. Oxidized sediment present at Seafloor in both top and bottom right of image.
13	E	Sparse (<10%)	Present (10-25%)	Shrimp	None	2	Soft, silty, light brown sediment with numerous tracks throughout image. Piece of wood present in bottom left and fish located at top and along right side of image.
14	A	Sparse (<10%)	Present (10-25%)	Shrimp	None	0	Soft, silty, light brown sediment with numerous tracks and clasts of various sized scattered throughout image- some with sediment settled on top. Fish vertebrae present along left side of image.
14	B	None	Abundant (25-75%)	Shrimp	None	0	Soft, silty, light brown sediment with numerous tracks, clasts, and rocks of various sized scattered throughout image- some with sediment settled on top.
14	C	None	Abundant (25-75%)	None	None	0	Soft, silty, light brown sediment with tracks and tubes scattered throughout.
15	A	Sparse (<10%)	Present (10-25%)	None	None	0	Soft, silty, light brown sediment with tracks and tubes scattered throughout.
15	B	Present (10-25%)	Present (10-25%)	None	None	0	Soft, silty, light brown sediment with tracks and tubes scattered throughout. Track aggregated in bottom right, with 1 large track going out the image top. Large burrow in top left.
15	D	Sparse (<10%)	Present (10-25%)	None	None	0	Soft, silty, light brown sediment with tracks and tubes scattered throughout.
16	A	None	Present (10-25%)	None	None	0	Soft, silty, light brown sediment with tracks and tubes scattered throughout.

Station ID	Replicate	Burrow Abundance	Track Abundance	Epifauna	Macroalgae and/or SAV	Number of Fish	Comment
16	B	Present (10-25%)	Abundant (25-75%)	None	None	0	Soft, silty, light brown sediment with abundant tracks and tubes throughout image. 2 larger burrows present in top left corner.
16	C	None	Abundant (25-75%)	None	None	0	Soft, silty, light brown sediment with abundant tracks and tubes throughout image. 2 large fish forage depressions.
17	A	Sparse (<10%)	Present (10-25%)	None	None	0	Soft, silty, light brown sediment with tracks centered around bottom right of image.
17	B	None	Present (10-25%)	Shrimp	None	0	Soft, silty, light brown sediment with tracks in top right of image. Seems like prism was dragged through part of the image.
17	C	Present (10-25%)	Present (10-25%)	Shrimp	None	0	Soft, silty, light brown sediment with tubes and tracks scattered throughout image. Large burrow present just under image center.
18	A	Sparse (<10%)	Present (10-25%)	None	None	0	Soft, silty, light brown sediment with tubes and tracks scattered throughout image.
18	B	Sparse (<10%)	Present (10-25%)	Shrimp	None	0	Soft, silty, light brown sediment with tubes and tracks scattered throughout image. Large burrow present in top right .
18	D	Sparse (<10%)	Sparse (<10%)	None	None	0	Soft, silty, light brown sediment with tubes scattered throughout image. Tracks are aggregated along left side of the image.
19	A	Sparse (<10%)	Abundant (25-75%)	Shrimp	None	0	Soft, silty, light brown sediment with tubes and numerous tracks scattered throughout image.
19	B	Sparse (<10%)	Present (10-25%)	Shrimp	None	0	Soft, silty, light brown sediment with numerous tubes scattered throughout image, but mainly concentrated throughout center.
19	D	Sparse (<10%)	Abundant (25-75%)	Shrimp	None	0	Soft, silty, light brown sediment with tubes scattered throughout image. Tracks are mainly located along right side of image.
20	A	Sparse (<10%)	Sparse (<10%)	None	None	0	Soft, silty, light brown sediment with numerous tubes and some tracks scattered throughout image.
20	B	Sparse (<10%)	Present (10-25%)	Shrimp	None	0	Soft, silty, light brown sediment with numerous tubes and some tracks scattered throughout image.
20	C	None	Sparse (<10%)	Shrimp	None	0	Soft, silty, light brown sediment with numerous tubes prevalent in the center of the image.
21	A	Sparse (<10%)	Present (10-25%)	None	None	0	Soft, silty, light brown sediment with tubes and tracks scattered throughout image.
21	B	Sparse (<10%)	Present (10-25%)	Shrimp	None	0	Soft, silty, light brown sediment with tubes and tracks scattered throughout image.
22	A	Sparse (<10%)	Abundant (25-75%)	None	None	0	Soft, silty, light brown sediment with tubes scattered throughout image. Heavy tracking through center of image.
22	B	None	Sparse (<10%)	Shrimp	None	0	Soft, silty, light brown sediment with tubes scattered throughout image.
22	D	Present (10-25%)	Present (10-25%)	Shrimp	None	0	Soft, silty, light brown sediment with tubes and tracks scattered throughout image. Several large burrows located the right side of image.
23	A	Present (10-25%)	Sparse (<10%)	Shrimp	None	0	Soft, silty, light brown sediment with numerous tubes prevalent throughout image. Burrows present along top half of image.
23	B	None	Abundant (25-75%)	Shrimp	None	0	Soft, silty, light brown sediment with numerous and tracks tubes prevalent throughout image.
23	C	IND	IND	IND	IND	IND	Image not viewable due to sediment cloud.
24	A	Present (10-25%)	Present (10-25%)	None	None	0	Soft, silty, light brown sediment with tracks, tubes, and burrows scattered throughout image.
24	B	None	Abundant (25-75%)	None	None	1	Soft, silty, light brown sediment with tubes scattered throughout image. Heavy tracking along right side of image.
24	D	Abundant (25-75%)	Present (10-25%)	None	None	0	Soft, silty, light brown sediment with tubes scattered throughout image. Tracks located along the right side of image, with large burrow located in the top left.

APPENDIX F - GRAIN SIZE SCALE FOR SEDIMENTS

APPENDIX F

GRAIN SIZE SCALE FOR SEDIMENTS

Phi (Φ) Size	Size Range (mm)	Size Class (Wentworth Class)
<-1	>2	Gravel
0 to –1	1 to 2	Very coarse sand
1 to 0	0.5 to 1	Coarse sand
2 to 1	0.25 to 0.5	Medium sand
3 to 2	0.125 to 0.25	Fine sand
4 to 3	0.0625 to 0.125	Very fine sand
>4	<0.0625	Silt/clay

APPENDIX G - NON-PARAMETRIC BOOTSTRAPPED CONFIDENCE LIMITS

APPENDIX E

Non-parametric Bootstrapped Confidence Limits

Bootstrapping is a statistical resampling procedure that uses the sample data to represent the entire population in order to construct confidence limits around population parameters. Bootstrapping assumes only that the sample data are representative of the underlying population, so random sampling is a prerequisite for appropriate application of this method.

Bootstrapping procedures entail resampling, with replacement, from the observed sample of size n. Each time the sample is resampled, a summary statistic (e.g., mean or standard deviation) of the bootstrapped sample is computed and stored. After repeating this procedure many times, a summary of the bootstrapped statistics is used to construct the confidence limit. For the bootstrap-*t* method (e.g., Manly 1997, pp. 56-59; or Lunneborg 2000, pp. 129-131), the bootstrapped statistic (T) is a pivotal statistic, which means that the distribution of T is the same for all values of the true mean (θ). The bootstrap-*t* is essentially the "Studentized" version (i.e., subtract the mean and divide by the standard error, as is done to obtain the Student *t*-distribution for the sample mean) of the statistic of interest. This approach is quite versatile, and can be applied to construct a confidence interval around any linear combination of means (Lunneborg 2000, p. 364).

For the purpose of constructing a confidence interval around the true value for the linear combination of means ($\Theta = \mu_{Ref} - \mu_{Mound}$) the pivotal statistic T for the true difference is defined as

$$T = \frac{d - \theta}{SE(d)} \qquad \text{(Eq. A-1)}$$

We assume that this is adequately approximated by the bootstrap sampling distribution of T, denoted T*:

$$T^* = \frac{d^* - \hat{\theta}}{SE(d^*)} \qquad \text{(Eq. A-2)}$$

This distribution is comprised of the studentized statistic (T^*_B) computed from a large number (B) of randomly chosen bootstrapped samples $y_1^*, y_2^*, \ldots y_B^*$ from each of the four groups or populations. Here, d^* is the linear combination of group means for the bootstrapped sample; $\hat{\theta}$ is the observed difference in sample means from the original samples; $SE(d^*)$ is the estimated standard error of the linear contrast.

The 5th and the 95th quantiles of the T^* distribution ($T^*_{0.05}$ and $T^*_{0.95}$, respectively) satisfy the equations:

$$\Pr[\frac{\theta - d}{SE(d)} > T^*_{0.05}] = 0.95 \quad \text{(Eq. A-3a)}$$

$$\Pr[\frac{\theta - d}{SE(d)} < T^*_{0.95}] = 0.95 \quad \text{(Eq. A-3b)}$$

Rearranging these equations yields 95% confidence in each of the following two inequalities:

$$\Pr[d + T^*_{0.05}\, SE(d) < \theta] = 0.95 \quad \text{(Eq. A-4a)}$$

$$\Pr[d + T^*_{0.95}\, SE(d) > \theta] = 0.95 \quad \text{(Eq. A-4b)}$$

Bootstrapping is used to estimate the values $T^*_{0.05}$, $T^*_{0.95}$ and $SE(d)$. The left side of equation A-4a represents the 95% lower confidence limit on the difference equation ($\mu_y - \mu_x$); the left side of equation A-4b is the 95% upper confidence limit on the difference equation. Based on the two one-sided testing (TOST) approach presented in McBride (1999), if the bounds computed by Equations A-4a and A-4b are fully contained within the interval [–δ , +δ], then we conclude equivalence within δ units.

The specific steps used to compute the 95% upper and 95% lower confidence limits on the difference between two means using the bootstrap-*t* method are described below.

1. Bootstrap (sample with replacement from the original sample of size n) B = 10,000 samples from each of the four populations (1 pooled reference group and 3 mounds) separately.
2. Compute the T^*_B statistic for each bootstrapped set of independent samples. T^*_i is the bootstrapped-*t* statistic computed from the i^{th} bootstrap sample, defined by the following equation

$$T^*_i = \frac{\sum_{j=1}^4 c_j \bar{y}^*_{ji} - \sum_{j=1}^4 c_j \bar{y}_j}{SE\left(\sum_{j=1}^4 c_j \bar{y}^*_{ji}\right)} = \frac{\sum_{j=1}^4 c_j \bar{y}^*_{ji} - \sum_{j=1}^4 c_j \bar{y}_j}{\sqrt{\sum_{j=1}^4 s^2_{y^*_{ji}} c_j^2 / n_j}} \quad \text{(Eq. A-5)}$$

   where $\bar{y}^*_{ji}$, and $s^2_{y^*_{ji}}$ are the means and variances for the i^{th} bootstrapped sample from the j^{th} group (j=1 to 4); and $\bar{y}_j$ is the observed mean for the j^{th} group. Multiplying these group means by their respective coefficients c_j (1/3, -1, -1, -1) and summing the products yields the difference equation we wish to test (Equation 1). This step produces 10,000 values of the bootstrapped-*t* statistic which comprise the "bootstrap-*t* distribution".
3. Compute the standard deviation of the 10,000 bootstrapped linear combinations, $\sum_{j=1}^4 c_j\, \bar{y}^*_{ji}$ and save it as $SE(d)$. This is the bootstrap estimate of the true standard error.
4. Find $T^*_{0.05}$ and $T^*_{0.95}$, the 5th and 95th quantiles of the bootstrap-*t* distribution generated in Step 2. These values satisfy Equations A- 3a and A-3b.

5. Applying Equations A-4a and A-4b using the values $T^*_{0.05}$ and $T^*_{0.95}$ found in Step 4 gives the bootstrap-*t* estimate of the 95% lower and upper confidence limits on the difference equation, i.e.,

$$95\%\ \text{LCL} = \sum_{j=1}^{4} c_j\, \bar{y}_j + T *_{0.05}\, SE(d) \qquad \text{(Eq. A-6a)}$$

$$95\%\ \text{UCL} = \sum_{j=1}^{4} c_j \bar{y}_j + T *_{0.95}\, SE(d) \qquad \text{(Eq. A-6b)}$$

where $(\sum_{j=1}^{4} c_j \bar{y}_j)$ is the linear combination expressing the difference between the mean of the reference group and the mean of the three disposal mounds based on the original sample observations, and *SE(d)* is the standard deviation of the bootstrapped differences computed in Step 3.

References

Lunneborg, Clifford E. 2000. Data Analysis by Resampling: Concepts and Applications. Duxbury. 556 pp. + Appendices.

Manly, Bryan F.J. 1997. Randomization, Bootstrap and Monte Carlo Methods in Biology. Second edition. Chapman & Hall, London. 340 pp. + Appendices